PERFORMANCE IMPROVEMENT OF A VAPOR COMPRESSION AIR CONDITIONING SYSTEM BY CONDENSATE AND FRESH WATER SOURCE

BY

NASIRU ISHAQ IBRAHIM

A Thesis Presented to the
DEANSHIP OF GRADUATE STUDIES

KING FAHD UNIVERSITY OF PETROLEUM & MINERALS

DHAHRAN, SAUDI ARABIA

In Partial Fulfillment of the
Requirements for the Degree of

MASTER OF SCIENCE

In

MECHANICAL ENGINEERING

SAFAR, 1435

DECEMBER, 2013

KING FAHD UNIVERSITY OF PETROLEUM & MINERALS

DHAHRAN- 31261, SAUDI ARABIA

DEANSHIP OF GRADUATE STUDIES

This thesis, written by **Nasiru Ishaq Ibrahim** under the direction of his thesis advisor and approved by his thesis committee, has been presented to and accepted by the Dean of Graduate Studies, in partial fulfillment of the requirements for the degree of **MASTER OF SCIENCE IN MECHANICAL ENGINEERING.**

Thesis Committee

_____

Dr. Abdulghani Al-Farayedhi
Advisor

_____

Dr. P. Gandhidasan
Member

_____

Dr. Zuhair M. Gasem

Department Chairman

_____

Dr. Abdelsalam Al-Sarkhi
Member

_____

Dr. Salam A. Zummo
Dean of Graduate Studies

_____26/12/13_____
Date

II

بسم الله الرحمن الرحيم

Dedicated

To My Parents and Family

ACKNOWLEDGMENTS

TABLE OF CONTENTS

LIST OF TABLES

LIST OF FIGURES

xv

xvi

NOMENCLATURE

A	area (m^2)
ADP	apparatus dew point
ARI	Air Conditioning and Refrigeration Institute
COP	coefficient of performance
C_p	specific heat capacity (kJ/kg-K)
$\dot{C}$	heat capacity rate (kW/K)
D	diameter (m)
dp	dew point
EER	energy efficiency rating
f''	fouling factor (W/K)
h	specific enthalpy (kJ/kg-K)
$\tilde{h}$	convective heat transfer coefficient (W/m^2-K)
k	thermal conductivity (W/m-K)
L	length (m)
NTU	number of transfer unit
M	mass of condensate in the storage tank (kg)
$\dot{m}$	mass flow rate, kg/s
P	pressure (kPa)
$\dot{Q}$	rate of heat transfer (kW)

T	temperature (^{o}C or K)
t	time (s or h)
UA	conductance (W/K)
WHO	World Health Organization
$\dot{W}$	rate of work (kW)

Greek Symbols

Δ	difference
ε	effectiveness
ϕ	relative humidity
η	efficiency
ω	specific humidity
δ	uncertainty value

Subscripts

a	air
avg	average
com	compressor
c	condenser, condensate
e	exit
ev	evaporator
f	fin
H	high
i	inside, initial, inlet
i,e	instrument error

L	low
max	maximum
min	minimum
o	outside
pc	precooler
r	refrigerant
r,e	random error
s	isentropic, surface
sat	saturated
sc	subcooler
sf	fin surface
t	tube
tot	total
w	water

ABSTRACT (ENGLISH)

Full Name : Nasiru Ishaq Ibrahim

Thesis Title : Performance Improvement of a Vapor Compression Air Conditioning System by Condensate and Fresh Water Source.

Major Field : Mechanical Engineering

Date of Degree : Safar, 1435, December, 2013

Considerable amount of electrical energy produced in the Kingdom of Saudi Arabia is consumed by air conditioning systems. In addition, water scarcity still exists in most of the arid and semi-arid countries. This thesis presents the outcome of a study conducted to bring down energy consumption and improve the performance of a vapor compression air conditioning system using condensate that is generated by the system. The base system used in the study is a 1.5 ton split type air conditioner. Three different options of system modifications are adopted to improve its performance. The three options are: option 'A'- air precooling before entering the evaporator using condensate, option 'B'- precooling the air entering the condenser by condensate and option 'C'- subcooling the refrigerant exiting the condenser using the condensate. Comparative study of the base system and the modified system is carried out. The results show that precooling the air entering the evaporator and condenser using condensate lowers the compressor discharge pressure. The discharge pressure also decreased significantly when subcooling is applied. The decrease in the discharge pressure resulted in the decrease in compressor power consumption to about 5% for option 'A', 4.8 % for option 'B' and 3.7% for option 'C' from experiments conducted for severest weather conditions. The severest weather conditions are 36 ^{o}C dry bulb temperature and 80% relative humidity obtained from the climate data of four major cities of Saudi Arabia. By decreasing the discharge pressure, the compressor's life expectancy can be improved. The coefficient of performance, COP is increased by about 30 %, 21% and 30% for options 'A', 'B' and 'C', respectively. The increase in the second law efficiencies obtained for options 'A', 'B', and 'C' are 24.85, 23.51 and 21.53%, respectively. The overall assessment of the three options is that option 'A' gives better system performance improvement followed by option 'B', then option

'C'. The rate of condensate extraction from the air conditioning system is studied and chemical analysis is carried out on the condensate sample to determine its quality. The amounts of condensate collected in Dhahran from the base system during the humid and hottest months of June, July, August and September are 1036, 1181, 2173 and 1781 kg, respectively, and these amounts are obtained experimentally on hourly basis. Analytical results of condensate extraction obtained by using hourly actual climate data are in good agreement with the experimental results. Condensate chemical analysis is conducted and the results are compared with the recommended guideline values of drinking water by World Health Organization. The Chemical analysis reveals that the condensate can be used as drinking water after undergoing simple bacterial removal process. It can also be used to improve the performance air conditioning systems and other applications such as cooling tower make up water and irrigation.

ABSTRACT (ARABIC)

الاسم الكامل: ناسيرو اسحاق ابراهيم

عنوان الرسالة: تحسين أداء أنظمة التكييف العاملة بضغط البخار باالتكثيف ومصدر مياه عذب

التخصص: هندسة ميكانيكية

تاريخ الدرجة العلمية:سفر1435. ديسيمبر 2013

يتم إستهلاك كميات كبيرة من الطاقة الكهربية المنتجة في المملكة العربية السعودية من قبل أنظمة التكييف. ومن جهة أخرى، لا تزال ندرة المياه موجودة في معظم البلدان القاحلة وشبه القاحلة. تقدم هذه الأطروحة نتائج دراسة أجريت لتقليل استهلاك الطاقة وتحسين أداء أنظمة التكييف التي تعمل بطريقة ضغط الغاز باستخدام البخار المكثَّف الناتج من قبل نظام التكييف. والنظام الأساسي المستخدم في هذه الدراسة هو مكيف هواء مشقوق بسعة 1.5 طن. . تم اعتماد ثلاثة خيارات مختلفة لتحسين أداء النظام و تقليل استهلاك الطاقة. الخيارات الثلاثة هي: الخيار "أ"، تبريد الهواء قبل دخوله المبخر باستخدام مكثف. الخيار "ب"، تبريد باستخدام مكثف. التكثيف ز الخيار "ج "تبريد الغاز المبرد الخارج من المكثف الهواء قبل دخوله المبخر باستخدام التكثيف. تم عمل دراسة مقارنة للنظام الاساسى وانظام المعدل. اظهرت النتائج ان عملية التبريد المسبق للهواء قبل المبخر والمكثف باستخدام مكثف. وقللت عملية التبريد المسبقة للهواء الداخل للمبخر والمكثف باستخدام الماء المكثَّف من ضغط التصريف للضاغط . أيضاً بشكل ملحوظ عندما تم تبريد الغاز المبرد لأقل من درجة الغليان. وأدى إنخفاض ضغط التصريف للمضخة إلى إنخفاض استهلاك الطاقة في المضخة إلى حوالي 5٪ للخيار "أ" ، و4.8 ٪ للخيار "ب"، و 3.7 ٪ للخيار "ث" الظروف المناخية الحادة هى 36 درجة مئوية و 80% رطوبة نسبية ماخوذة من بيانات الطقس للاربع مدن الرئيسية فى المملكة العربية السعودية. ومن خلال خفض ضغط التصريف، يمكن تحسين متوسط العمر المتوقع للمضخة. وتم زيادة معامل الأداء (COP) بنحو 31 ٪ ، 21 ٪ و 30 ٪ للخيارات "أ" و"ب" و"ث" على التوالي. وكانت الزيادة في الكفاءة للقانون الثاني للخيارات "أ" و"ب" و"ث" هي 24.85، 23.51، و21.53 ٪ على التوالي. وتبين من التقييم العام للخيارات الثلاثة أن الخيار "أ" يعطي أفضل تحسين لأداء النظام، يليها الخيار "ب" ثم الخيار "ث". وتم دراسة معدل استخراج الماء المكثف من نظام تكييف الهواء الذي يعتبر مصدرا إضافياً للماء بالإضافة إلى تحليله كيميائياً لتحديد درجة نقائه. وكانت كمية الماء المكثف من خلال النظام في منطقة الظهران خلال الأشهر يونيو ويوليو وأغسطس وسبتمبر هي 1036, 1076 ، 1181، 2173، و1781 كجم على التوالي، وتم جمع هذه الكميات في التجربة كل ساعة. وكانت النتائج التحليلية لعملية التكثيف والتي تم حسابها لكل ساعة باستخدام البيانات المناخية الفعلية في إتفاق جيد مع النتائج التجريبية. تم اجراء التحاليل الكيميائية والتى تمت مقارنة نتائجها مع الموصى بها للماء المقطر من منظمة الصحة . أظهرت التحاليل الكيميائية الماء المكثف أنه يمكن استخدامه على أنه ماء مقطر بعد عملية ازالة البكتيريا ، وايضا يمكن استخدامه لتحسين اداء انظمة وتطبيقات تكييف الهواء كما فتعويض مياه أبراج التبريد،والري.

CHAPTER 1

INTRODUCTION

1.1. Background

Air conditioning can be described as a process of controlling temperature, moisture content, cleanliness, quality and circulation of air current in accordance with the requirement of thermal comfort. The rapid growth in population and industrialization has resulted in a greater demand of using air conditioning systems and consequently energy consumption across the globe. The global climate change also makes air conditioning systems design a necessary integral part to maintain suitable indoor conditions in modern buildings [1]. For example, air conditioning systems consumes up to 52 % of the electric energy in the Kingdom of Saudi Arabia (KSA) where summer seasons are generally hot and humid [2]. The energy consumption in other countries of similar climate conditions is expected to be in the same range.

Thermodynamic cycles such as vapor compression, vapor absorption and gas cycles are used in refrigeration and air conditioning applications. But vapor compression cycle is most widely used in residential air conditioning applications and is considered in this thesis. Typical application of a vapor compression air conditioning (VCAC) system is removing thermal energy from the interior of a building and rejecting it outside the building. This thermal energy is sometimes called the "space cooling load" and it can be

either sensible or a combination of sensible and latent components depending on the level of humidity in the air. The removal and rejection of the load from the interior to the exterior of a building is governed by heat exchangers generally known as evaporators and condensers, respectively. Majority of VCAC systems operate with air-cooled condensers. Under extreme climate conditions, the VCAC systems suffered the problems of over-heating, and reduced system performance. This eventually leads to increase in the pressure ratio across the compressor thereby increasing the power consumption. Local and international building codes require the new institutional, commercial and industrial buildings to have high volumes of outdoor ventilation air without compromising comfort and indoor air quality. This high demand of outside air requirement creates another energy penalty for air conditioning systems.

Developing the existing air conditioning systems and reducing energy consumption requires consideration of the seasonal variation of climates, in addition to the building energy loads. The primary factors that affect air conditioning systems performance are the air humidity and temperature. One aspect of achieving energy efficiency in buildings must be through the improvement of the existing air conditioning systems and equipment and it is obvious that the improvement will come as research is done.

Shortage of fresh water supply still exists in many developing and arid countries across the globe. Therefore, new techniques of supplementing fresh water supply at low cost are needed and one such techniques is the use of air conditioners condensate as additional source of water. Atmospheric air is a mixture of water vapor and many other gases. Considerable amount of water is contained in the atmosphere and this amount becomes high in hot and humid climates [3, 4]. The water vapor normally condenses over the

evaporator coil surface when the surface temperature becomes lower than the dew point temperature of the air. In hot and humid climates, huge amount of condensate usually flows-out of the evaporator and in most cases it is considered as a waste. In regions where climate conditions with high humidity prevail like those in some parts of Saudi Arabia, the cooling process can result in appreciable amount of water. If the condensed water is not properly handled, it can cause damage to building walls and wets the ground surface. The condensate can be utilized to improve the performance of air conditioning system and serve as an additional source of water.

1.2.   Principle of Operation of a Vapor Compression Air Conditioning System

The conventional VCAC system comprises of four basic components: evaporator, compressor, condenser and expansion valve as shown in Fig. 1.1. In a typical vapor compression cycle, low temperature and pressure mixture of vapor and liquid refrigerant enters the evaporator at state **4**. The refrigerant mixture absorbs heat from the warmed air that is passing through the evaporator and exit as a saturated vapor, state **1**. The compressor is used to compress the refrigerant vapor to higher pressure and temperature. The high pressure superheated vapor then enters an air cooled-condenser at state **2** where it is cooled by flowing air stream and exit as a liquid, state **3**. The liquid refrigerant passes through an expansion valve where it is expanded at constant enthalpy and the pressure suddenly decreased, becoming a saturated mixture of liquid and vapor and the cycle continues. Figures 1.2 and 1.3 show the corresponding P-h and T-s diagrams of the simple VCAC.
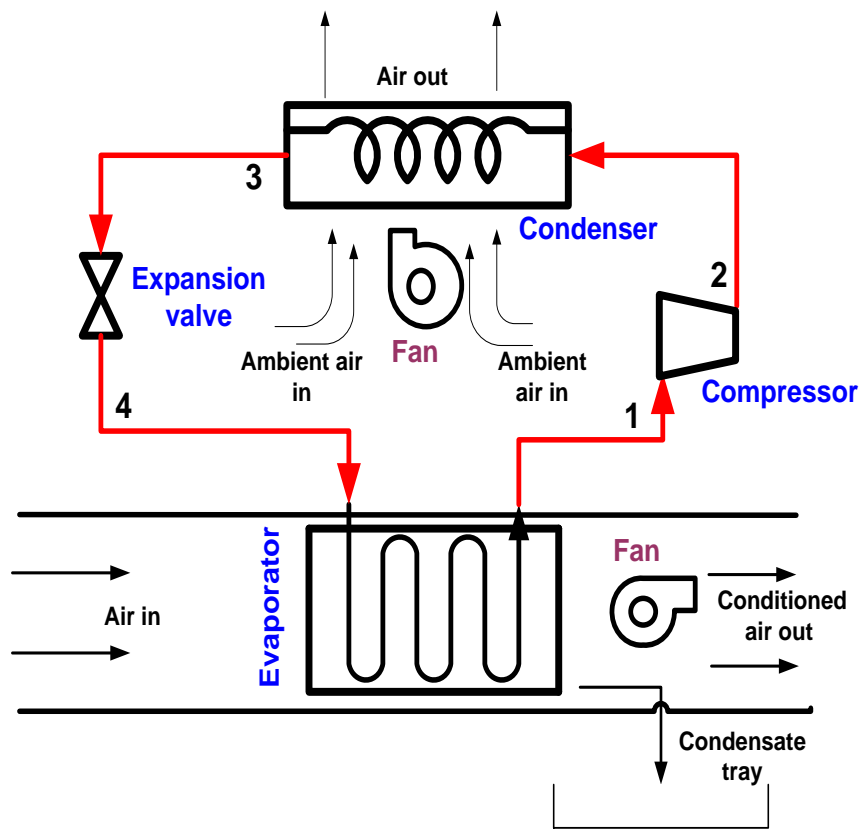
Figure 1.1 Basic components of conventional vapor compression system.
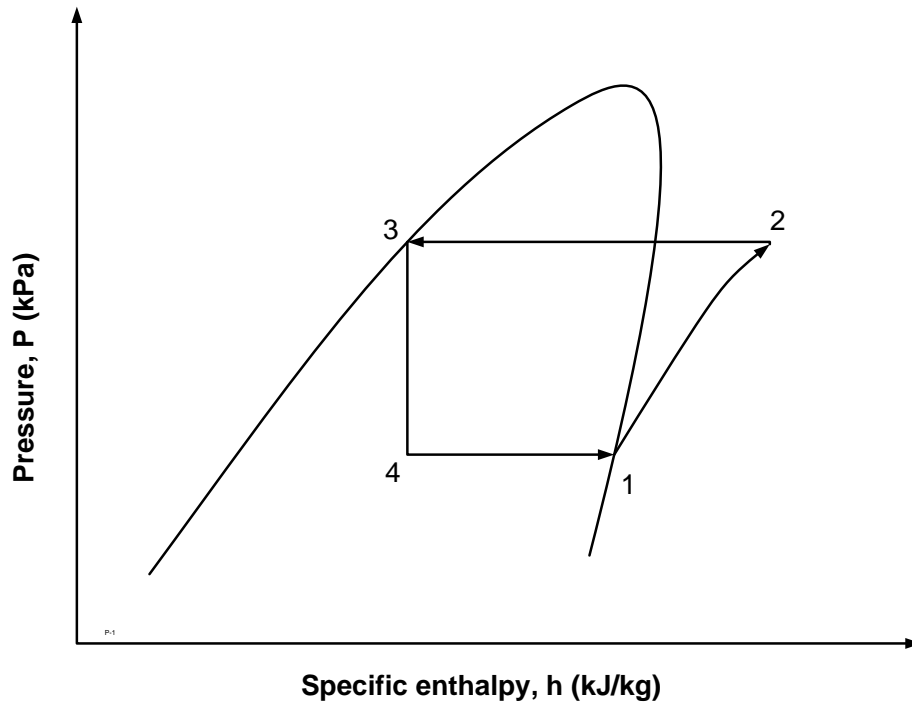
Figure 1.2 Schematic of pressure versus enthalpy diagram of conventional simple vapor compression cycle.
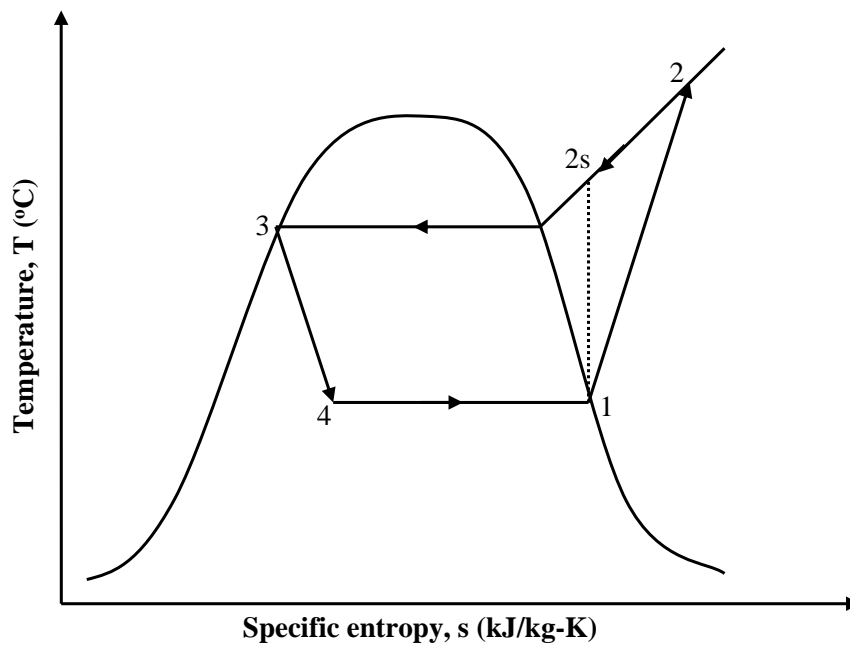
Figure 1.3 Schematic of temperature versus entropy diagram of conventional vapor compression cycle.

1.3. Objectives of the Thesis

The main objectives of the thesis research are:

1. To improve the performance of a vapor compression air conditioning system using condensate.

2. To use the condensate as additional water source and to test its quality.

The above objectives will be achieved by incorporating the following options:

- Option 'A': Precooling the air stream entering the evaporator using condensate.

- Option 'B': Precooling the air before entering the condenser using condensate.

- Option 'C': Subcooling the liquid refrigerant exiting the condenser using the condensate.

The thesis research is accomplished through the following steps:

i. Literature review will be carried out regarding the performance enhancement techniques of vapor compression systems and water vapor extraction from air conditioners.

ii. Climate data (temperature and relative humidity) for Dhahran, Saudi Arabia will be collected and used in the study.

iii. Analytical investigation will be carried out using some of the available climate data to estimate the rate of condensate extraction from an air conditioning system and the results will be validated with experiment. Analytical study and validation will also be carried out for option 'A' to evaluate the system performance.

iv.　Experiments will be conducted in Dhahran by using a 1.5-ton capacity base VCAC system. The performance of the base VCAC system will be compared with the performance of the system after modifications. Modifications on the system involves the following:

a) Addition of a precooler suitable for precooling the air entering the evaporator, using the air conditioner condensate.

b) Addition of a precooler for precooling the air stream before entering the condenser using the condensate.

c) Incorporation of a subcooler suitable for subcooling the liquid refrigerant exiting the condenser using the condensate.

v.　Overall performance evaluation of the modified air conditioning system will then be carried out.

Finally, chemical analysis of the condensate will be performed and the results will be compared with international standard guideline for water quality.

CHAPTER 2

LITERATURE REVIEW

2.1. Introduction

This chapter begins with literature survey on atmospheric water vapor condensation, followed by survey on various performance improvement techniques of VCAC systems. Studies related to the second law analysis applied to vapor compression systems are also reviewed.

2.2. Atmospheric Water Vapor Condensation as a Water Source

Condensation of water vapor occurs in different ways as reported in [3, 4]. One of the common ways is by surface cooling such as evaporator coils in air conditioning systems. Khalil [5] presented a theoretical study on cooling and dehumidification process where the controlling parameters of heat and mass transfer rate are optimized for the climate conditions of United Arab Emirates (UAE). An experimental study was carried out to obtain water for irrigation in Bahrain where three condensation surfaces are tested: aluminum, glass and polyethylene foil, [6]. The authors show that the hourly average quantities of condensate collected on these surfaces are 1.3, 0.8 and 0.3 kg/m^2, respectively. Habeebullah [7, 8] investigated theoretically the limits of water production from evaporator coil using summer climate data of Jeddah, KSA. He indicated that the daily variation of condensate yield follows similar pattern to relative humidity where the

minimum occurs during midday hours. Another study was carried out on a combined heat pump-dehumidification system in Jeddah, KSA for water production [8]. The water yield from the combined system is 0.618 m^3/day in January and 2.23 m^3/day in September. Elsarrag and Al Horr [9] studied experimentally water recovery from atmospheric air using a packaged unit air conditioner and tilted solar absorption/desorption system. They found that the average rate of condensed water from the air conditioning system is about 7.2 l/day per kW of cooling. Brayant and Ahmad [10] reported that over 660,000 gallons of water was captured within 140 days from condensate drains of 600 tons air conditioning unit in a commercial building in Doha, Qatar.

Large capacity air conditioning systems operating in hot and humid areas generates huge quantities of condensate. Guz [11] reported an hourly condensate production rate from a typical building in San Antonio as between 0.1 and 0.3 gallons of water per ton of cooling. Khan and Al-Zubaidy [12] presented a theoretical study on condensate recovery from cooling coil using Dubai weather conditions. They reported that about 2600 liters of condensate is produced from a HVAC system consisting of fresh air handling units. Their calculation is carried out by fixing cooling coil exit air temperature (12.77^{o}C). It is to be noted that cooling coil exit air temperature and humidity ratio depends on the capacity of the cooling coil and the coil inlet air temperature and humidity which affects the rate of condensate extraction. Therefore, a more general model that considers the variation of the coil exit air temperature as a result of the variation of inlet air conditions and coil capacity is thought in the present study. The inlet air conditions are the temperature and humidity.

Recently, Mahvi et al. [13] studied quantity and chemical quality of condensate obtained from different air conditioners operating in Bandar Abbas, Iran during the months of March to December. They reported that each air conditioner produced about 36 liters of water per day on average and split types generated more water than window air conditioners. The authors concluded that after undergoing a simple disinfection on the condensate sample, it will have no adverse effect on consumer health, adding that the water has suitable quality for many industrial uses.

Loveless et al. [14] identified areas in the world with the greatest condensate collection potential, given special consideration to areas having water scarcity. They tested few samples of condensate collected from different locations in Saudi Arabia. The authors stated that the quality of the collected condensate is close to that of distilled water, and after low-cost polishing treatments, the condensate quality may reach that of the portable water.

Domestic water demands in the Kingdom have increased from 502 million m^3 (MCM) in 1980 to about 2350 MCM in 2000 and is expected to be about 6450 MCM in 2025 [15]. Air conditioners condensate can be used to supplement the domestic water demand.

The above studies revealed that considerable amount of condensate can be extracted from the air conditioning systems. However, the purpose of which the condensate is extracted is solely to serve as an alternative water source for domestic uses. In order to have the maximum benefit of this technology, the present research focuses on utilizing the condensate to boost the performance of air conditioning systems. US patents [16-19] proposed the ideas of collecting condensate and circulating it through liquid-line and

super-heated vapor line to subcool the refrigerant. Although different approaches, all the above patents focuses on subcooling the refrigerant only. This thesis goes beyond that to include precooling the air before entering the evaporator and condenser.

2.3. Evaporative Cooling to Enhance Condenser Performance

One of the methods of performance improvement and energy saving techniques in VCAC systems is evaporative cooling to augment condenser performance. Evaporative cooling in this kind of application can be achieved in two ways; the first is by direct injection of water over the condenser coil. This method is associated with the problem of scaling and corrosion potential on the condenser coil and hence it is not widely accepted. The second method is by injecting water into evaporative media pad located in front of the condenser to precool the incoming air stream or by mist precooling. The second method is also divided into two, direct and indirect evaporative precooling. Chodak and Murphy [20] presented an experimental study to improve the efficiency of condensing unit of an air conditioner using a direct evaporative precooler. They concluded that a significant reduction in power is realized. Hajidavalloo and Eghtedari [21, 22] in their experimental study also indicated that using evaporatively-cooled air condenser in hot weather conditions, reduction in power consumption can be achieved up to 20% and the coefficient of performance can be improved to about 50%. Delfani et al. [23] in their study used indirect evaporative cooler as a precooling unit for conventional packaged unit air conditioner. Their results show that indirect evaporative cooler can reduce electrical energy consumption by about 55% during cooling season.

Waly et al. [24] carried out experimental investigation on the effect of precooling inlet air to condensers of air-conditioning units. Three different methods of precooling the

condenser air are considered; the cooling pads (CP) setup, the cooling mesh (CM) setup and the shading setup. All the three setup were applied to split air-conditioning units during the peak summer period in Kuwait. The results showed significant drop in power consumption ranging from 8.1 to 20.5% and an increase in cooling capacity ranging from 6.4 to 7.8% by using the CP and CM setups, respectively, which in turn, resulted in an increase in the coefficient of performance (COP) of the units by 36–59%.

A technique of using condensate drain to precool inlet air to the condenser of a 1.5 ton split air conditioner has been investigated using mathematical model [25]. For typical weather conditions of Beirut, the simulation results have shown that the drained condensate would be sufficient for air precooling in October only, resulting in 5.3% energy saving and the synchronized spray of condensate is found to last for six operating hours in a particular day in June and eight hours in August. This resulted in a total daily reduction in the consumed energy of 5% in June and 4.5% in August. It is to be noted that evaporative cooler is used in the above study using the condensate to precool the air entering the condenser. In the present study, a cross flow fin-tube heat exchanger is used for the same purpose which allows re-circulation of the condensate; hence the problem of condensate lost due to evaporation when using evaporative cooling is eliminated.

Mist precooling as a technique of improving the performance of air-cooled chillers has been reported by many researchers. Cansevdi et al. [26] indicated that using water spray mist precooling under ambient temperatures ranging from $20^{o}C$ to $39^{o}C$, the energy efficiency rating (EER) is increased from 2.96 to 3.36, corresponding to a rise of 3.5% in the EER, while an increase of 5.9 % in the cooling capacity is achieved. Yu and Chan, Tissot et al. [27, 28] indicated that effective cooling of air before the condenser through

mist precooling greatly influence the performance of the conventional system and reduction in power consumption. It is to be noted that these evaporative cooling techniques require additional source of water. In the present work, condensate is used as the coolant using a precooler that is placed upstream the condenser.

2.4. Refrigerant Subcooling

Subcooling is a process of further cooling refrigerant after exiting the condenser to a temperature below the saturation temperature of the refrigerant. Refrigerant subcooling modifies a conventional vapor compression system through the addition of heat exchanger downstream of the condenser. Subcooling increases the system's cooling effect and reduces the amount of energy required to run the system by reducing compressor power.

U.S. department of energy [29] reported three types of subcooling, (a) suction-liquid line subcooling (b) using small secondary vapor-compression system for subcooling the main system (this type is generally referred to as "mechanical subcooling"), and (c) using external heat sink.

2.4.1. Suction-liquid Line Subcooling

Suction-liquid line heat exchangers are used to subcool the refrigerant exiting the condenser by suction of cold refrigerant vapor from the evaporator. A suction-liquid line system has more cooling effect than a conventional vapor-compression system of the same condenser and compressor size, but the power consumption of the compressor may increases due to the additional super heat to the suction-line refrigerant by the heat

exchanger, where the compressor must work harder than when it is closed to the saturated-vapor line [30]. The overall effect of using a suction-liquid line heat exchanger in terms of thermodynamic efficiency depends on the type of refrigerant and operating conditions. Experimental investigation of the effects of subcooling using suction-liquid line heat exchanger on the performance of a domestic refrigeration system for different refrigerants is in [31]. The author stated that the compressor work input for all the investigated refrigerants decreases as the subcooling effectiveness increases.

2.4.2. Mechanical Subcooling

In mechanical subcooling, two refrigeration cycles are coupled together with a subcooling heat exchanger located downstream of the condenser. Mechanical subcooling is applicable to both low and medium temperature applications. Miller [32] noted that deep mechanical subcooling can results in 20% to 30% savings in input energy to compressors, capital saving through reduction in equipment size, and reduction in maintenance cost by as much as 60%. Different techniques are used in achieving mechanical subcooling.

Khan and Zubair [33] presented numerical simulation on the improvement of performance of refrigeration cycle by integrated mechanical subcooling. The simulation shows that performance improvement of air conditioning system can be as much as 20% during peak periods of high condensing temperatures, while high-temperature and low-temperature refrigeration systems will achieve energy saving up to 20 and 40%, respectively under the same conditions. Design and system analysis of dedicated mechanical subcooling of vapor compression refrigeration system has been carried out

14

and reported in [34]. They demonstrated that the performance of the overall cycle is improved over the conventional cycle. Qureshi et al. [35] carried out experimental study to improve the performance of a vapor compression system using dedicated mechanical subcooling. They reported about 21 % increase in second law efficiency of the system with subcooling.

2.4.3. External Heat Sink Subcooling

External heat sink subcooling technology is applicable to high temperature refrigeration and air conditioning applications. This system consists of a heat exchanger placed downstream the condenser. Liquid refrigerant is circulated through the heat exchanger, where it is further subcooled by counter flow water coming from a mini-cooling tower via a pump. After absorbing heat from the refrigerant due to subcooling, the warmed water is circulated back to the cooling tower where it is cool again by evaporation and the cycle continues [29].

There are limited studies in the literature with regards to external heat subcooling both numerical and experimental. In areas where there is water scarcity, this method may not be applicable. It can be noted that all the previous studies of subcooling techniques uses either a separate water source as the subcooling medium or employed dual-systems which in turn needs additional cost.

Although all the above mentioned techniques have been demonstrated and explained in a number of publications, the idea of using condensate to accomplish such techniques is quite new and at initial stage.

2.5. Hybrid Cooling

Hybrid cooling is one of the new cooling processes that received significant attention by different research institutes and universities. The basic concept of hybrid cooling involves the combination or integration of two or more cooling systems to improve the overall system performance. Hybrid cooling system directly combines vapor-compression system (VCS) or vapor-absorption system (VAS) with a desiccant dehumidification system. The desiccant section handles the latent heat load and dehumidifies the air, and the VCS or VAS handle the sensible heat load and provide the cooling. Using a desiccant to carry the latent load leaves only the sensible load for the cooling coil, resulting in operating the cooling coil at a lower load; hence, less input energy into the vapor compression refrigeration system is required [36]. Incorporating desiccant system to the conventional vapor-compression system reduces cooling loads and allows air conditioning systems to operate more efficiently.

Two types of desiccant are commonly used in cooling applications; solid and liquid desiccants. When solid desiccant is employed, the heat rejected from the condenser in the vapor-compression system is used to activate the solid desiccant, which is integrated directly into the condenser. Experimental investigation on a hybrid solid desiccant-R407C vapor compression air conditioner is presented in [37]. The authors reported that solid desiccant-based hybrid air conditioning system reduces the compressor electric power and the number of electric unit (kW-h) by 10.2%.

Mei and Dai [38] presented a comprehensive review on liquid-desiccant dehumidification for air conditioning application. Dai et al. [39] performed experimental study on hybrid cooling system. The system comprises of sections of desiccant dehumidification,

evaporative cooling and vapor compression air conditioning. They concluded that the new system can have more cooling production than the simple vapor compression system alone by 20-30%, and significant reduction in electric power consumption. Other studies have also shown that hybrid vapor compression system is more promising under high ambient conditions and significant performance improvement as well as energy saving can be achieved over conventional VCAC systems [40, 41].

The main disadvantage of liquid desiccant systems is the corrosive nature of the desiccant solution and the components of the system are greatly affected with time. Solid desiccant systems on the other hand require large volumes of desiccant and with time, efficiency of the desiccant bed can be reduced due to dust and foreign matter deposited in the pore. This problem can be addressed by additional air filtering, which may necessitate additional cost as a result of increased pressure drop through the system. In addition, maintenance cost will be escalated because filters need periodic cleaning and replacement. Therefore cost remains the prohibiting factor for desiccant systems.

2.6. Thermal Energy Storage Systems

Thermal energy storage technology integrated with conventional VCAC system is found to be one of the important technologies for energy management. Thermal storage systems are used to preserve energy in thermal reservoirs for later usage. For cooling applications, the cool energy is usually stored in form of sensible heat (chilled water storage) or latent heat (ice storage) [42]. Cool thermal storage systems are used to shift the power consumption from the peak to the off-peak periods. Due to the lower temperature during

night, thermal storage systems would consume less operating energy compare to the conventional air conditioning systems [42].

Chilled water thermal storage system consists of a storage tank, a packaged chiller or built-up refrigeration system, interconnecting piping, pumps and controls. Chilled water is produced by the chiller during the off-peak period at night and stored in the tank. The chilled water is then circulated through the cooling coil to achieve the required comfort during the peak period. Ice storage system is similar to water storage system with some additional components.

Different methods and application as well as assessment of thermal energy storage system have been studied by Dincer [43]. Study on the use of ice and chilled water cool thermal storage in Kuwait is also reported in [44, 45] and different operating strategies such as full and partial storage have been addressed by the authors. They found that ice cool thermal storage can reduce the electrical energy consumption during the peak periods of cooling demand. Yau and Behzad [46] presented a comprehensive review on cool thermal storage technologies and operating strategies for building applications. They concluded that localized parameters such as electricity demand trend, the peak and off-peak hours, electricity tariff rate, the system initial cost and the energy policy have to be considered through various case studies in different countries with different climates. It is to be noted that cool thermal storage technology may not be feasible in areas where there is no availability of water.

2.7. Second Law Analysis

Actual vapor compression systems are associated with various irreversible processes as a result of heat transfer between the system and the surrounding at a finite temperature difference. Exergy analysis which is based on the second law of thermodynamics provides an important criterion for evaluating the performance of such systems.

There has been substantial number of studies on the second law/exergy analysis of refrigeration and heat pump systems. Leidenfrost et al. [47] investigated the performance of a refrigeration system using R12 as the refrigerant based on exergy analysis. In this study, refrigeration load was kept constant while removing heat from a cold storage medium. Three different condensers – air, water and evaporative-cooled condensers are evaluated as functions of relative humidity of the ambient air through the determination of exergetic losses and the needed power for the thermodynamic cycle. It was found that wetting the condenser with water requires only 1% of the overall power consumption but reduces the consumption by 30% as compared with the air-cooled condenser. It is also stated that precooling the air by a water spray before it enters an air-cooled condenser is of benefit only at relative humidity 65% or less.

Bejan [48] presented second law analysis for a refrigeration system in which he refuted the conventional view expressed by Strobridge [49] that the second law efficiency of actual refrigeration cycle does not depend on the evaporator temperature by offering two models to explain the claim. He shows that the exergetic efficiency decreases as the evaporating temperature decreases.

Akau and Schoenhals [50] studied a heat pump system experimentally using water as the heat source and heat sink. They concluded that the computed values of the second law efficiency for heat pump operating under a well defined set of conditions depends upon the task performed on the ideal system used as the reference.

Yumrutas et al. [51] presented a computational model based on the exergy analysis to investigate the effects of evaporating and condensing temperatures on the pressure losses, exergy losses, second law efficiency and COP of a vapor compression refrigeration cycle. They stated that evaporating and condensing temperatures have strong effects on the exergy losses in the evaporator and condenser, second law efficiency and COP of the cycle but little effects on the other components of the cycle. They also found that the total exergy loss decreases with decreasing temperature difference between the evaporator and refrigerated space and between the condenser and the outside air.

Bilgen et al. [52] studied heat pump–air conditioner systems theoretically and experimentally using first and second law of thermodynamics. They found that the exergy efficiency is a decreasing function of load, varying from 0.35 to 0.22. The authors recommended that to improve the performance of the heat pump system, each component may be further study from exergy usage and economic point of view.

Arora and Kaushik [53] carried out detailed theoretical exergy analysis of an actual vapor compression refrigeration cycle where a model is developed for computing COP, exergy destruction, exergy efficiency and efficiency defects considering three different refrigerant; R502, R404A and R507A. They concluded that the worst component in terms of exergy destruction is the condenser followed by the compressor, the throttling valve

and the evaporator, respectively. They also found that increase in dead state temperature has a positive effect on exergy efficiency while COP of both R404A and 507A is improved by subcooling of the condensed liquid refrigerant.

An exergy analysis of multistage cascade low temperature refrigeration system used in olefin plants is presented in [54]. In this study, expressions for exergy efficiency and exergy destruction for each component of the refrigeration system and the relations for the total exergy destruction and overall exergetic efficiency are developed. They found that the major irreversibilities on the refrigeration system are due to losses within compression component and driving forces across the heat exchangers.

Venkataramanamurthy and Kumar [55] carried out comparative energy and second law analysis of R22, R436b vapor compression refrigeration system experimentally. A vapor compression cycle initially designed to operate with R-22 is used in their study. They examined the effect of evaporating temperature on the exergy losses, the second law efficiency and the COP of the refrigeration cycle. They found that the second law efficiency is very low, although the first law efficiency was within a normal range. The author mentioned that the reasons for such low efficiency are due to large exergy destructions in the compressor and the condenser.

Several researchers [56-58] used exergy concept for comparative performance evaluation of refrigeration systems with alternative refrigerants. Ahamed et al. [59] presented a comprehensive review on exergy analysis of vapor compression refrigeration system. The author pointed out that exergy depends on the evaporating temperature, condensing temperature, subcooling and compressor pressure as well as environmental temperature.

CHAPTER 3

THEORETICAL STUDY OF A VAPOR

COMPRESSION AIR CONDITIONING SYSTEM

3.1. Introduction

This chapter gives the detailed theoretical framework of the VCAC system under study. The modified system under study consists of three additional heat exchangers incorporated to the conventional system together with a condensate tank as shown in Fig 3.1. Two heat exchangers are used for air precooling at the evaporator and the condenser inlets while the other heat exchanger is used for refrigerant subcooling downstream of the condenser. The conventional VCAC system is analyzed considering the four basic components of the system. Using the three additional heat exchangers, the three options of performance improvement as mentioned in the objectives are studied.

3.2. Thermodynamic Performance of VCAC System and Condensate Extraction

The thermodynamic performance analysis of conventional VCAC system from energy point of view and the rate of condensate extraction from the system are studied and presented in this section.
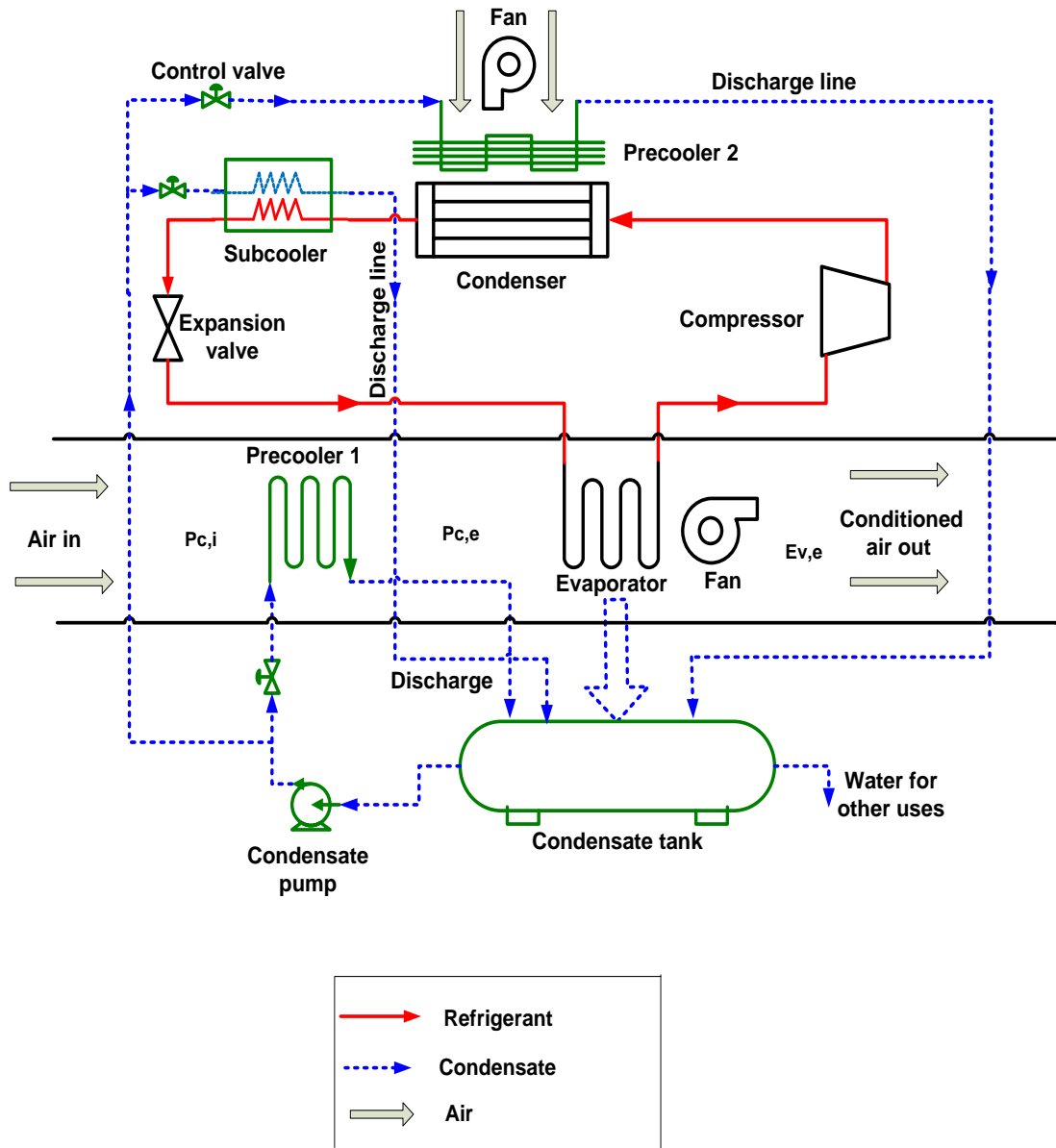
Figure 3.1 Schematic of the modified air conditioning system.

In order to determine the heat transfer and thermodynamics properties of the refrigerant, each component of the system is taken as a single unit. The following assumptions are made in the analytical aspect of the study:

1. Steady state condition of the whole VCAC system.

2. Pressure losses in the refrigerant lines are neglected.

3. Heat gains and heat loses from the system or to the system are neglected.

4. Adiabatic compressor and expansion valve.

5. Saturated states at the evaporator and condenser outlets.

Heat transfer rate to and from the cycle heat exchangers occurs by convection of flowing fluid streams with finite mass flow rates and specific heats. Therefore, the rate of heat transfer in the evaporator can be written as:

$$\dot{Q}_{ev} = \dot{m}_{a,ev}\left(h_{a,ev,i} - h_{a,ev,e}\right) = \dot{m}_r(h_1 - h_4) \tag{3.1}$$

Similarly, the rate of heat transfer from the condenser to the sink is written as:

$$\dot{Q}_c = \varepsilon_c \dot{m}_{a,c} C_{p,a,c}\left(T_3 - T_{a,c,i}\right) = \dot{m}_r(h_2 - h_3) \tag{3.2}$$

Isentropic compressor work is expressed as:

$$\dot{W}_{com,s} = \dot{m}_r(h_{2s} - h_1) \tag{3.3}$$

And the actual compressor work input as:

$$\dot{W}_{com} = \dot{m}_r(h_2 - h_1) \tag{3.4a}$$

or

$$\dot{W}_{com} = \frac{\dot{W}_{com,s}}{\eta_s} \tag{3.4b}$$

Using the first law of thermodynamics and considering the fact that change in internal energy is zero for a cyclic process, the overall energy balance of the cycle can be written as:

$$\dot{Q}_c - \dot{Q}_{ev} - \dot{W}_{com} = 0 \tag{3.5}$$

The measure of performance of refrigeration cycle is the coefficient of performance (COP) and is expressed as the cooling effect produced per unit work input.

$$COP = \dot{Q}_{ev}/\dot{W}_{com} \tag{3.6}$$

The second law efficiency of the system is defined as:

$$\eta_{II} = \frac{COP}{COP_{max}} \tag{3.7}$$

where

$$COP_{max} = \frac{T_L}{T_H - T_L} \tag{3.8}$$

and T_L is the mean temperature during the transfer of heat in the evaporator and is defined as[60]:

$$T_L = \frac{T_{a,ev,i} - T_{a,ev,e}}{ln\left(\frac{T_{a,ev,i}}{T_{a,ev,e}}\right)} \tag{3.9}$$

The ambient air temperature, which is the temperature of the air entering the condenser, $T_{a,c,i}$ is considered as the high temperature T_H throughout the analysis.

3.2.1. Condensate Extraction Considering the Complete VCAC System

In order to achieve the objectives of this study, it is necessary to first examine the quantity of condensate that can be obtained from the air conditioning system. Cooling with dehumidification is one of the applications of air conditioning systems where moist

air is processed to suit human comfort. This process is carried out in a heat exchanger containing a refrigerant or a secondary coolant such as chilled water or brine solution. In a cooling with dehumidification process, both humidity ratio and temperature of the air entering the evaporator decreases. When there is no moisture removal in the process, but only temperature decrease, the energy transfer is called 'sensible cooling'. When there is decrease in both temperature and humidity ratio as the air passes over the cooling coil, then the energy transferred is 'latent cooling'. In this case, moisture is removed in the form of liquid water, called *condensate.*

Consider a cooling section of a VCAC system in Fig. 3.2 where moist air passes over the cooling coil of an evaporator. When the evaporator coil surface temperature becomes lower than the dew point temperature of the entering air stream, the water vapor condenses over the coils. Psychrometric representation of the cooling/dehumidification process is shown in Fig. 3.3. As the air enters the coil at state (i), part of the air stream will come into direct contact with the coil surface and will be cooled to temperature almost equal to T_s, where T_s is the coil surface temperature.

Point 's' is termed as the apparatus dew point (ADP). The cold air in contact with the cooling coil is then mixed with the remaining air stream that is not in direct contact with the surface and exit at state (e) as shown in the Figure. The actual air exit at state (e) is located somewhere between point s and *dp* and may not necessarily be on the saturation curve [7, 61].

The temperature of the resulting mixture of the two air streams at the evaporator exit is expected to be greater than the coil surface temperature. The air properties (temperature and humidity ratio) at the exit of the evaporator are not known in the analytical study.

26
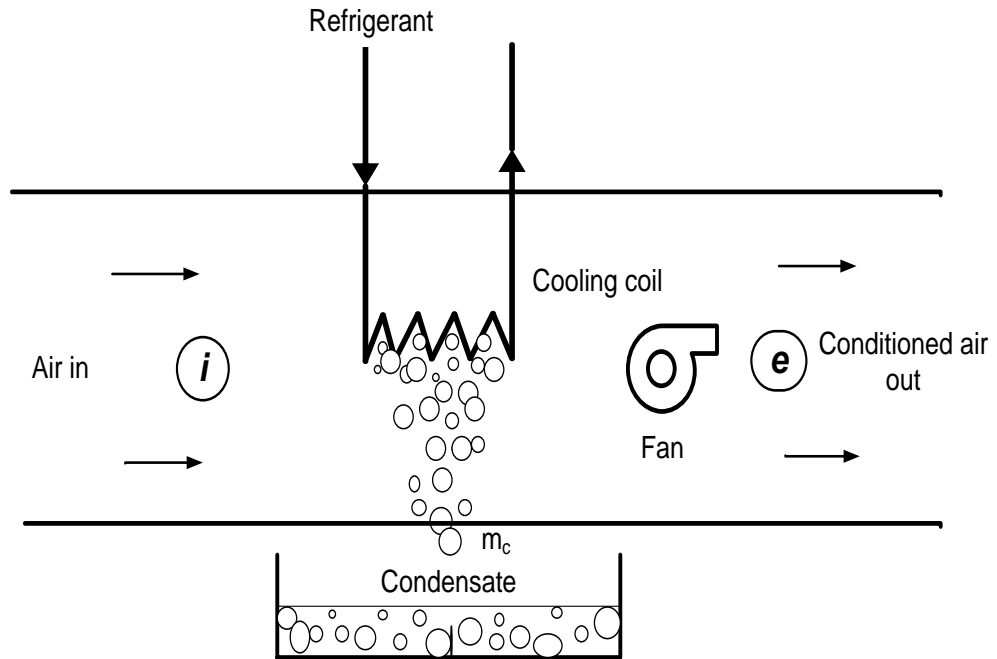
Figure 3.2 Schematic of a cooling with dehumidification process.
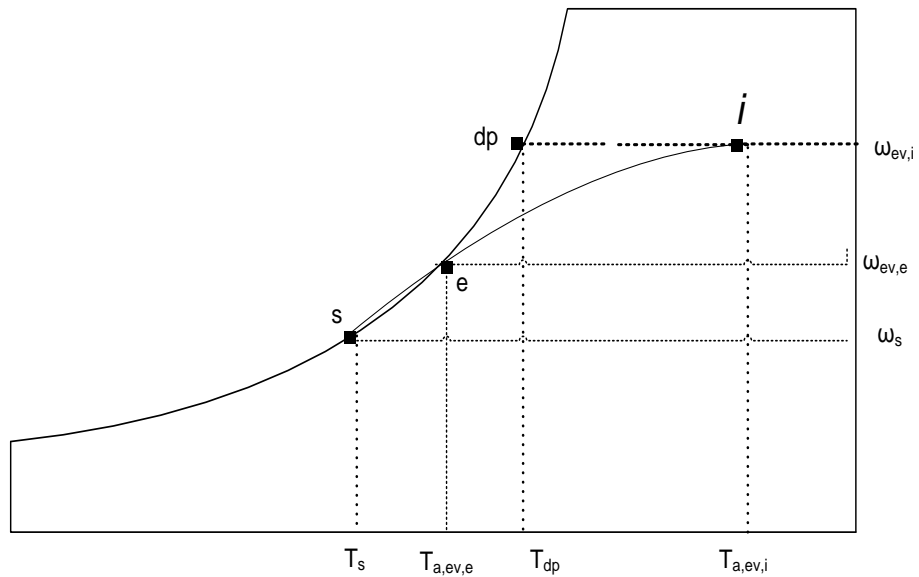
Figure 3.3 Psychrometric representation of cooling and dehumidification process.

27

The temperature and humidity ratio of the air stream leaving the evaporator at state (e) depends on the temperature of the refrigerant circulating in the evaporator, the evaporator thermal capacity, the inlet air humidity ratio and its flow rate. The rate of condensate extraction can be determined for any given air conditioning system of known nominal capacity and air flow rate across the evaporator. If the properties of the air at the evaporator inlet are known, the outlet air enthalpy can be determined using Eq. (3.1).

Evaporator effectiveness is defined as the ratio of actual heat transfer to the maximum possible heat transfer. In this case, the effectiveness is expressed in terms of the enthalpy of air-water mixture in order to take into account the effect of both heat and mass transfer occurring simultaneously at the coil surface [61]:

$$\varepsilon_{ev} = \frac{h_{a,ev,i} - h_{a,ev,e}}{h_{a,ev,i} - h_{a,min}} = \frac{\omega_{ev,i} - \omega_{ev,e}}{\omega_{ev,i} - \omega_{ev,min}} \tag{3.10}$$

The minimum enthalpy $h_{a,min,}$ and minimum humidity ratio $\omega_{ev,min}$ of the air are determined at the evaporating temperature. The evaporating temperature usually ranges from -1.1 ^{o}C to above for high temperature applications such as air conditioning [29]. The effectiveness of the evaporator is computed in the analytical study by assuming an initial guess value of the evaporating temperature from the above range after which the humidity ratio of the exit air, $\omega_{ev,e}$ is determined. Applying mass balance across the evaporator coil, the rate of condensate extraction from the coil is calculated as:

$$\dot{m}_c = \dot{m}_{a,ev}(\omega_{ev,i} - \omega_{ev,e}) \tag{3.11}$$

The daily condensate production is obtained by integrating the average value of condensate extracted per hour over the day as:

$$m_{c,day} = \int_0^{24} \dot{m}_{c,avg} dt \qquad (3.12)$$

The above property-dependent equations for system performance analysis and condensate extraction are coded in Engineering Equations Solver (EES) software [62] during the analytical studies. Applying the first law of thermodynamics to all components of the VCAC system, the assumed evaporating temperature is commented out after which the guessed value is updated.

The input parameters to the above model equations are the evaporator inlet air temperature and relative humidity, atmospheric pressure, flow rate of air entering the evaporator and condenser, temperature of air entering the condenser and condenser effectiveness. The rate of heat transfer at the evaporator and the evaporating temperature values are assumed at the beginning and then commented out once the program is completely coded.

3.2.2 Condensate Extraction Considering Only the Evaporator

Another approach of estimating the rate of condensate extraction is by considering only the evaporator as a heat exchanger in which both heat and mass transfer occurs concurrently. Evaporators used in air conditioning systems are mostly finned-tube cross-flow heat exchangers. In cooling applications, these heat exchangers may be treated as dry or wet depending on whether condensation occurs or not. There are two approaches in which these heat exchangers can be analyzed: (a) design-based analysis and (b) performance-based analysis [63]. The design-based analysis involves calculation of the necessary surface area and the number of rows and columns of tube where operating conditions are specified. The operating conditions are the air and refrigerant flow rates

and air inlet and exit temperatures and humidity. The performance-based analysis is the one in which the coil surface area is known so that the final air exit states can be determined for various operating conditions. The performance-based analysis can be carried out by one of the following methods: the dry coil/wet coil analysis which is based on NTU-effectiveness method, the enthalpy-based effectiveness [61], the total enthalpy method [64, 65] or the fin efficiency weighing method [7]. Details of all the various approaches of analyzing evaporators is beyond the scope of this study and only the enthalpy effectiveness approach [61] will be discussed further.

The flow rates and inlet temperatures of air and refrigerant, pressures and coil geometry information are required when applying the enthalpy-based effectiveness method of evaporator analysis. The heat transfer rate at the evaporator is the rate at which heat is removed from the space by the cooling system [66]. The heat transfer rate is already given as Eq. (3.1). The rate of condensate extraction can be computed once the evaporator exit air humidity ratio is determined. The evaporator thermal capacity is a function of its geometrical dimensions. Evaporator geometric information can be used to calculate various thermal resistances which affect the total coil conductance. The coil conductance can be written as [61]:

$$UA = \left[\frac{f''}{\pi D_{in}L_t} + \frac{\ln\left(D_o/D_i\right)}{2\pi k_m L_t} + \frac{1}{\pi D_{in}L_t \tilde{h}_r} + \left(\frac{C_{p,a}}{C_{p,a,sat}}\right)\frac{1}{\tilde{h}_a A_{tot}\eta_o} \right]^{-1} \quad (3.13)$$

In order to calculate the coil conductance, it is necessary to determine the convective heat transfer coefficients on the refrigerant and air sides, ($\tilde{h}_r$ and $\tilde{h}_a$). Different correlations are available in literature for determining the convective heat transfer coefficients. Some of

the correlations are built-in in EES software and they can be accessed easily. The software implements Shah's correlations for obtaining $\tilde{h}_r$, while Kays and London's procedure for finned circular tube heat exchanger is implemented for the air-side heat transfer coefficient $\tilde{h}_a$ [67, 68].

The outer surface efficiency is related to the fin efficiency and the heat exchanger geometry given as:

$$\eta_o = 1 - \frac{A_{sf}}{A_{tot}}(1 - \eta_f) \qquad (3.14)$$

and $C_{p,a,sat}$ is the saturation specific heat capacity of the humid air defined as:

$$C_{p,a,sat} = \left(\frac{\partial h}{\partial T}\right)_{P,\emptyset=1} \approx \frac{h_{a,e,i}(T_{a,ev,i}, P_a, \emptyset=1) - h_{a,ev,e}(T_{a,ev,e}, P_a, \emptyset=1)}{(T_{a,ev,i} - T_{a,ev,,e})} \qquad (3.15)$$

The ratio of saturation specific heat capacity of the humid air to the normal specific heat capacity, $(C_{p,a,sat}/C_{p,a})$ given in Eq. (3.13) which is always greater than unity, represents the effect of mass transfer as an augmentation to convective heat transfer coefficient on the air side. The evaporator exit air temperature $T_{a,ev,e}$, is required in solving Eq. (3.15). Therefore, the solution starts with an initial guess value for $T_{a,ev,e}$ after which the value is updated as the calculation proceeds.

The number of transfer unit, *NTU* can be determined from the coil conductance. Knowing the *NTU*, the effectiveness of the coil can be computed using the **ε**-*NTU* solution for cross-flow heat exchanger from which the actual exit air properties can be determined using enthalpy-effectiveness relation given as Eq. (3.10). Finally, the rate of condensate extraction can be calculated from the mass balance across the cooling coil as given in Eq. (3.11).

3.3 Performance Study of the Modified VCAC System

The equations for analyzing the performance of conventional VCAC system and evaluating the rate of condensate extraction from the evaporator coil have been presented in section 3.2. Equations used in evaluating the performance of the modified system by considering the three different performance improvement options of the VCAC system are presented in this section.

3.3.1 Option 'A': Evaporator Inlet Air Precooling

The purpose of precooling the air stream before entering the evaporator is to increase the system performance and reduce power consumption. In order to achieve the precooling, a precooler is placed across the air path, allowing heat transfer between the air and the cold fluid as shown in Fig 3.4. The cold fluid in this case is the condensate that is generated by the VCAC system. The air is precooled sensibly as it passes through the precooler by circulating the collected condensate. The air then enters the evaporator where it is further cooled and dehumidified. The information presented here together with that in section 3.2 are used in the analytical study and some of the equations are used in analyzing the experimental data for this option.

The heat transfer rate on the condensate side of the precooler is written as:

$$\dot{Q}_{pc,ev} = \dot{m}_w C_{p,w}\left(T_{w,e} - T_{w,i}\right) \tag{3.16}$$

It is assumed that no heat loss or gain on the water pipelines. The heat transfer rate on the air side of the precooler is given as:

$$\dot{Q}_{pc,ev} = \dot{m}_{a,pc} C_{p,a}\left(T_{a,i} - T_{a,e}\right) \tag{3.17}$$
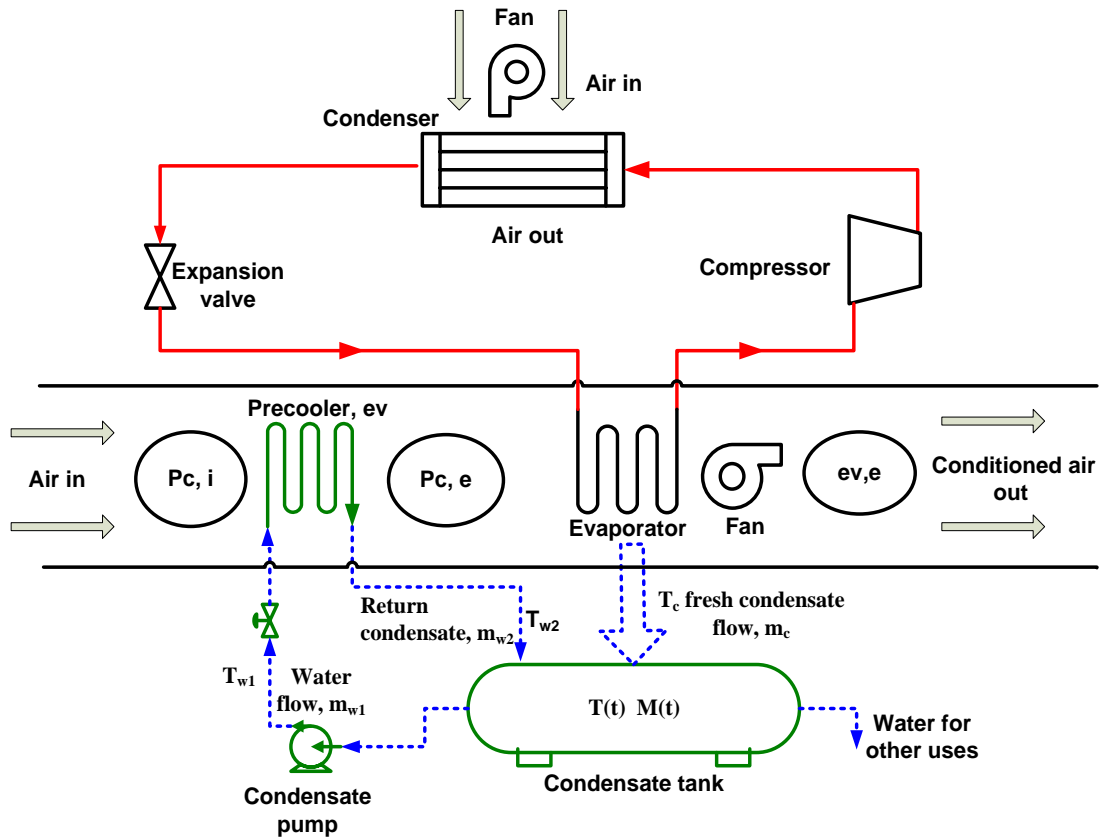
Figure 3.4 Schematic of the modified system integrated with air precooler - Option 'A'.

and the heat transfer rate in the precooler between the two fluids as:

$$\dot{Q}_{pc,ev} = \varepsilon_{pc}\dot{C}_{min,pc}(T_{a,i} - T_{w,i}) \tag{3.18}$$

3.3.2 Option 'B': Condenser Inlet Air Precooling

The purpose of precooling the air stream before entering the condenser is to improve the rate of heat rejection from the hot refrigerant to the surrounding, thus increasing the COP of the system and reducing the compressor power consumption. Schematic of the VCAC system integrated with condenser air precooler is shown in Fig. 3.5. The information presented here together with that in section 3.2 are used in analyzing the experimental data for this option.

The rate of heat transfer in the precooler at the condensate side is given as:

$$\dot{Q}_{pc,c} = \dot{m}_w C_{p,w}(T_{w,e} - T_{w,i}) \tag{3.19}$$

and at the air side as:

$$\dot{Q}_{pc,c} = \dot{m}_{a,c} C_{p,a}(T_{a,i} - T_{a,e}) \tag{3.20}$$

The heat transfer rate between the two fluids is also written as:

$$\dot{Q}_{pc,c} = \varepsilon_{pc,c}\dot{C}_{min,pc,c}(T_{a,i} - T_{w,i}) \tag{3.21}$$

3.3.3   Option 'C': Refrigerant Subcooling Downstream of the Condenser

The conventional VCAC system presented in the previous section is also integrated with subcooler to lower the temperature of the refrigerant exiting the condenser using condensate. Schematic of the system with subcooler and the corresponding P-h diagrams are shown in Fig. 3.6 and 3.7 respectively.
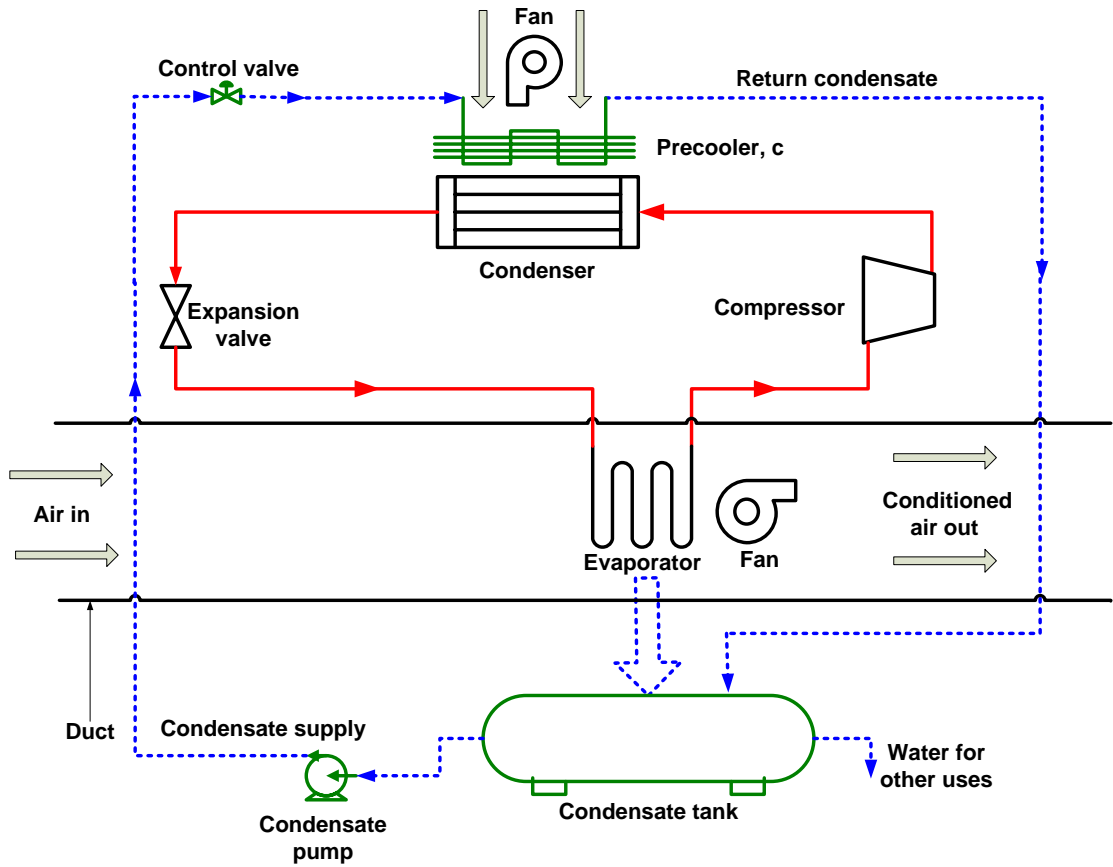
Figure 3.5 Schematic of the modified system integrated with condenser air precooler - Option 'B'.
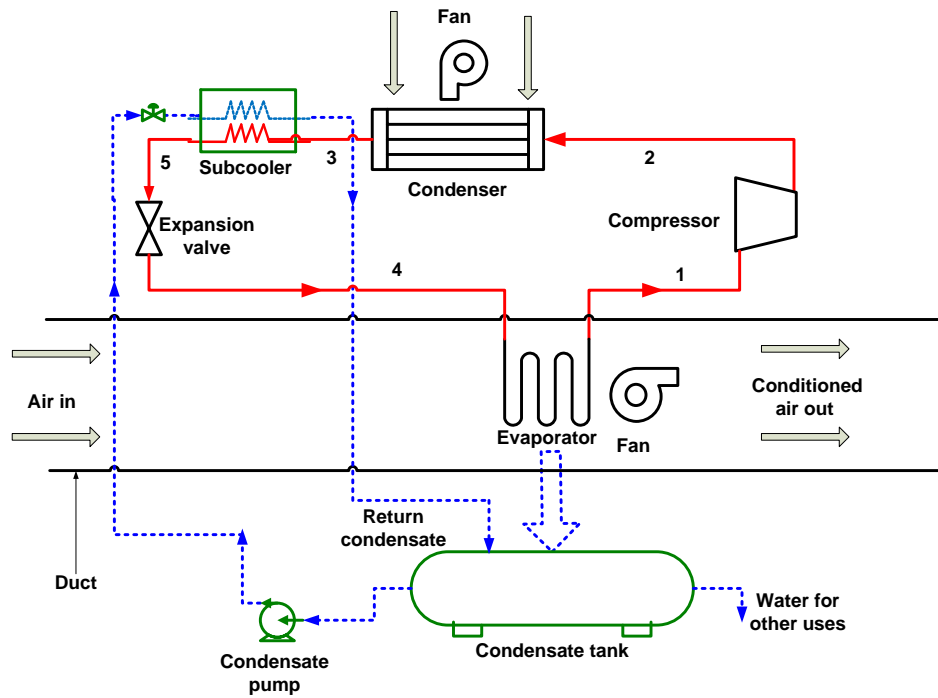
Figure 3.6 Schematic of the modified system integrated with subcooler - Option 'C'.
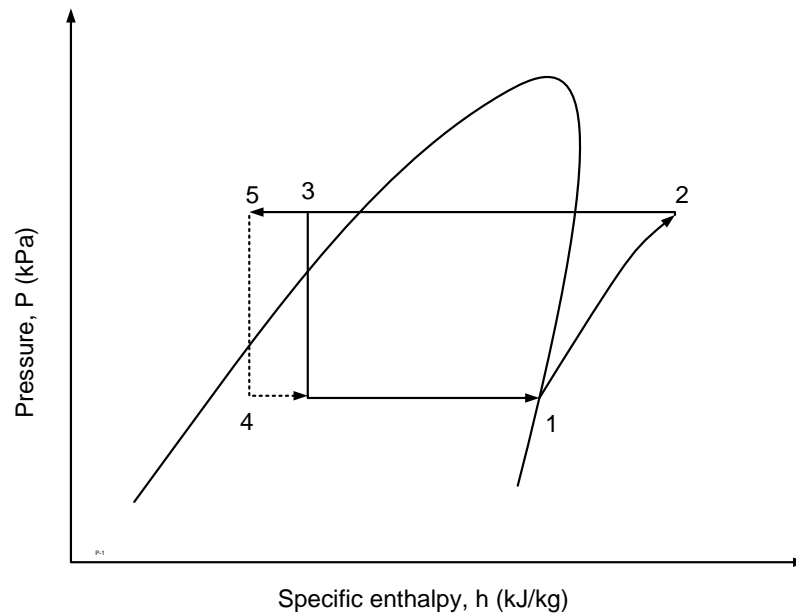
Figure 3.7 Pressure-enthalpy diagram of the modified system - Option 'C'.

The detailed heat transfer equations of the four components of simple VCAC system are given in section 3.2 and the heat transfer equations across the subcooler are added here for the analysis of the modified system with option 'C'. The rate of heat transfer between the refrigerant flowing through the subcooler and the condensate is given as:

$$\dot{Q}_{sc} = \dot{m}_r C_{p,sc} \varepsilon_{sc} (T_3 - T_{w,i}) = \dot{m}_r (h_3 - h_5) \tag{3.22}$$

The rate of heat transfer in the subcooler from the water side can is written as:

$$\dot{Q}_{sc} = \dot{m}_w C_{p,w} \Delta T_w \tag{3.23}$$

3.3.4   Condensate Temperature Change During Air Precooling: Analytical Study

After precooling the air in the precoolers or subcooling the refrigerant, the condensate is circulated back to the condensate tank. The condensate temperature in the tank may rise to an extent that it may no longer provide the required precooling or subcooling. It is therefore imperative to estimate the condensate temperature rise in the tank for a particular period of operation. Equations governing the accumulation of condensate and changes in condensate temperature within the tank are obtained by applying mass and energy balance. Note that this procedure is used in the analytical study only because the condensate temperature in the tank is measured directly during the experiment. The following assumptions are used in the formulation of the mathematical equation governing the change in condensate temperature in the storage tank.

1. The volume of the tank remains fixed relative to the coordinate frame.
2. The tank is well insulated so that heat gain from surrounding to the condensate is neglected.

3. The state of mass of condensate within the tank may change with time, and at any instant of time, the state is assumed uniform throughout the entire volume.

4. Specific heat capacity of condensate is constant.

5. The mass flow rates of condensate leaving and entering the tank are equal.

Schematic of the control volume of condensate tank is shown in Fig. 3.8. At the beginning of the precooling operation, the tank is initially filled with cold condensate of mass M_i and at a temperature, T_i which is collected earlier from the air conditioning system.

The parameters $M(t)$ and $T(t)$ represent the mass and the temperature of condensate in the tank at any time.

The mass balance for the condensate tank can be written as:

$$\frac{dM}{dt} = \dot{m}_c \tag{3.24}$$

where $\dot{m}_c$ is the mass flow rate of fresh condensate from the evaporator coil.

By integrating the above equation, the expression for mass of condensate accumulated in the tank at any given time is obtained as:

$$M = \dot{m}_c t + M_i \tag{3.25}$$

The energy balance on the condensate tank provides:

$$c_p \frac{d(MT)}{dt} = \dot{m}_w c_p (T_{w2} - T_{w1}) - \dot{m}_c c_p T_c \tag{3.26}$$
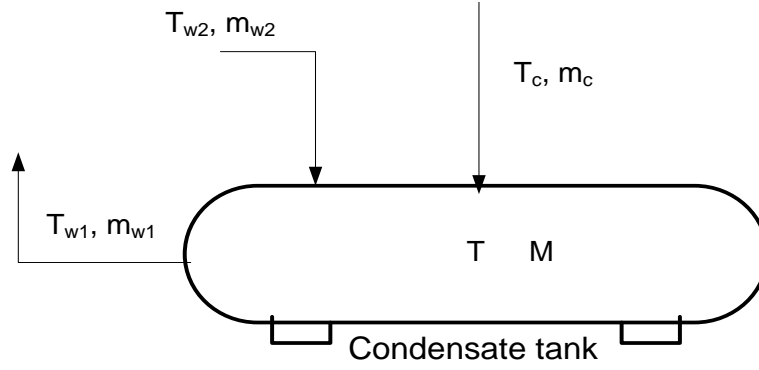
Figure 3.8 Control volume of condensate-storage tank.

Eq. (3.26) can be re-arranged as:

$$\frac{dT}{dt} + T\frac{dM}{dt} = \dot{m}_w(T_{w2} - T_{w1}) - \dot{m}_c T_c \tag{3.27}$$

Substituting Eq. (3.24) and (3.25) into Eq. (3.27) gives the rate of change of condensate temperature inside the tank which is a first-order linear differential equation.

$$\frac{dT}{dt} + \left(\frac{\dot{m}_c}{\dot{m}_c t + M_i}\right)T = \frac{\dot{m}_w(T_{w2} - T_{w1}) - \dot{m}_c T_c}{(\dot{m}_c t + M_i)} \tag{3.28}$$

Applying the initial conditions, initial condensate temperature in the tank $T = T_i$ at time $t = 0$, the condensate temperature in the tank as a function of time is found:

$$T(t) = \frac{[\dot{m}_w(T_{w2} - T_{w1}) - \dot{m}_c T_c]t}{\dot{m}_c t + M_i} + \frac{T_i M_i}{\dot{m}_c t + M_i} \tag{3.29}$$

The instantaneous condensate temperature in the tank when the system is subjected to precooling during the day time can be calculated using Eq. (3.29). During the night time, the condensate temperature in the tank at any time can be determined by considering $\dot{m}_w$ to be zero in Eq. (3.29).

39

CHAPTER 4

CLIMATE DATA

4.1.   Overview of the Kingdom of Saudi Arabia

The Kingdom of Saudi Arabia is the world's largest oil producing country and holds about 25% of the world's crude oil reserves. The kingdom's 2011 population is estimated to be about 26 million and the annual population growth rate as of 2011 is 1.5%. The rapid growth in population created higher demand of energy in the Kingdom. As mentioned in the literature survey, considerable amount of electrical energy is consumed by air conditioning systems due to severe weather conditions. The weather conditions in Saudi Arabia are drastically changing from one region to another.

Riyadh is the largest city with a population of about 5.2 million, lies in the central region and is the capital of the Kingdom and is characterized as hot and dry due to extreme temperature and low humidity in summer. Jeddah is the second largest city with a population of about 3.4 million. Jeddah is located on the Tihamah coastal plain in the western region. It is characterized with a high humidity most of the year, very hot in the summer and cooler in the winter. Western Saudi Arabia is dominated by the mountain chain running the entire length of the country parallel to the Red Sea. These western mountains induce convective cloudiness by causing the moist air to rise which resulted in greater rainfall. Rain usually falls in small amount in December. Dammam city lies in

eastern region on the Arabian Gulf coast with a population of about 0.9 million. Dhahran is closer to Dammam and the distance between them is about 20 km. The weather conditions of Dhahran and Jeddah are similar.

Jazan lies in the southwest corner of Saudi Arabia and is situated on the coast of the Red Sea and serves a large agricultural heartland that has a population of 1.5 million. Asir is a province located also in the southwest of the country, with an area of about 81,000 km² and an estimated population of 1,563,000, its capital is Abha. The southwest region experiences high humidity but not as hot as the western and eastern regions. Actual climate data is used in this study with emphases on Dhahran climate.

4.2. Dhahran Climate Data

The use of condensate to improve the performance of air conditioning systems can only be applicable to areas where high relative humidity and temperature prevails. In this thesis, the study of the climate data is restricted only to Dhahran area where the experimental work is carried out.

Dhahran, Saudi Arabia is located at 26.3^o N, 50.2^o E. Dhahran's climate is characterized by extremely hot, humid summers, and cool winters. Temperatures can rise up to about 50 °C in the summer, coupled with extreme humidity, 70-100%. In winter, the temperature rarely falls below 3 °C with rain falling mostly between the months of November and May.

The climate data used in this study is obtained from Jeddah Regional Climate Center (JRCC) under the patronage of the Presidency of Meteorology and Environment (PME). The data is presented on the basis of hourly average, daily average and monthly average.

The recorded hourly weather data is used in the study in estimating the rate of condensate extraction and served as a guide in the performance study of the VCAC system. Due to the bulkiness of the climate data, only that of monthly average and few hourly data of some selected days are presented.

Monthly maximum and mean temperatures of the years 2009 to 2012 are compared in Figs. 4.1 and 4.2, respectively. It can be observed that there is slight variation in the annual temperatures of the area. Maximum temperature during the summer months of March to November ranges from 30 to 48 ^{o}C. Peak values of temperature are found in the months of June, July and August while the mean temperatures are in the range of 25 to 38 ^{o}C. Similarly, the maximum relative humidity for the whole year ranges from 75 to 100 % while the mean values ranges from 30 to nearly 70 % as shown in Figs. 4.3 and 4.4. The high mean relative humidity of the ambient air that prevails for long period indicates that appreciable amount of condensate can be captured from the cooling devices. The climate date is also presented in Table 4.1.

In order to have a closer view in to the climatic conditions, hourly climate data of typical summer days of Dhahran is presented in Figs. 4.5 - 4.26 and Table 4.2. The climate data presented is of the average day of each month [69]. These figures indicate that there is an inverse trend between the ambient air temperature and relative humidity. The humidity increases when the air temperature decreases and vice-versa. During the midnight, down to early morning hours, the relative humidity is high, which then decreases during the day hours. This is a clear indication that more condensate will be extracted during night hours.
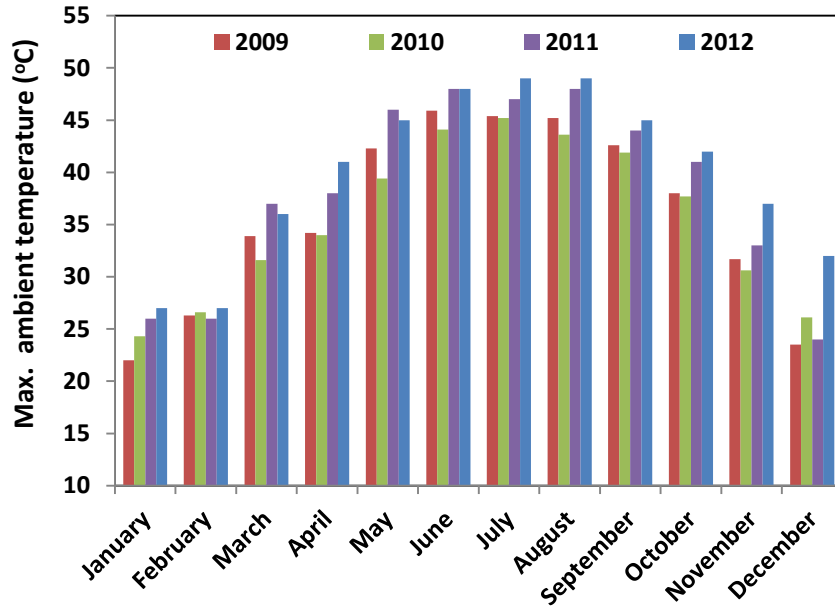
Figure 4.1 Comparison of monthly maximum temperature of the years 2009 to 2012 in Dhahran.
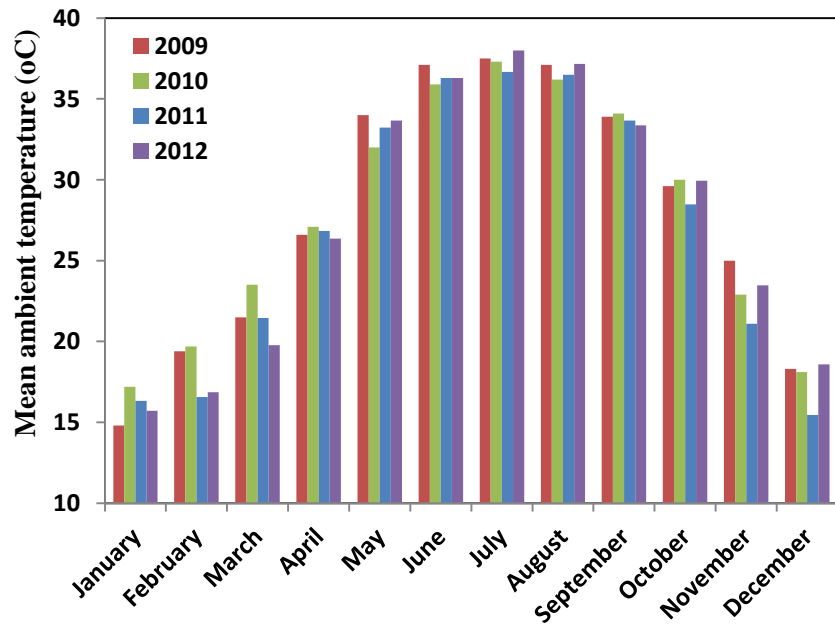
Figure 4.2 Comparison of monthly mean temperature of the years 2009 to 2012 in Dhahran.
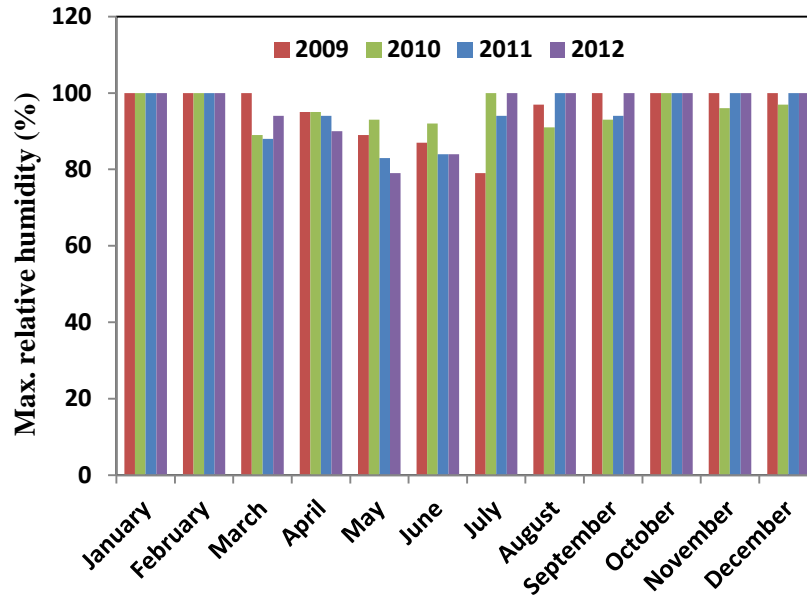
Figure 4.3 Comparison of monthly maximum relative humidity of the years 2009 to 2012 in Dhahran.
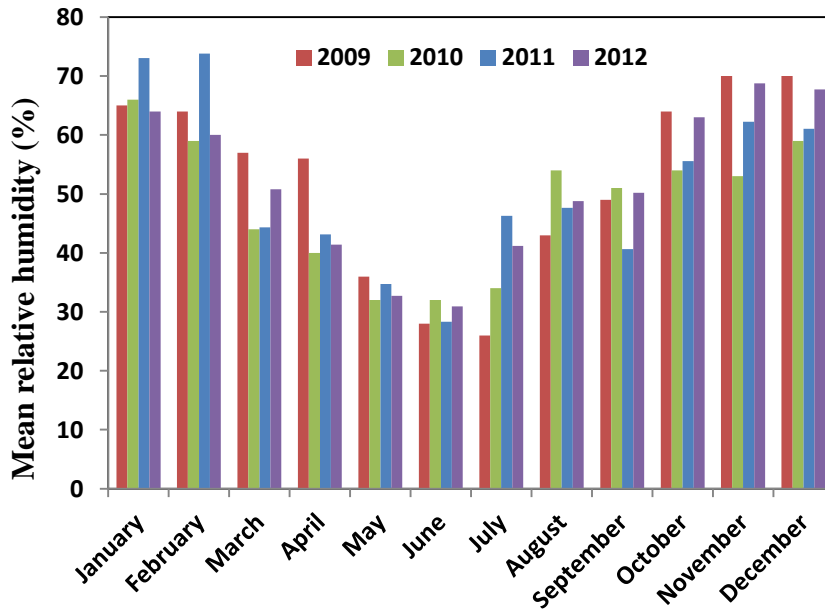
Figure 4.4 Comparison of monthly mean relative humidity of the years 2009 to 2012 in Dhahran.

Table 4.1 Summary of Dhahran maximum and minimum temperature and relative humidity: 2009 – 2012.

	T_max (°C)				T_mean (°C)			
Month	2009	2010	2011	2012	2009	2010	2011	2012
January	22	24.3	26	27	14.8	17.2	16.3	15.7
February	26.3	26.6	26	27	19.4	19.7	16.6	16.9
March	33.9	31.6	37	36	21.5	23.5	21.5	19.8
April	34.2	34	38	41	26.6	27.1	26.8	26.4
May	42.3	39.4	46	45	34	32	33.2	33.7
June	45.9	44.1	48	48	37.1	35.9	36.3	36.3
July	45.4	45.2	47	49	37.5	37.3	36.7	38.0
August	45.2	43.6	48	49	37.1	36.2	36.5	37.2
September	42.6	41.9	44	45	33.9	34.1	33.7	33.4
October	38	37.7	41	42	29.6	30	28.5	29.9
November	31.7	30.6	33	37	25	22.9	21.1	23.5
December	23.5	26.1	24	32	18.3	18.1	15.5	18.6

	Φ_max (%)				Φ_mean (%)			
Month	2009	2010	2011	2012	2009	2010	2011	2012
January	100	100	100	100	65	66	73.0	64.0
February	100	100	100	100	64	59	73.8	60.0
March	100	89	88	94	57	44	44.3	50.8
April	95	95	94	90	56	40	43.1	41.4
May	89	93	83	79	36	32	34.7	32.7
June	87	92	84	84	28	32	28.3	30.9
July	79	100	94	100	26	34	46.3	41.2
August	97	91	100	100	43	54	47.6	48.8
September	100	93	94	100	49	51	40.6	50.2
October	100	100	100	100	64	54	55.5	63.0
November	100	96	100	100	70	53	62.2	68.8
December	100	97	100	100	70	59	61.0	67.7
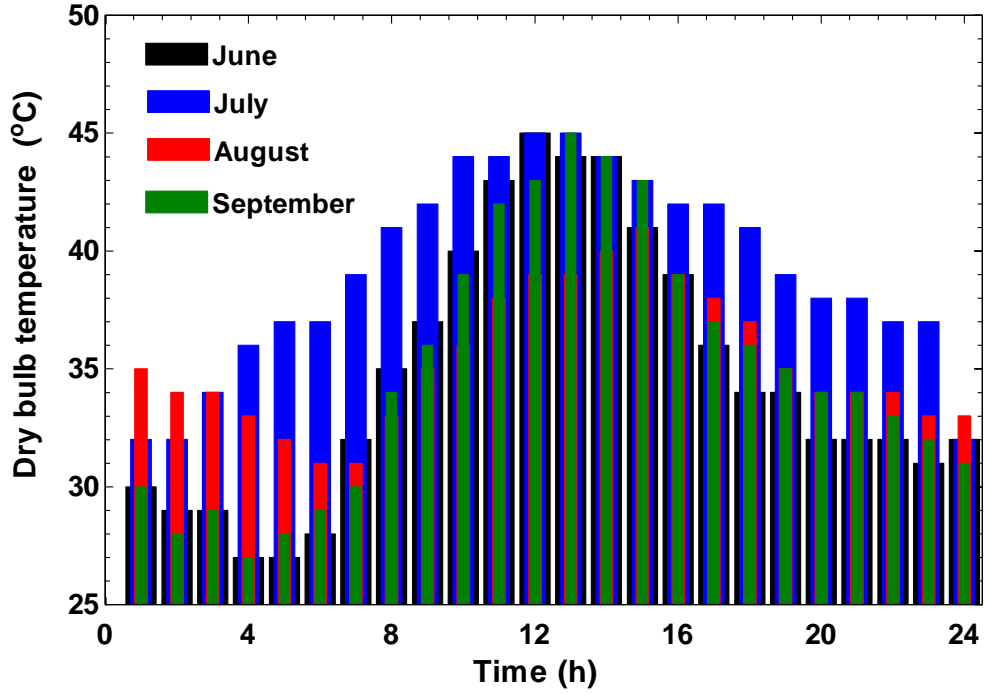
Figure 4.5 Variations of Ambient dry bulb temperature of typical days in June through September, Dhahran.
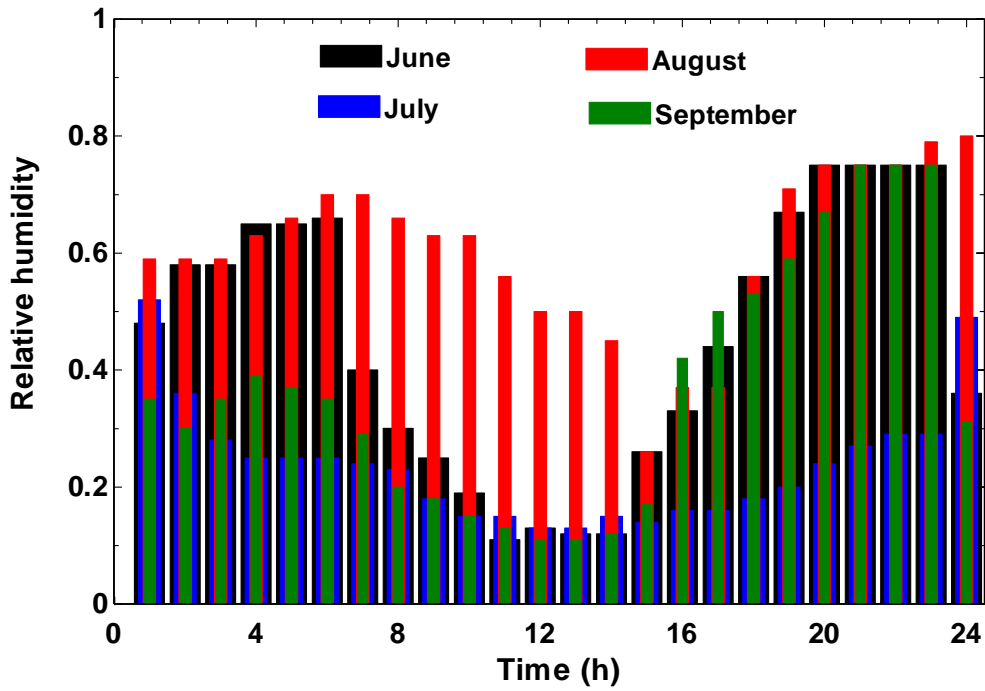
Figure 4.6 Variations of Ambient relative humidity of typical days in June through September, Dhahran.

Table 4.2 Hourly variations of ambient temperature and relative humidity of typical days in June through September, Dhahran.

Time	June		July		August		September	
	T (^{o}C)	ϕ	T (^{o}C)	ϕ	T (^{o}C)	ϕ	T (^{o}C)	ϕ
1:00 AM	30	0.48	32	0.52	35	0.59	30	0.35
2:00 AM	29	0.58	32	0.36	34	0.59	28	0.3
3:00 AM	29	0.58	34	0.28	34	0.59	29	0.35
4:00 AM	27	0.65	36	0.25	33	0.63	27	0.39
5:00 AM	27	0.65	37	0.25	32	0.66	28	0.37
6:00 AM	28	0.66	37	0.25	31	0.7	29	0.35
7:00 AM	32	0.4	39	0.24	31	0.7	30	0.29
8:00 AM	35	0.3	41	0.23	33	0.66	34	0.2
9:00 AM	37	0.25	42	0.18	35	0.63	36	0.18
10:00 AM	40	0.19	44	0.15	36	0.63	39	0.15
11:00 AM	43	0.11	44	0.15	38	0.56	42	0.13
Noon	45	0.13	45	0.13	39	0.5	43	0.11
1:00 PM	44	0.12	45	0.13	39	0.5	45	0.11
2:00 PM	44	0.12	44	0.15	40	0.45	44	0.12
3:00 PM	41	0.26	43	0.14	41	0.26	43	0.17
4:00 PM	39	0.33	42	0.16	39	0.37	39	0.42
5:00 PM	36	0.44	42	0.16	38	0.37	37	0.5
6:00 PM	34	0.56	41	0.18	37	0.56	36	0.53
7:00 PM	34	0.67	39	0.2	35	0.71	35	0.59
8:00 PM	32	0.75	38	0.24	34	0.75	34	0.67
9:00 PM	32	0.75	38	0.27	34	0.75	34	0.75
10:00 PM	32	0.75	37	0.29	34	0.75	33	0.75
11:00 PM	31	0.75	37	0.29	33	0.79	32	0.75
12:00 AM	32	0.76	32	0.49	33	0.8	31	0.75

4.3. Air Conditioners Usage in Saudi Arabia

Saudi air conditioning market is the biggest market in the Middle East and North Africa regions. A recently published report by TechSci Research [70] reported that air conditioners market in Saudi Arabia is expected to grow at the annual rate of 8.7% during the period from 2012 to 2017. Saudi Arabia remains a very promising market for air-conditioning products, due to its hot climate, high per capita income and rapid population growth and it is expected that Saudi air conditioners market will reach about SR 7.5 billion revenues by 2017. The domestic production of air conditioners has gradually increased in the Kingdom due to the high demand of air conditioners. It is estimated that due to increasing demand of split air conditioners the market share of window air conditioners is expected to witness almost 10% drop in next five years. It is interesting to note that the present study is highly suitable for split air conditioners.

Air-conditioning products are considered a necessity and are installed in almost all buildings throughout the country. It is to be noted that the central region, Riyadh has the largest sales, accounting for about 35%, followed by the western region, around Jeddah which accounts for around 25%. A further 15% of sales are in the east of the country, Dammam, with the other 25% shared between all other regions.

Conventional VCAC systems are popular in the Kingdom and absorption chillers are not popular due to their high price. Currently all packaged products sold in Saudi Arabia are fitted with the refrigerant R-22 and hence, in this thesis, R-22 is used.

CHAPTER 5

EXPERIMENTAL SET-UP

5.1. The Experimentation Room

The experimental phase begins with the experimentation room design and its construction. A site close to the entrance of heat engines lab, located in building 26, KFUPM is dedicated for the experiment. With the site selected, the general specifications of the room suitable for operating a 1.5 ton capacity air conditioner are set up. To ensure reliability and durability, joist of 50 mm x 100 mm s4s kiln dried wood is used as the structural frame of the room which is strong enough to serve the purpose. The joist is bolted on a steel frame with lag bolts and common nails with steel cleats and 18mm thick × 1.2 m × 2.4 m plywood is laid on top of the floor deck. A 50 mm x 100 mm s4s kiln dried wood vertical studs are used for the exterior and interior walls which are nailed to top and bottom wood runner. In order to minimize heat gain or loss through the walls, a 50 mm thick fiberglass is used in the interior walls; 18mm polyester laminated plywood is used in the exterior walls.

The roof frame is made from fabricated wood structures trusses 50 mm × 100 mm s4s kiln dried wood complete with bracing and purlins, a 50 mm thick fiberglass insulation one side with aluminum face vapor barrier fill the void of roof and a 0.35 mm pre-

finished corrugated ridge/side trims. Access door is tightly sealed against air and mixture leakages.

A climate chamber has been fabricated for generating various climate conditions ranging from 25 to 45°C temperature and 10 to 95% relative humidity and the schematic of the experimentation room with the climate chamber is shown in Fig 5.1. This chamber is able to generate actual climate conditions for estimating the amount of condensate that can be extracted from the system. The casing of the chamber is made up of Plexiglass of 10 mm thickness, 2.48 m length, 0.38 m width and 0.35 m height. A heater capacity of 6 kW connected to a temperature controller is placed at one end of the climate chamber. The heater is used to warm up the air that is forced in to the climate chamber by a blower in order to get the required air temperature at the exit of the chamber.

Three humidifying pads each of 10 cm thickness are placed inside the climate chamber next to the heater and are located 10 cm apart from each other. A tank of size 47 x 47 x 45 cm^3 is filled with water and connected to a pump which circulates the water through the humidifying pads to humidify the air until the required humidity is achieved. Humidification of the air can results in cooling the air evaporatively, which consequently will make it difficult to generate high temperatures (say 45°C) at the exit of the climate chamber. For this reason, four heaters each of 1 kW are installed inside the water tank for heating the water in order to avoid undesirable cooling of the air at this stage as a result of humidification and to have control of both temperature and humidity of the air at the same time. The air heater and the water heaters are connected to different temperature controllers using thermocouple. The temperature controllers are digital switch setting type, model: T4L-B3RK4C.
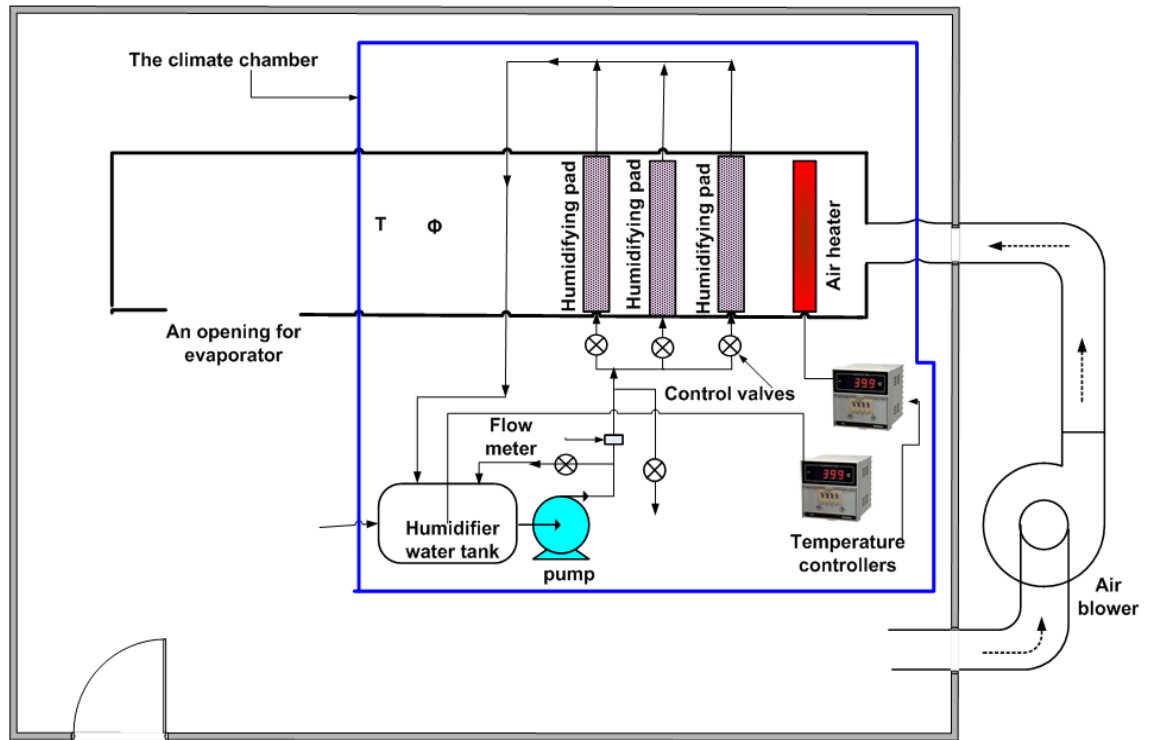
Figure 5.1 Schematic of the experimentation room with climate chamber inside.

One thermocouple is placed closed to the heater element and another inside the water. The temperature controllers are adjusted based on the required climate conditions to be generated in the chamber. Regulator valves are fitted along the water line for regulating the flow of water manually in order to get the required relative humidity. Photograph of the climate chamber is shown in Appendix A, Fig. A-1.

5.2.   The Base System

The base system is a stand-alone 1.5 ton split type VCAC system manufactured by Zamil, model: MWZ18CHIXFTQ &KZC18CSPHIQ without the additional heat exchangers. The specifications of the base system are listed in Table 5.1.

Table 5.1 Characteristics of the base air conditioning system.

Parameter	Value
Cooling capacity @ 27 ^{o}C DB/19 ^{o}C WB and 35 ^{o}C DB outdoor	4.747 kW
Power input	2.075 kW
Current input	9.7 Amps
EER	7.81
Refrigerant 22 charge	1.3 kg
Compressor type – Rotary	-
Evaporator face area	0.259 m^2
Volume flow rate of air at evaporator side, measured	0.135 m^3/s
Condenser face area	0.548 m^2
Volume flow rate of air at condenser side, measured	0.73 m^3/s

5.3.   Installation of Air Precooler for Option 'A'

A suitable heat exchanger or precooler is designed and installed on the base system to lower the air before entering the evaporator. The precooler is placed in the climate chamber after the humidifying pads and before the evaporator. Based on the present

application where the requirement is to lower the temperature of air entering the evaporator, the size of the precooler is 0.118 m^2 face area. The condensate temperature at the inlet and outlet of the precooler is recorded using thermocouples. The air temperatures and the relative humidity before and after the precooler are also recorded. Schematic of the experimental rig of this option is shown in Fig. 5.2. The upper part of the evaporator which is the air inlet is inserted inside the climate chamber at one end and the air that is at controlled temperature and relative humidity is directed to the evaporator which is serving as the load to the VCAC system. Photographs of the precooler and the experimental rig are shown in Appendix A, Figs. A-2 and A-3.

5.4.   Installation of Air Precooler for Option 'B'

The precooler of option 'B' is a finned-tube cross flow heat exchanger designed for precooling the air entering the condenser. The precooler consists of copper tube and aluminum fins and is having one column, twenty numbers of tube rows and face area of 0.79 m^2. The precooler is curved so that it covers the entire L-shaped condenser face. The gap between the condenser and precooler is covered at the top by an insulation material so that the air stream that may likely by-pass the precooler is prevented from escaping. Photographs of the precooler before and after installation are also shown in Appendix A. The two ends of the precooler tube are connected to the pipe in which condensate is circulating, entering from one side and exiting through the other side. The condensate temperatures at the inlet and exit of the precooler are measured as well as the air temperature before and after the precooler using thermocouples. Schematic of the experimental rig with option B is shown in Fig. 5.3 and the photographs of the precooler before and after installation are shown in Appendix A, Figs. A-4 to A-6.

53
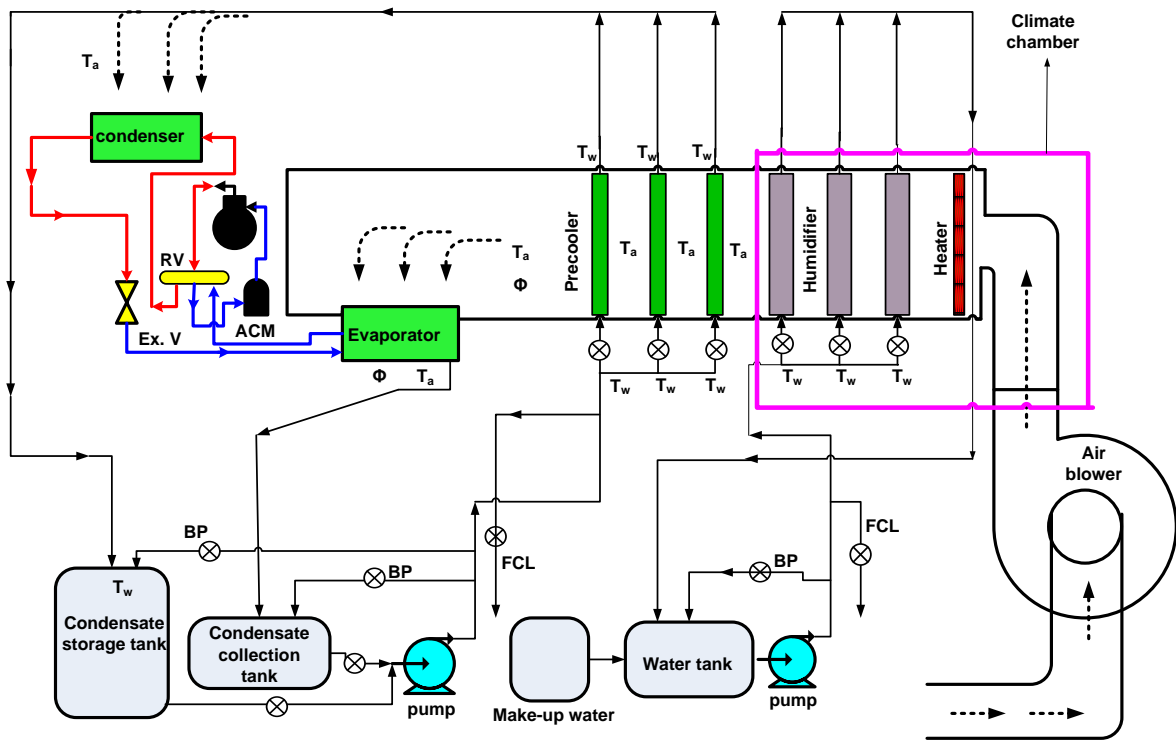
Figure 5.2 Schematic of experimental rig for option 'A'.
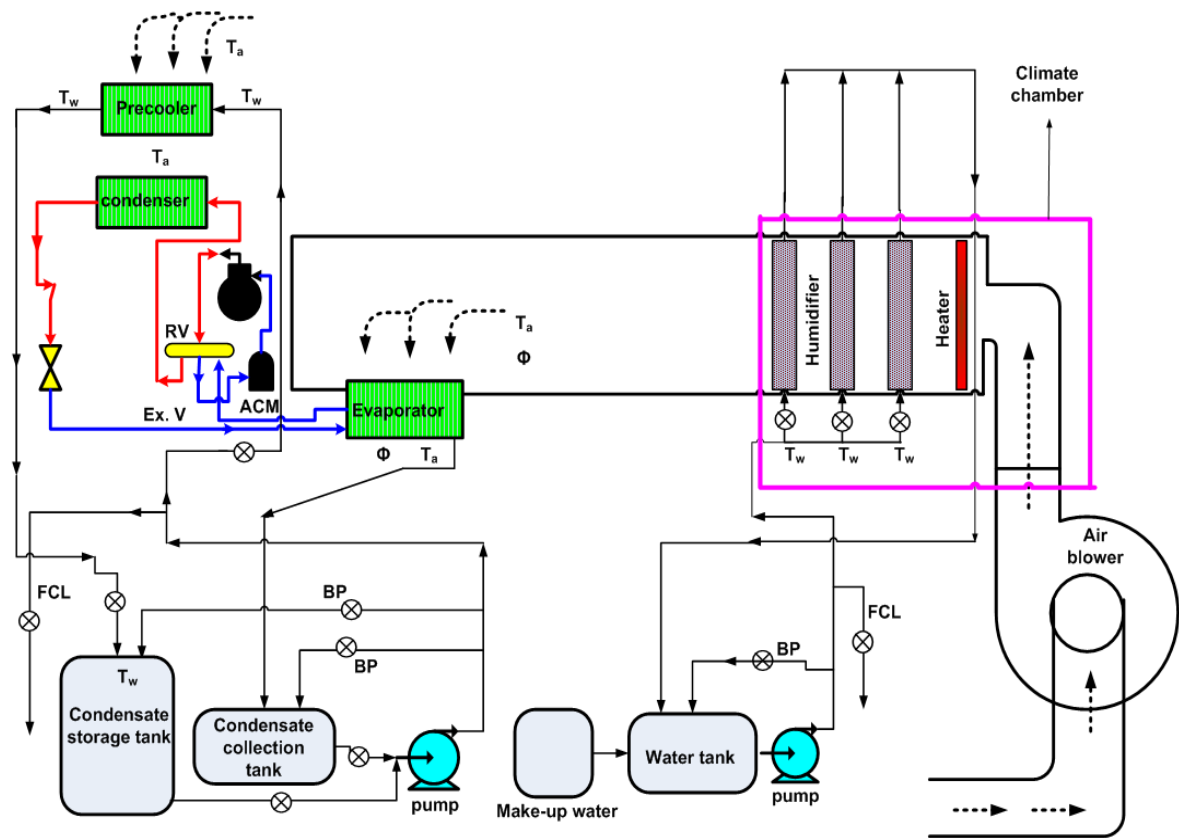
Figure 5.3 Schematic of experimental rig with option 'B'.

5.5. Installation of Refrigerant Subcooler for Option 'C'

The refrigerant subcooler used in the experiment is also finned-tube type heat exchanger having copper tube and aluminum fins. Schematic of the experimental rig with option 'C' is shown in Fig. 5.4. The face area of the heat exchanger is 0.0644 m^2 and consists of two columns and nine tube rows. This small size heat exchanger is designed so as to keep the pressure drop of the refrigerant minimum. The subcooler is enclosed inside a special casing of galvanized iron. The galvanized iron casing is made in such a way that it allows the passage of condensate across the subcooler while refrigerant is circulating through the subcooler tube. Photographs of the subcooler with casing before and after installation on the base air conditioning system are shown in Appendix A, Figs. A-7 to A-10.

5.6. The Complete Experimental Set-up and Instrumentation

The complete experimental set-up comprises the experimentation room, the base air conditioning system, the climate chamber and the additional heat exchangers for the three options.

The climate chamber which also contains the evaporator of the air conditioning unit is placed inside the room. An air blower located outside the experimentation room is ducted to the climate chamber in order to compensate the drop in air flow to the evaporator as a result of the precoolers and humidifying pads that are placed along the air path inside the chamber. The blower is used to supply air into the chamber.

Condensate dripping from the evaporator is collected directly using a small rectangular Plexiglass tray and is directed to a collection tank of 250 L capacity which is kept inside

56
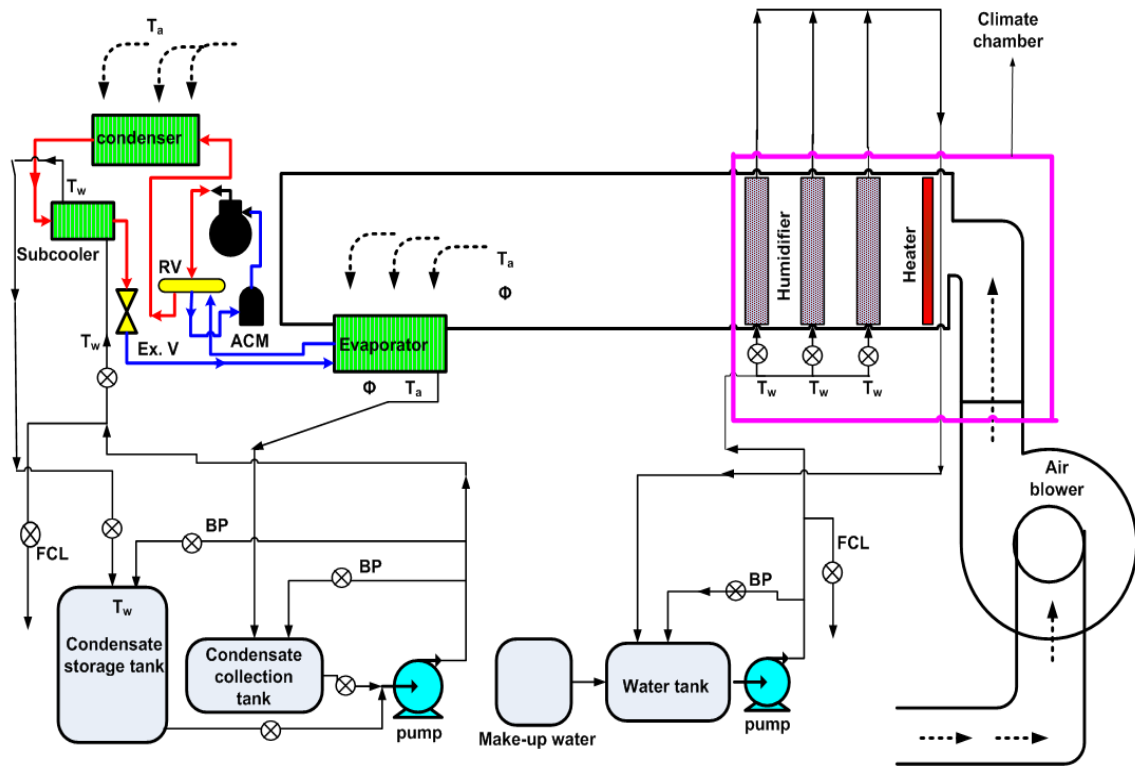
Figure 5.4 Schematic of experimental rig with option 'C'.

the room. The condensate-collection tank is connected to the condensate storage tank of 1000 L capacity located outside the room. The storage tank is connected to a centrifugal pump which delivers the condensate to the various additional heat exchangers.

The outdoor unit which comprises the condenser and compressor of the air conditioning system is also located outside the room. The precooler for option 'B' is installed just behind the condenser as seen before. The subcooler is installed after the condenser tube and before the expansion valve. Schematic of the complete experimental set-up is shown in Fig. 5.5. The mass flow rates of condensate circulating through the precoolers and subcooler are measured using special type flow transmitters of accuracy ±2 % full scale. The transmitter displays the measured flow rate digitally and transmits the flow signal to a computer at a time. The temperatures of air, condensate and refrigerant are measured using type-T thermocouples at the various locations shown in Figs. 5.5 and 5.6. Surface type thermocouples are used to measure the temperature of condensate and refrigerants at various locations. The thermocouples are placed over the surfaces of the pipes while isolated from the surrounding using insulation. The mass flow rate of air is measured indirectly by measuring the speed of the air using a hydro-thermo anemometer of accuracy ±2%.

The refrigerant pressures at locations indicated in Fig. 5.6 are measured using pressure transducers PX309 series, Omega each of accuracy 0.25%. The compressor power consumption is measured by the use of current transmitter; model number PM – H721LC with an accuracy of ±2 %. The relative humidity of the air is measured using relative humidity transmitters capable of measuring from 3 to 95%. The accuracy of the humidity
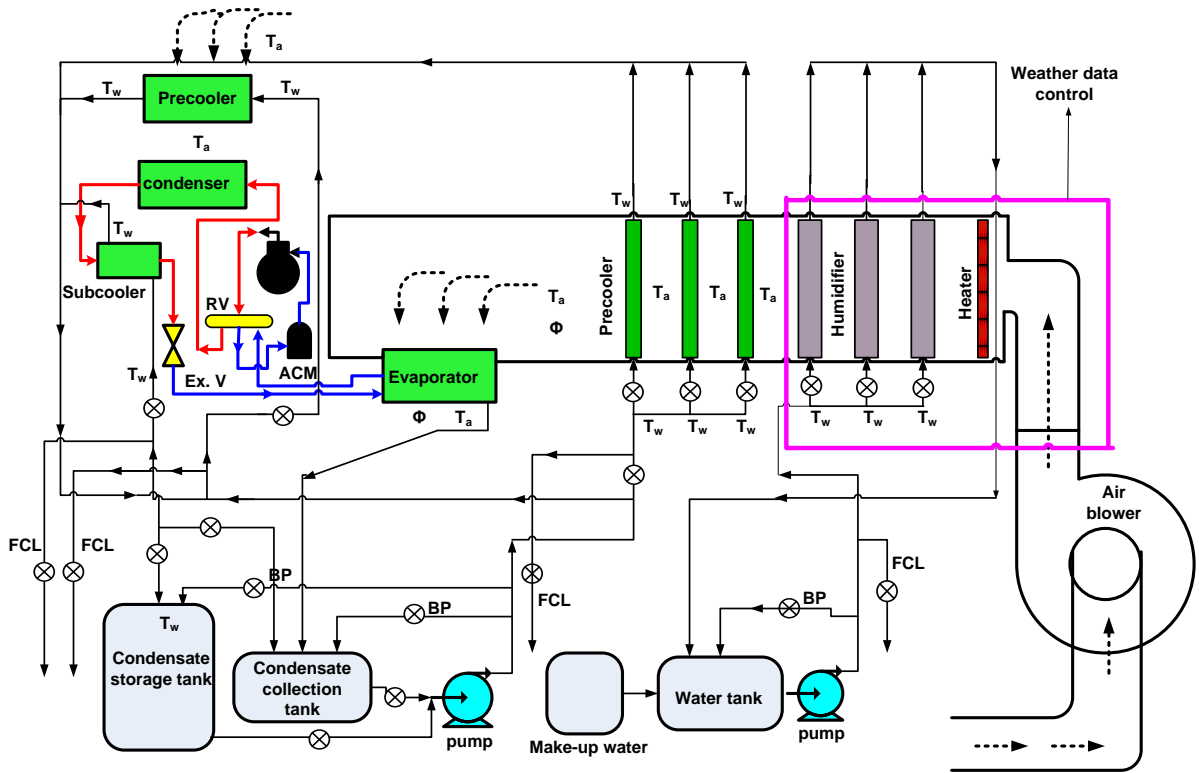
Figure 5.5 Schematic of the complete experimental set-up.

ACM - accumulator T_a - air temperature

BP - by-pass T_w - water temperature

FCL - flow calibration line   RV - reversing valve

Ex. V - expansion valve

transmitter is ±2.5 % for the range of 20 – 80% relative humidity and ±3.1% below 20% and above 80% relative humidity. All the sensors are connected to a central data acquisition (DAQ) system from National Instruments that collects, display and stores the various measurements in a data file.
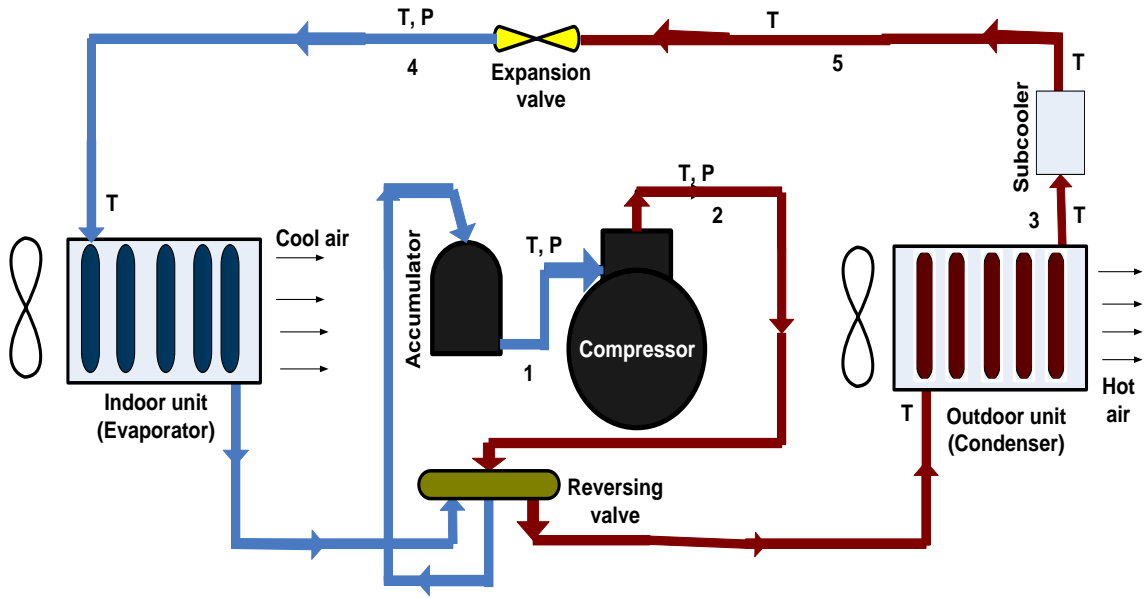
Figure 5.6 Schematic of the air conditioning system showing the temperature and pressure measurement locations.

CHAPTER 6

RESULTS AND DISCUSSIONS

This chapter presents the experimental results of the modified VCAC system for options 'A', 'B' and 'C'. Comparison of experimental and analytical results for option 'A' and condensate extraction from the air conditioning system are also discussed. The performance of the modified system and power consumption are compared with base system results. The base system results are the results obtained without the use of the three options. Engineering Equation Solver (EES) software is used in solving the various equations and obtaining thermo-physical properties of the fluid involved.

6.1.   Condensate Extraction from the Air Conditioning System

Extraction of condensate from the air conditioning system is strongly influenced by the climate conditions. The climate data of Dhahran, Saudi Arabia has been presented in chapter four and the data for several years show similar characteristics. The recorded climate data consists of temperature and relative humidity of the air which ranges between 27 - 47 $^{\circ}$C and the relative humidity reaching up to about 90 % and rarely to 100 % during the summer periods. In the this study, only the summer months of June, July, August and September are considered for condensate collection from the VCAC system experimentally and analytically using the hourly climate data. The hourly climate data is chosen in order to get the best estimate of condensate extraction rate because there are

limited cases in the literature where hourly climate data is used experimentally for the prediction or estimation of condensate production except for a few days. The hourly climate data is used in its original form in the analytical calculations while in the experimental aspect; the data is broken down into 32 sets for simplicity. The algorithms used in breaking the temperature and relative humidity are shown in Appendix B. Experiments are performed for the 32 sets of data to estimate the rate of condensate extraction from the base VCAC system. The corresponding rates of condensate extraction obtained for each group are shown in Table 6.1. The first two columns represent the 32 sets of temperature and relative humidity, respectively while the last column is the corresponding hourly extracted condensate. In these experiments, each data set is considered separate and the temperature and relative humidity of the air are generated in the climate chamber while the VCAC system is running. The temperature and humidity of the air in the climate chamber are measured using thermocouples and humidity sensors, respectively. The thermocouples and humidity sensors are connected to a data acquisition system which records and displays the data. Collection of condensate began by the use of stop watch after the temperature and humidity of the air in the climate chamber reached steady state. The volumetric flow rate of air through the evaporator is $0.135m^3/s$ which is also used in the analytical calculations.

After completing the experiments for the 32 groups, a computer code is written in Matlab which is used to pick the experimental condensate given in Table 6.1 and match it with the corresponding hourly climate data stored in excel sheets using the algorithms shown in Appendix B and the code is also presented in the same Appendix.

Table 6.1 The 32 sets of experimental data and the corresponding amount of condensate extracted from the VCAC system.

T (°C)	Φ (%)	Condensate extraction rate (kg/h)
25	40	1.1
25	50	1.4
25	60	2.0
25	70	2.8
25	80	3.16
25	90	3.48
30	20	0.6
30	30	0.8
30	40	1.6
30	50	2.5
30	60	2.8
30	70	3.2
30	80	3.9
30	90	4.4
30	95	5.7
35	20	0.8
35	30	1
35	40	2.2
35	50	2.68
35	60	3.48
35	70	4.24
35	80	5.1
35	90	5.4
40	10	0.36
40	20	0.9
40	30	1.52
40	40	2.4
40	50	3.42
40	60	3.7
45	10	0.4
45	20	0.9
45	40	3.3

These results represent the experimental condensate that can be extracted in Dhahran considering 100 % outdoor air goes to the evaporator. The program reads-in the hourly experimental condensate values and assigns each value to the appropriate temperature and humidity combinations that are arranged in two columns in excel sheets. The experimental condensate is obtained for each hour of the summer months; from June to September. The cumulative sum of the hourly values of the extracted condensate gives the corresponding amount of daily condensate while the cumulative daily condensate gives the corresponding monthly extracted condensate.

Analytical study is also carried out to estimate the rate of condensate extraction from the VCAC system using the model equations presented in chapter 3 without the precooling options and the results of condensate extracted are compared with the experimental results. The model equations presented in chapter 3 are coded in EES which relates the cooling capacity of the air conditioning system, flow rate of air and the thermo-physical properties of the fluid involved; namely air and R-22. The nominal cooling capacity of the base system given in Table 5.1 is used in the model as the initial guest value and the flow rates of air across the evaporator and the condenser given in the table are also used. The isentropic efficiency of the compressor is taken as 0.65 [33].

Analytical results given in Fig. 6.1 show the effect of relative humidity on the rate of condensate extraction using the climate data for the average day of the month of August. It is noted that the variation of condensate extraction followed the variation pattern of relative humidity. This means that the rate of condensate extraction mainly depends on the relative humidity. The effect of evaporator inlet air temperature on the rate of condensate
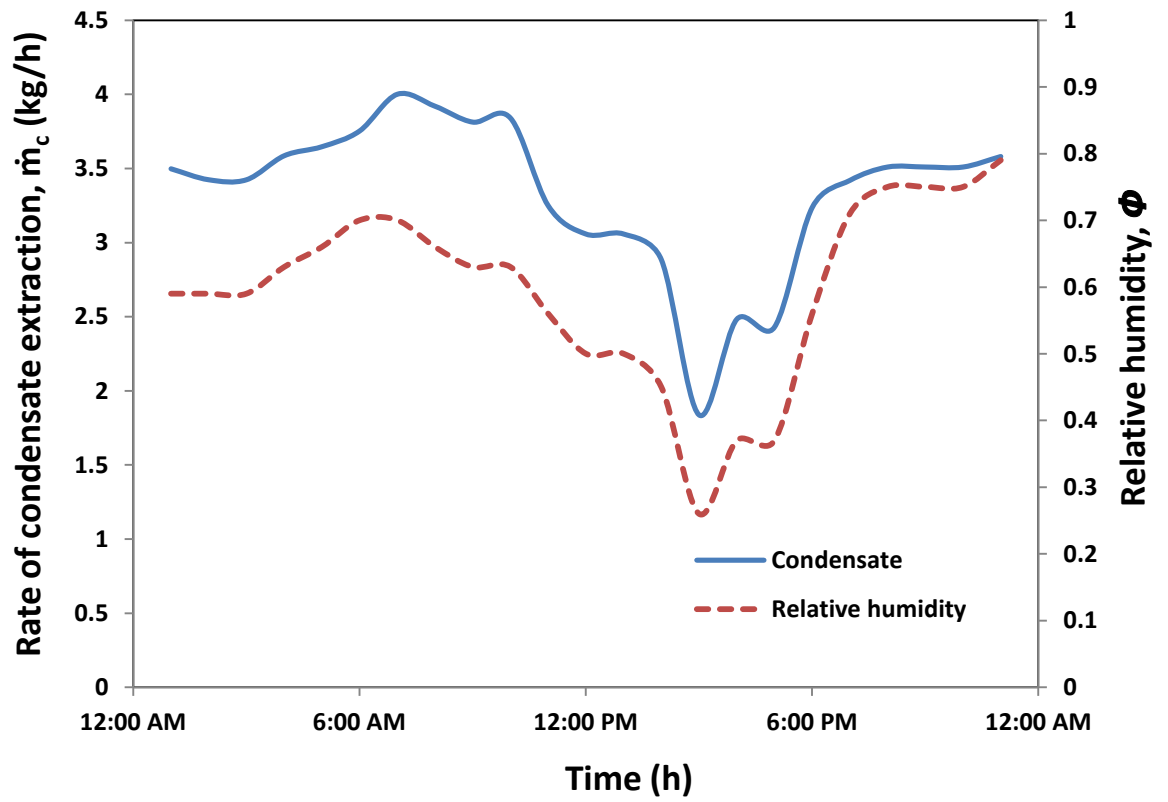
Figure 6.1 Hourly variations of condensate extraction rate and relative humidity for a typical day of August, Dhahran.

extraction as a function of relative humidity is shown in Fig 6.2 of the analytical results. It is clear that the rate of condensate extraction increases sharply with increase in the relative humidity due to higher water vapor content in the air. It is also observed that the rate of condensate extraction is higher at higher air temperatures.

Before presenting the monthly extracted condensate, hourly rate of condensate extraction of typical summer days are presented both experimental and analytical using the climate data given in Table 4.2. The sample results are summarized in Table 6.2. Observing the trend of the hourly climate data in Table 4.2 and the corresponding hourly condensate extraction rate, it can be concluded that the extracted condensate is high at higher humidity. Experimental and analytical daily condensate extraction in Dhahran for the months of June through September are summarized in Table 6.3 and presented in Figs. 6.3 – 6.6. It is observed that the comparison of analytical results is in good agreement with the experimental results. Monthly amounts of condensate extraction are obtained from the daily condensate and the results are also shown in Table 6.3. It is noted that the quantity of condensate is highest in August and this is as a result of high humidity in August compared to the other months.

6.1.1. Condensate Chemical Analysis

A sample of condensate is collected from the VCAC system under study when 100 % outdoor air is sent to the evaporator of the system. The sample is collected directly into sterilized bottles. Chemical analysis is then carried out on the collected sample at the Center for Environment and Water, Research Institute, KFUPM. The tests conducted on
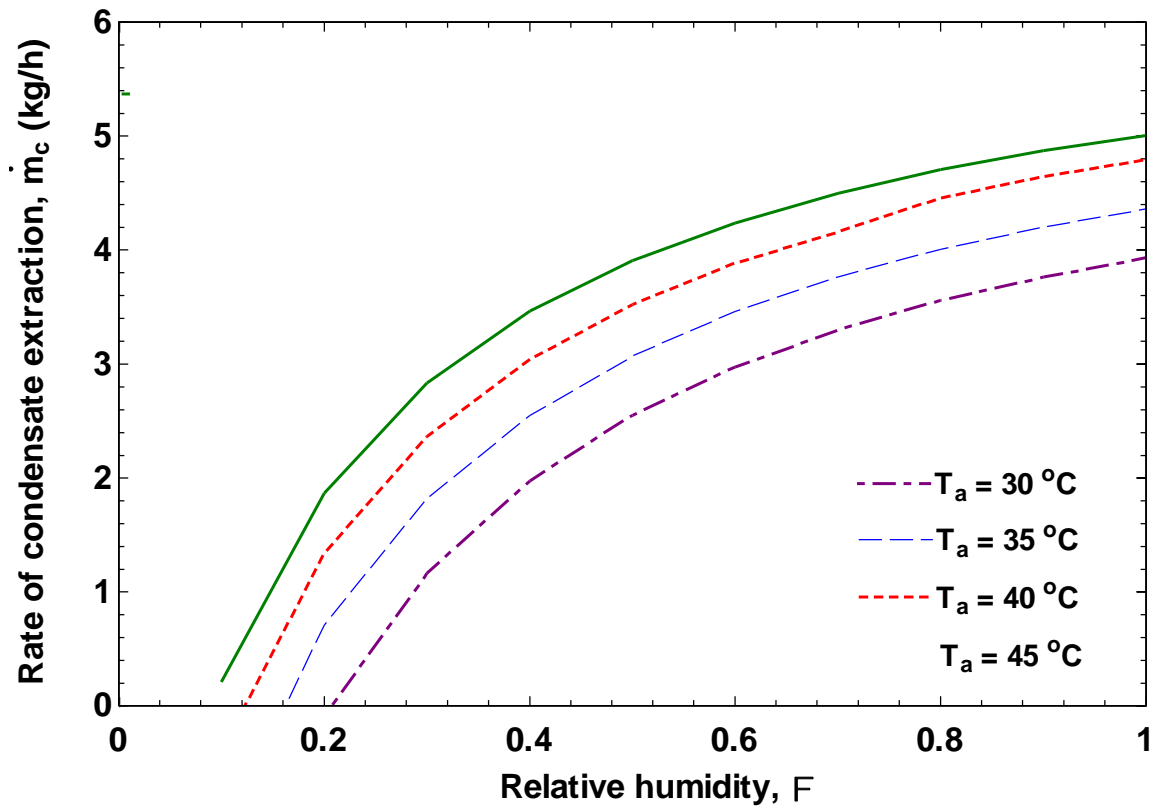
Figure 6.2 Variation of condensate extraction rate with relative humidity at different dry bulb temperatures.

Table 6.2 Comparison of condensate extraction rate for typical days in June through September, Dhahran.

Time	June Condensate (kg/h)		July Condensate (kg/h)		August Condensate (kg/h)		September Condensate (kg/h)	
	Experimental	Analytical	Experimental	Analytical	Experimental	Analytical	Experimental	Analytical
1:00 AM	2.5	2.5	2.5	2.7	3.5	3.5	1.6	1.6
2:00 AM	2.8	2.9	1.6	1.8	3.5	3.4	0.8	0.9
3:00 AM	2.8	2.9	1.0	1.3	3.5	3.4	1.6	1.6
4:00 AM	2.8	3.3	1.0	1.2	2.8	3.6	1.1	1.7
5:00 AM	2.8	3.3	1.0	1.3	3.2	3.6	1.6	1.6
6:00 AM	3.2	3.3	1.0	1.3	3.2	3.8	1.6	1.6
7:00 AM	1.6	2.3	0.9	1.4	3.2	4.0	0.8	1.1
8:00 AM	1.0	1.6	0.9	1.5	3.2	3.9	0.8	0.5
9:00 AM	1.0	1.3	0.9	1.0	3.5	3.8	0.8	0.5
10:00 AM	0.9	1.1	0.9	0.8	3.5	3.8	0.9	0.4
11:00 AM	0.4	0.2	0.9	0.8	3.7	3.1	0.4	0.4
Noon	0.4	0.7	0.4	0.5	3.3	3.0	0.4	0.2
1:00 PM	0.4	0.5	0.4	0.5	3.3	3.0	0.4	0.3
2:00 PM	0.4	0.5	0.9	0.7	3.3	2.9	0.4	0.4
3:00 PM	1.5	2.2	0.4	0.5	1.5	1.8	0.9	1.0
4:00 PM	1.5	2.5	0.9	0.7	2.4	2.4	2.4	2.6
5:00 PM	2.2	2.9	0.9	0.7	2.4	2.5	2.7	3.4
6:00 PM	3.5	3.3	0.9	1.2	3.5	3.3	2.7	3.6
7:00 PM	4.2	3.7	0.9	0.9	4.2	3.4	3.5	2.9
8:00 PM	3.9	3.8	0.9	1.2	5.1	3.6	4.2	3.1
9:00 PM	3.9	3.8	1.5	1.5	5.1	3.6	5.1	3.3
10:00 PM	3.9	3.8	1.0	1.5	5.1	3.6	3.9	3.7
11:00 PM	3.9	3.6	1.0	1.5	3.9	3.5	3.9	3.6
12:00 AM	3.9	3.9	2.5	2.7	3.9	3.5	0.8	1.4
Yield/day (kg)	55.5	59.8	25.2	29.5	83.7	80.1	43.2	41.3

Table 6.3 Experimental and analytical daily condensate extraction for the months of June through September.

Days	Condensate (kg/day)							
	June		July		August		September	
	Experimental	Aanalytical	Experimental	Aanalytical	Experimental	Aanalytical	Experimental	Aanalytical
1	15.6	8.5	15.0	15.0	86.9	79.4	71.6	70.1
2	24.9	22.2	13.4	11.5	85.0	76.0	74.9	73.7
3	66.4	69.8	17.0	19.5	76.2	70.8	45.0	50.4
4	64.8	67.3	31.9	33.6	63.3	64.9	63.7	62.5
5	43.5	51.4	46.0	49.8	59.4	59.0	56.0	62.0
6	45.1	50.0	14.7	14.7	58.3	63.4	61.8	67.7
7	16.7	14.7	22.1	31.4	31.7	33.0	83.2	81.2
8	18.8	18.9	50.8	54.2	31.8	41.9	54.0	60.0
9	13.8	6.5	86.4	77.1	70.5	68.1	53.9	55.4
10	14.8	13.8	64.8	71.7	69.2	70.6	60.7	65.8
11	55.5	56.6	66.9	67.5	62.3	70.1	36.9	42.5
12	64.6	68.7	63.5	73.8	62.0	66.7	31.9	37.2
13	35.4	38.3	58.7	57.5	58.3	61.7	56.1	63.9
14	50.8	58.4	52.7	56.1	64.0	71.6	40.1	49.0
15	34.7	39.4	51.0	60.5	63.2	71.1	43.2	41.0
16	56.3	56.5	37.3	50.4	83.7	80.1	51.5	56.7
17	60.1	62.7	25.2	33.2	85.6	85.4	54.1	62.3
18	65.4	68.4	24.5	33.3	71.0	71.9	60.2	67.8
19	47.2	55.5	26.9	32.2	77.7	70.3	67.5	69.3
20	44.0	48.5	18.2	14.5	64.8	68.2	79.0	80.9
21	27.0	29.9	35.5	38.1	81.7	89.9	71.2	73.7
22	16.2	15.3	53.5	55.8	87.9	84.4	73.0	75.8
23	13.6	9.4	24.8	28.7	80.2	81.9	66.4	70.6
24	13.0	5.4	15.7	19.7	70.5	70.8	61.2	75.1
25	19.8	26.2	24.6	32.7	74.9	72.3	69.2	77.2
26	24.2	32.5	20.3	30.9	85.4	76.0	76.4	79.5
27	19.9	25.0	19.5	28.6	84.2	80.6	60.0	63.2
28	25.7	30.5	21.4	29.6	99.1	82.9	40.8	45.5
29	19.8	25.9	40.4	52.7	79.7	72.9	52.2	63.3
30	18.5	28.1	65.8	70.5	55.2	56.8	65.7	76.4
31			72.6	70.5	49.2	53.7		
Daily Average Condensate	34.5	36.8	38.1	42.4	70.1	69.9	59.4	64.0
Monthly Condensate (kg)	1036.4	1104.5	1181.0	1315.4	2172.7	2166.2	1781.4	1919.6
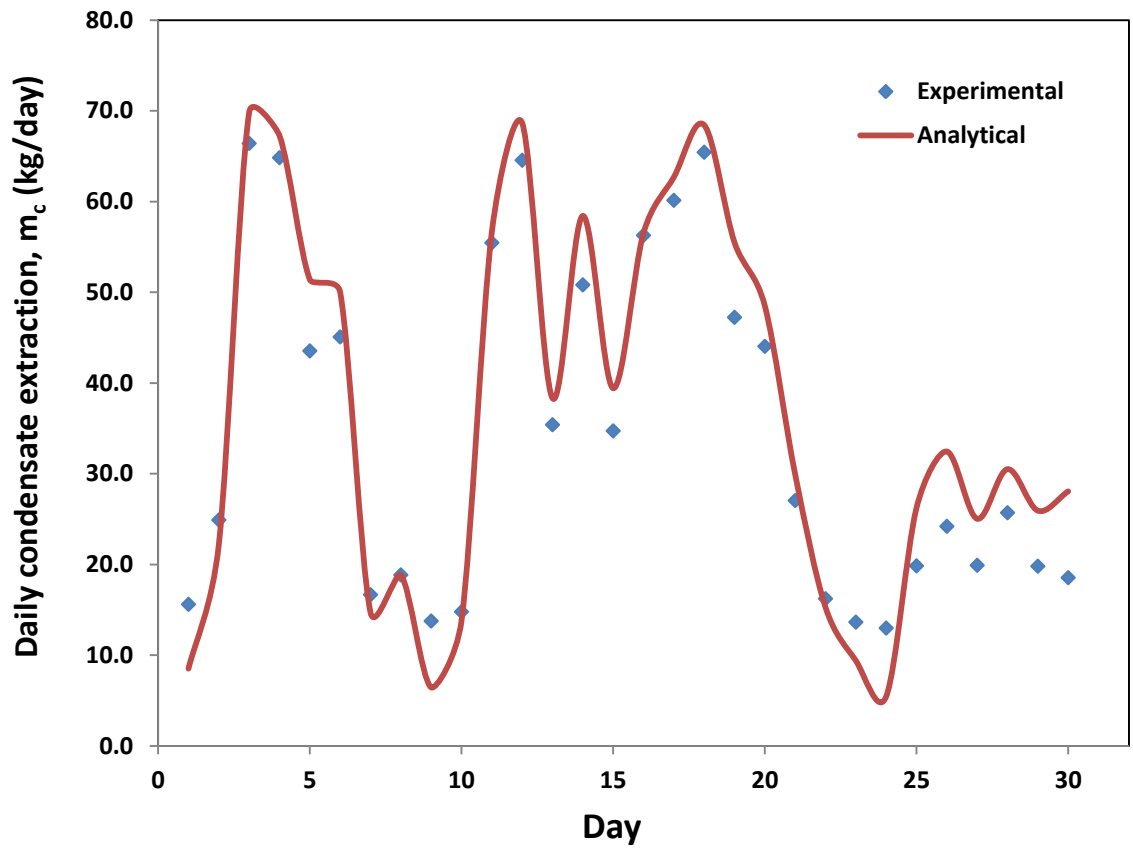
Figure 6.3 Comparison of analytical with experimental rate of condensate extraction for the month of June.
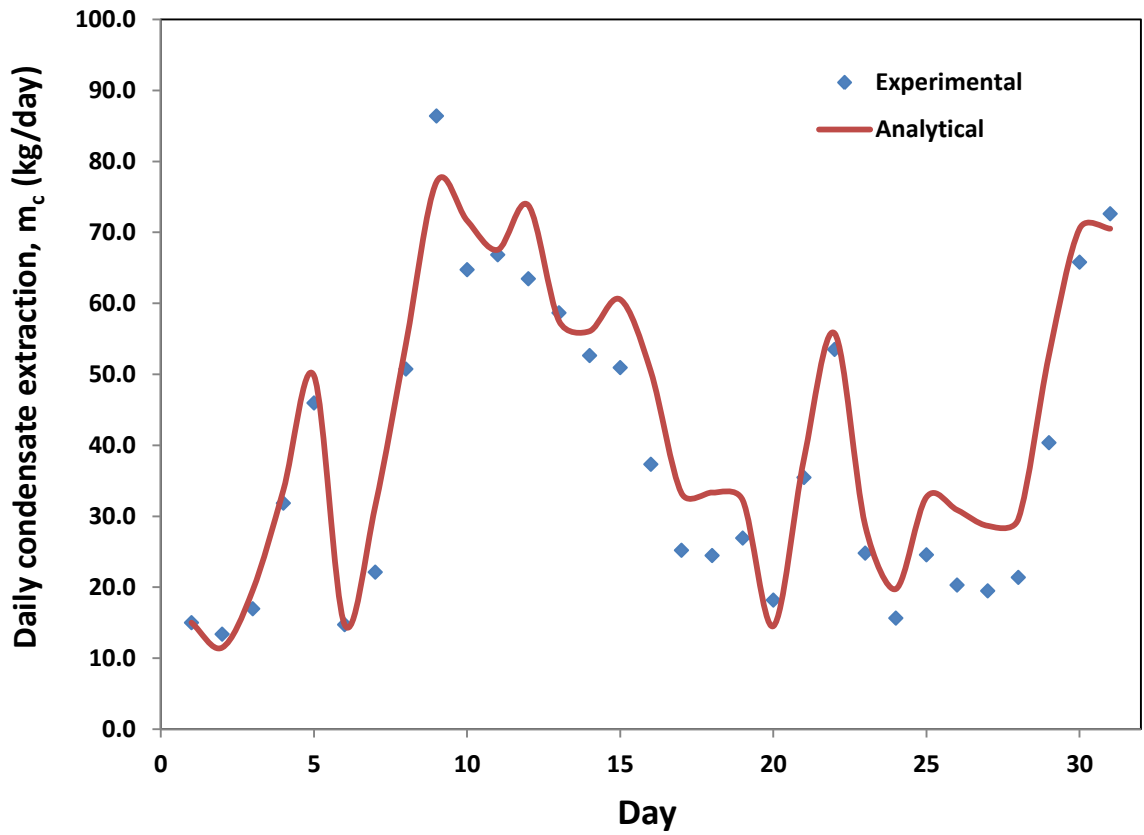
Figure 6.4 Comparison of analytical with experimental rate of condensate extraction for the month of July.
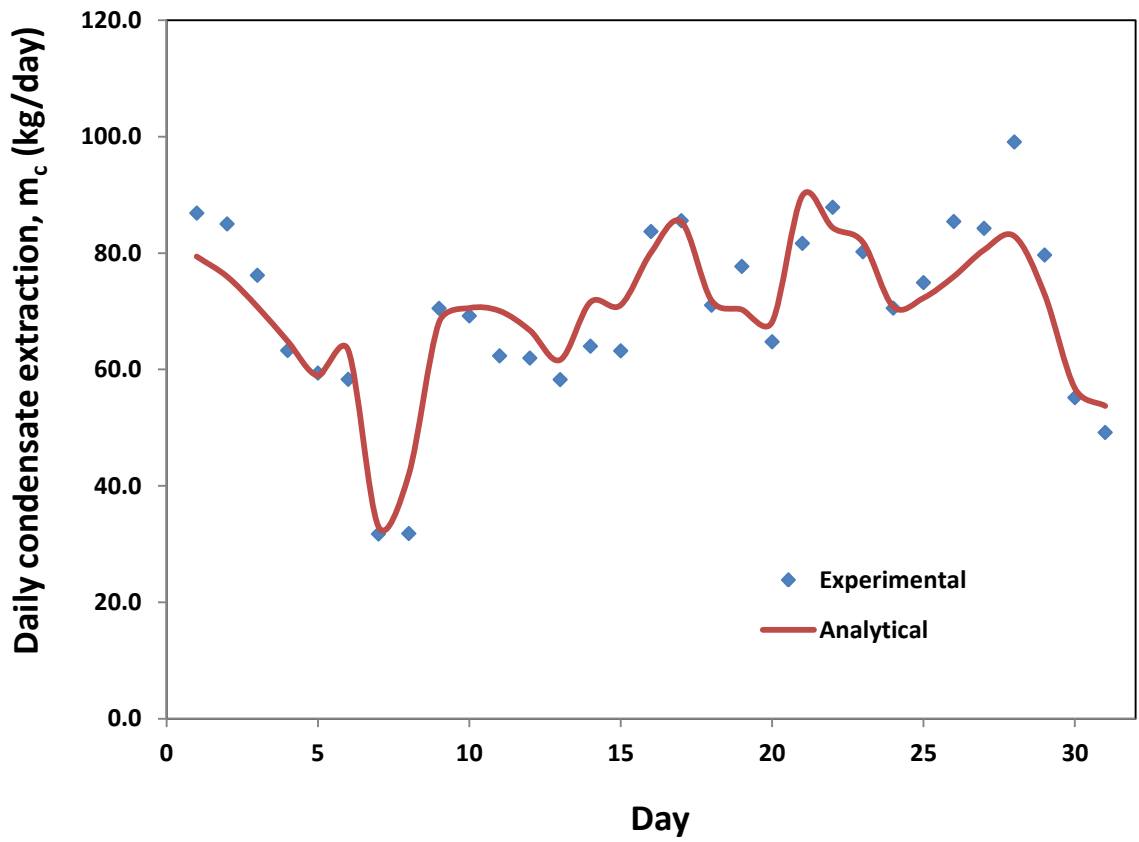
Figure 6.5 Comparison of analytical with experimental rate of condensate extraction for the month of August.
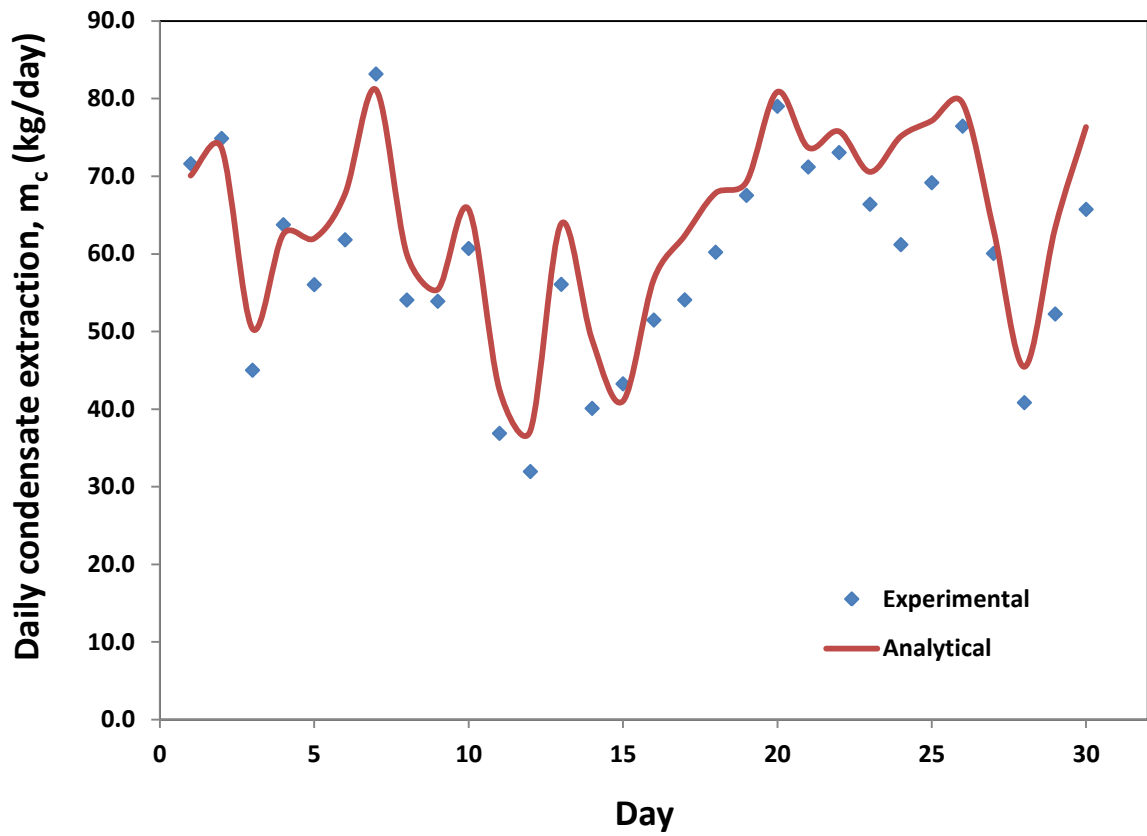
Figure 6.6 Comparison of analytical with experimental rate of condensate extraction for the month of September.

the sample includes: Total dissolved solids (TDS), turbidity, Electrical Conductivity (EC), pH, carbonates and metals.

Table 6.4 shows the results from the chemical analysis compared with KSA and World Health Organization, (WHO)'s maximum accepted values as reference. The findings in this table show that all the obtained results are within the limit of recommended values by WHO and KSA. It is reported that portable water produced by multi-stage flash and reverse osmoses seawater desalination processes have TDS of about 50 mg/l after post-treatment processes [14]. By comparison, condensate of this quality can be used for non-drinking applications as well, such as irrigation, cooling towers make-up water, municipal uses and above all, improving the a performance of air conditioning systems. Looking at the chlorine content found in the condensate sample, it is concluded that the condensate can be classified as distilled water and this is what make the condensate suitable for the above mentioned applications due to its less corrosion potential.

The present results also show that the quality of the tested condensate is very close to that of the drinking water. By undergoing simple bacterial removal and post-treatment processes, the condensate may be fit for drinking.

6.2. System Performance Analysis

The experimental results of the three performance improvement options mentioned earlier in the previous chapter are discussed in this section. A program is written in Engineering Equation Solver (EES) to determine the properties of the fluids such as enthalpy using the experimental data.

Table 6.4 Chemical concentrations in condensate sample compared with WHO acceptable limits.

Property	Condensate Value	KSA Guideline Value	WHO Guideline Value	Conclusion
pH	6.52	6.5 – 8	6.5 – 8.5	Within the limit
Turbidity	2.01 NTU	5 NTU	< 5 NTU	Within KSA limit
TDS	27 mg/l	1500 mg/l	< 600 mg/l	Within KSA limit
Cu	0.019 mg/l	2 mg/l	1 mg/l	Within the limit
Fe	N/A	0.3 mg/l	0.3 mg/l	Not available
Mn	0.007 mg/l	0.4 mg/l	0.1 mg/l	Within the limit
Mg	0.933 mg/l	N/A	N/A	Not compared
Na	0.428 mg/l	200 mg/l	N/A	Within the limit
Zn	0.02 mg/l	3 mg/l	5 mg/l	Within the limit
Hg	N/A	0.001 mg/l	0.001 mg/l	Not available
Ca	5.08 mg/l	N/A	N/A	Not compared
Cd	N/A	0.003 mg/l	N/A	Not available
Chloride	0.7 mg/l	250 mg/l	250 mg/l	Within the limit
Fluoride	N/A	1.5 mg/l	1.5 mg/l	Not available
Nitrate	1.71 mg/l	50 mg/l	10 mg/l	Within the limit
Sulphate	5.38 mg/l	500 mg/l	400 mg/l	Within the limit
Ba	0.01 mg/l	0.7 mg/l	N/A	Within the limit
Sr	0.023 mg/l	N/A	N/A	Not compared

The fluids in this case are the air and refrigerant (R-22). The following assumptions are made in the analysis of the experimental data:

- Pressure losses and heat gains or losses in the refrigerant lines are neglected.

- Heat gain across the boundaries of the precoolers and subcooler is neglected.

- Pressure of air entering the evaporator is assumed atmospheric.

The actual compressor power consumption is measured using a current transmitter while the rate of heat transfer in the evaporator is obtained by using the measured inlet and exit temperature and relative humidity of the air and its flow rate.

6.2.1. Results for Evaporator Air Precooling: Option 'A'

Experimental and analytical results for evaporator air precooling are presented in this section. Before the commencement of the experiment, a start-up amount of condensate was collected within several days and stored in the condensate-storage tank of $1m^3$ capacity for conducting the experiments with the air precooling options. In this option, two categories of experiments are carried out. In the first category, experiments are conducted at the severest weather conditions of Saudi Arabia while in the second category, other intermediate conditions are used. The severest weather conditions are 36 ^{o}C dry-bulb temperature and 80% relative humidity and are obtained from the climate data and the details are presented in the next section.

6.2.1.a Experimental and Analytical Results for Severest Weather Conditions: Option 'A'

Air conditioning systems are used for providing comfort in buildings. Some buildings such as hospitals require high volume of air. This is the main reason why in this kind of building, 100 % outdoor air is taken and cooled by the cooling system and then the cold air is blown into the building interior. In this part of the study, the air conditioning system is tested considering 100% outdoor air entering into the evaporator. The severest weather conditions are used as the testing conditions. The severest conditions are determined by finding the maximum enthalpy of the air considering the air as a mixture of dry air and water vapor. Therefore, the maximum enthalpy is determined at the severest combination of the air temperature and relative humidity of four different cities of Saudi Arabia as shown in Table 6.5. The maximum enthalpy is found at Dhahran and Jeddah climate conditions and the corresponding temperature and relative humidity at which the maximum enthalpy is obtained are the severest conditions (36 $^{\circ}$C and 80%). The reason for using the maximum enthalpy in determining the severest conditions is because the humid air consists of the sensible and latent heat components which formed the load that must be remove by the cooling section of the VCAC system.

In this category, two sets of experiments are carried out for comparison. The first is the base system experiment, without operating the air precooler while the second experiment includes the precooler. During the two experiments, the information given in Table 6.6 is used. The results of the two experiments are compared in order to evaluate the advantage of the modified system with option 'A' over the base VCAC system. About two hours experiments are performed for the baseline and the modified system under the same

Table 6.5 Enthalpies of severest weather conditions in major cities of Saudi Arabia.

T (^{o}C)	Φ	h (kJ/kg)	City
34	0.89	112.5	Dhahran
36	0.8	114.9	
30	0.89	91.82	Jazan
38	0.6	103.6	
31	0.94	100.5	Jeddah
36	0.8	114.9	
32	0.46	67.4	Riyadh
31	0.38	58.5	

Table 6.6 Experimental conditions of options 'A', 'B' and 'C' for severest weather conditions.

Parameter	Value
Evaporator entering air temperature	36 ^{o}C
Evaporator entering air relative humidity	80%
Volumetric flow rate of air to the evaporator	0.146 m^3/s
Ambient air temperature	35-38 ^{o}C
Initial condensate water temperature at the precooler inlet	24.9 ^{o}C
Mass flow rate of condensate through the precooler	0.16 kg/s
Volume of condensate-tank	1 m^3

experimental conditions highlighted previously. Experimental data was recorded in every minute and then the averages of every 12 readings are used in plotting the results. Analytical results are also obtained using the model equations presented in chapter 3. The values of the volumetric flow rate of air to the evaporator, the temperature and relative humidity of the air at the evaporator inlet that are used during the experiments are also used in the analytical computation as input parameters. Parameters computed by the analytical model includes evaporating and condensing temperatures, evaporator exit air temperature, cooling effect, coefficient of performance, compressor power and the second law efficiency.

Variation of precooler inlet and exit air temperatures are shown in Fig. 6.7 and the precooler effectiveness in Fig 6.8. About 5.7 $^{\circ}$C air temperature drop 'ΔT' is achieved by the precooler as indicated in the figures. Lowering the air temperature before entering the evaporator reduces the sensible heat load to the evaporator. The positive effect of reducing the sensible heat load is lower pressure difference across the compressor as shown in Fig. 6.9. The decrease in pressure difference across the compressor resulted in the decrease in compressor power consumption as shown in Fig. 6.10. The compressor power obtained from the base system and the modified system both experimental and analytical are also compared. About 5% reduction in compressor power consumption is realized from the experimental results. Comparison of COP obtained from the base system with that of the modified system is shown in Fig. 6.11. It is noted that there is significant increase in COP of about 31% when option 'A' is applied. The increase in COP as a result of air precooling before entering the evaporator is due to decrease in compressor power. Evaporator exit air temperature also decreased as a result of lowering
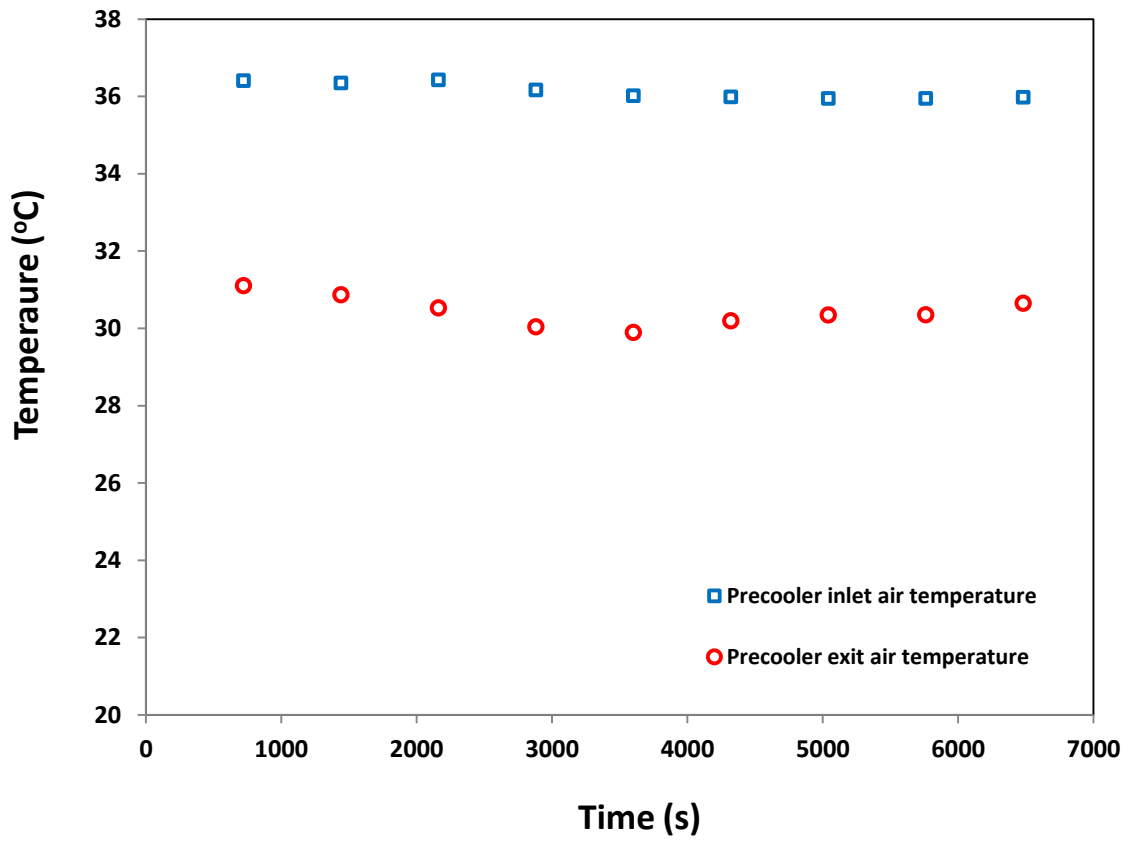
Figure 6.7 Air temperatures across precooler of option 'A' for severest weather conditions.
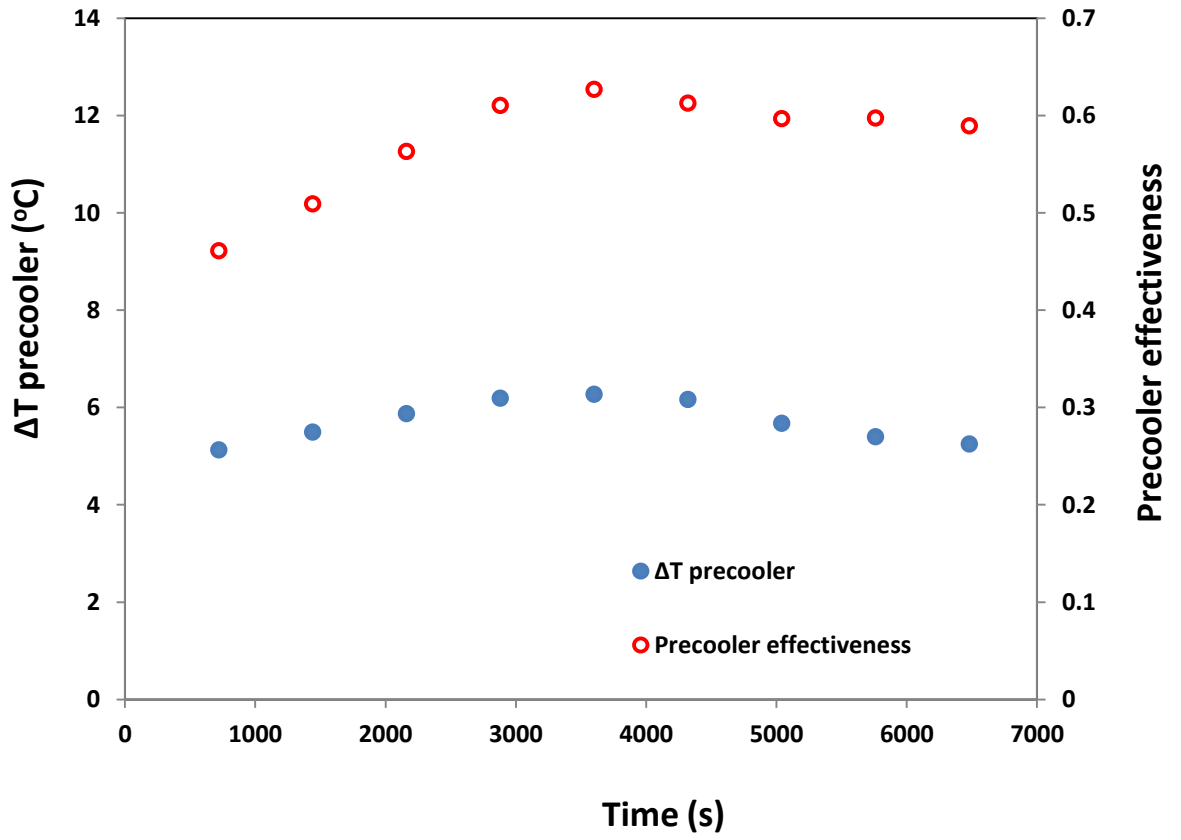
Figure 6.8 Variation of ΔT and precooler effectiveness of option 'A' for severest weather conditions.
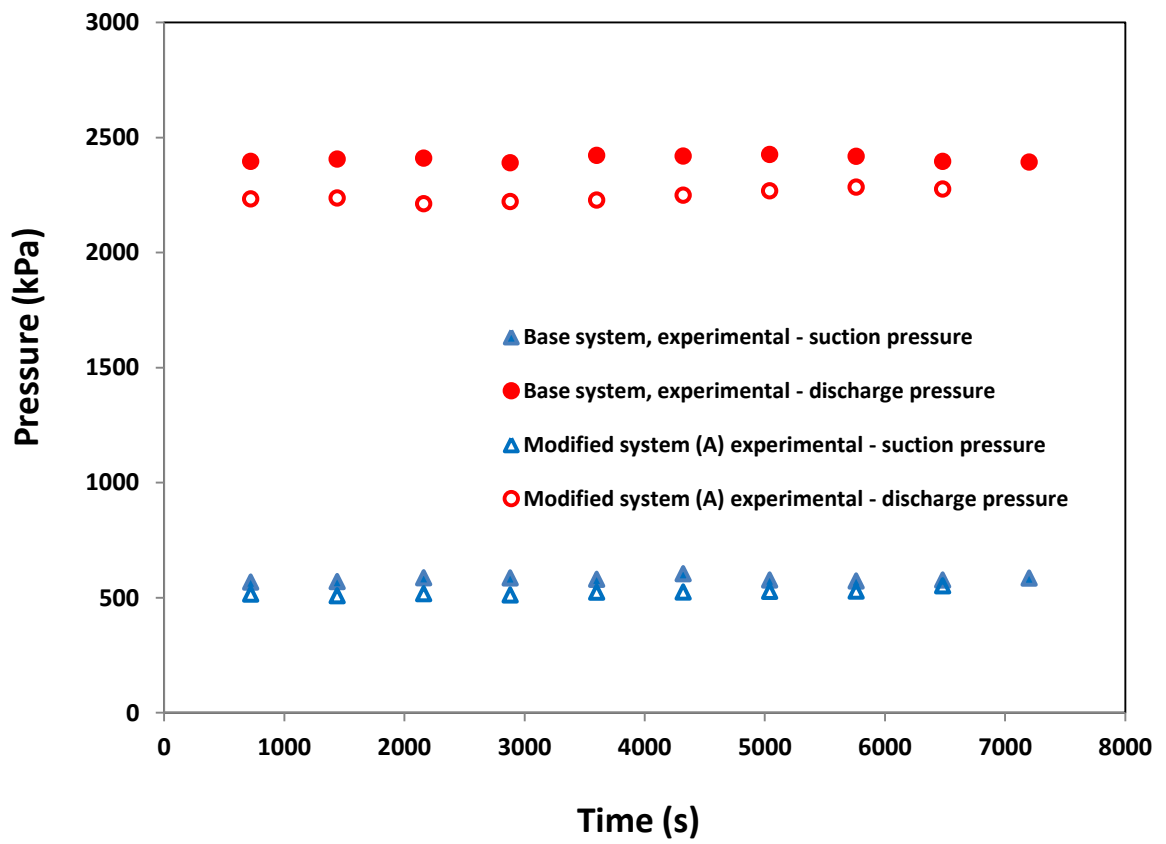
Figure 6.9 Comparison of compressor pressures of base system with option 'A' for severest weather conditions.
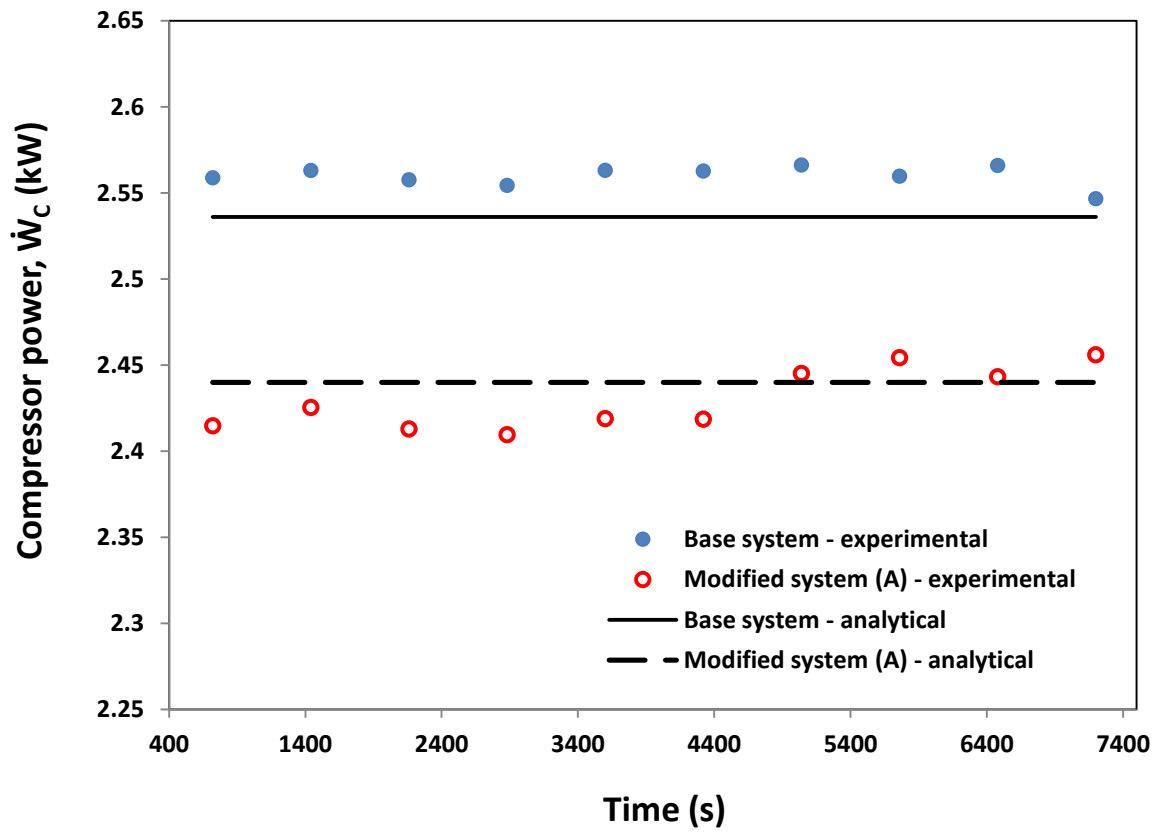
Figure 6.10 Comparison of compressor power of base system with option 'A' for severest weather conditions.
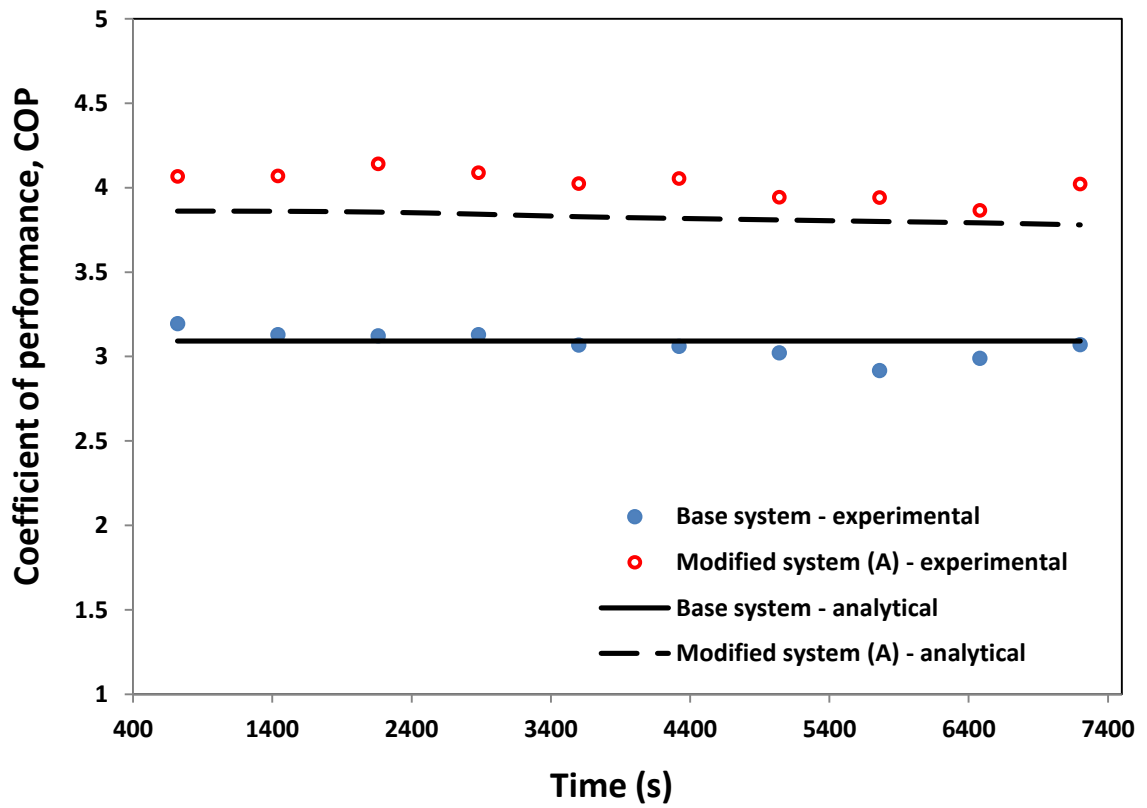
Figure 6.11 Comparison of COP of base system with option 'A' for severest weather conditions.

the air temperature before entering the evaporator using condensate as depicted in Fig. 6.12. The decrease in evaporator exit air temperature means that a better cooling is achieved due to air precooling at the evaporator inlet. Comparison of the second law efficiency obtained from the base system with the modified system is shown in Fig. 6.13. The second law efficiency is increased to about 25% when the air entering the evaporator is lowered. The increase in the second law efficiency is due to the combined effect of the decrease in evaporator exit air temperature and the increase in COP.

Variation of condensate temperature in the tank with time is shown in Fig. 6.14. The condensate temperature increases because after exiting the precooler, it is re-circulated back to the tank. Only about 2.3 $^{\circ}$C increase in the condensate temperature is noticed during the two hours experiment. This is a clear indication that the precooling technique will last long even if the condensate is re-circulated back to the tank provided the tank is large ($\geq 1\ m^3$). Using the analytical model and assuming the air precooling is maintained for eight hours during the day time (on-precooling) and then stopped at night when the air temperature is relatively low (off-precooling), then the variation of condensate temperature inside the tank during these periods is presented in Fig. 6.15. The initial amount of condensate before the precooling is 1000 kg and at the end of the precooling, the amount is increased to 1054 kg due to continuous collection of fresh condensate at the rate of 6.8 kg/h. During the off-precooling period, the 54 kg of condensate is removed from the tank so that the condensate temperature within the tank can be reduced more while continuously collecting fresh condensate as preparation for the following day. The 54 kg of condensate that is removed from the tank can be used for other purposes such as washing and cleaning.
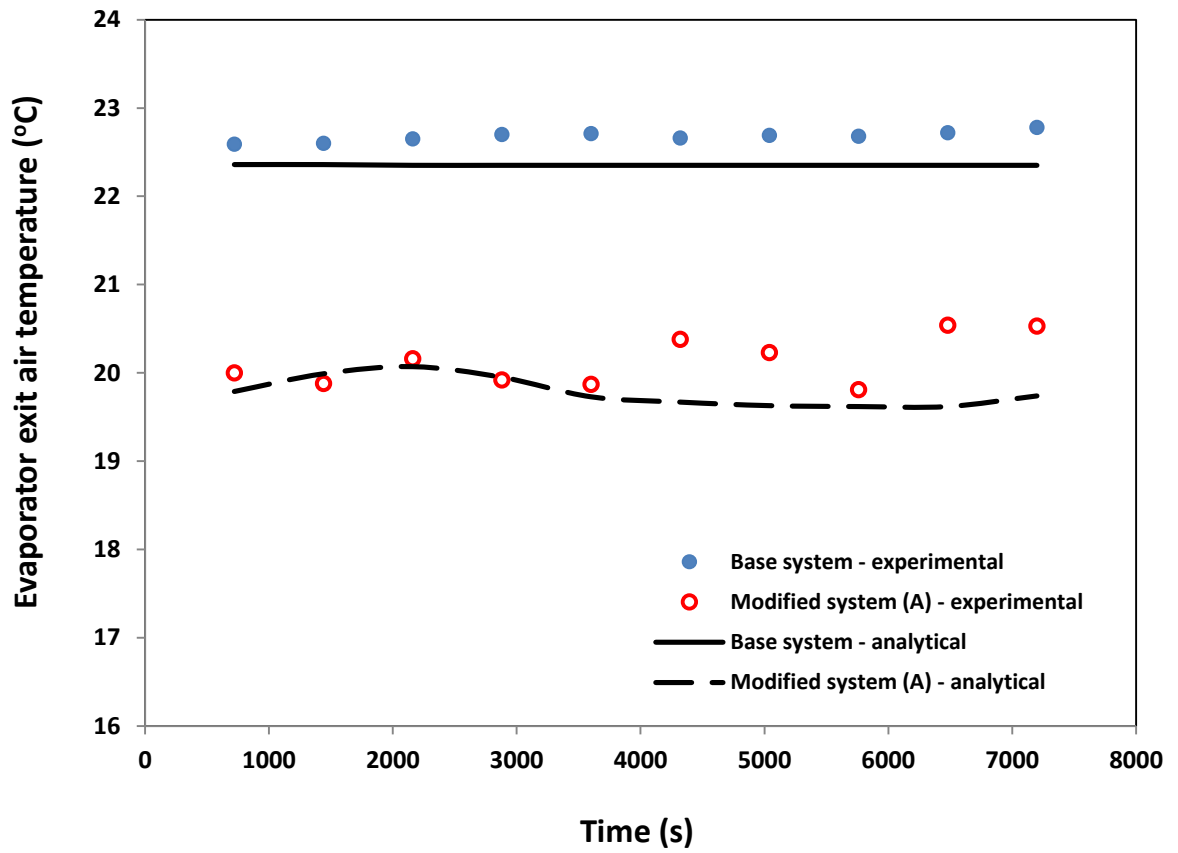
Figure 6.12 Comparison of evaporator exit air temperature of base system with option 'A' for severest weather conditions.
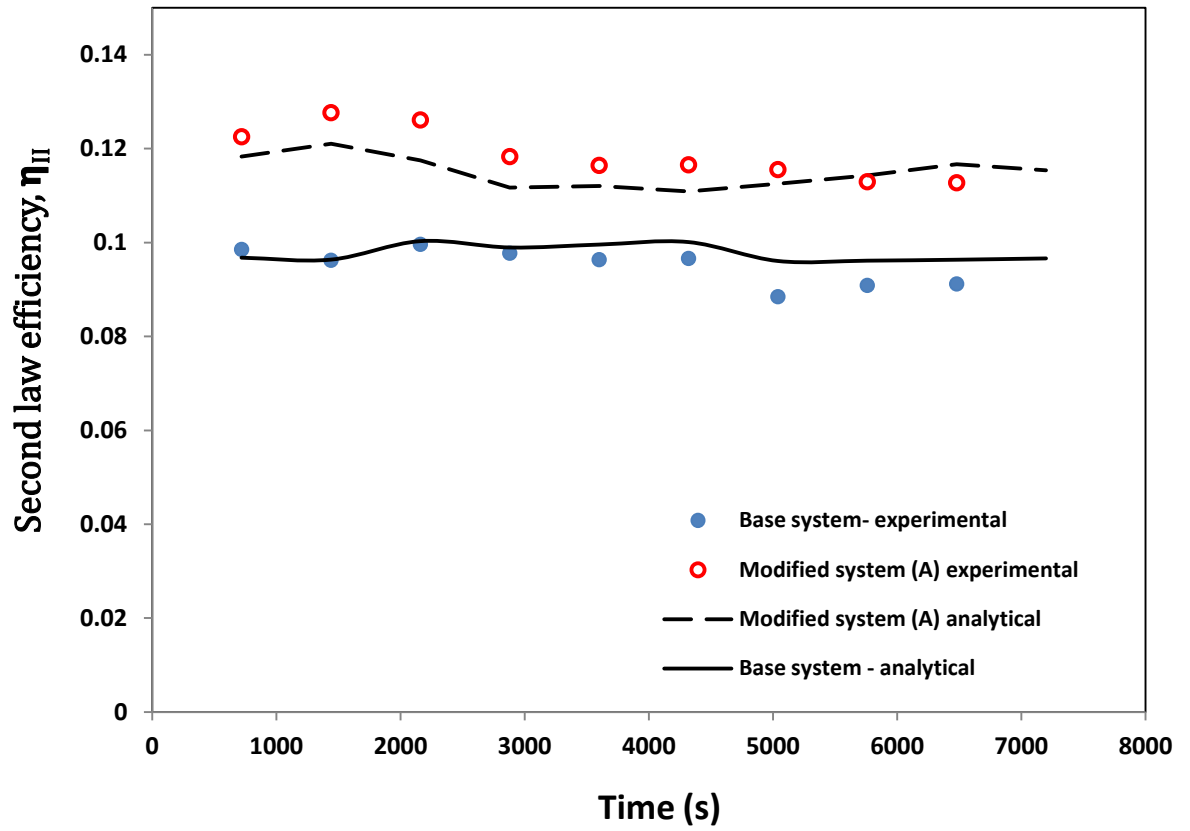
Figure 6.13 Comparison of second law efficiency of base system with option 'A' for severest weather conditions.
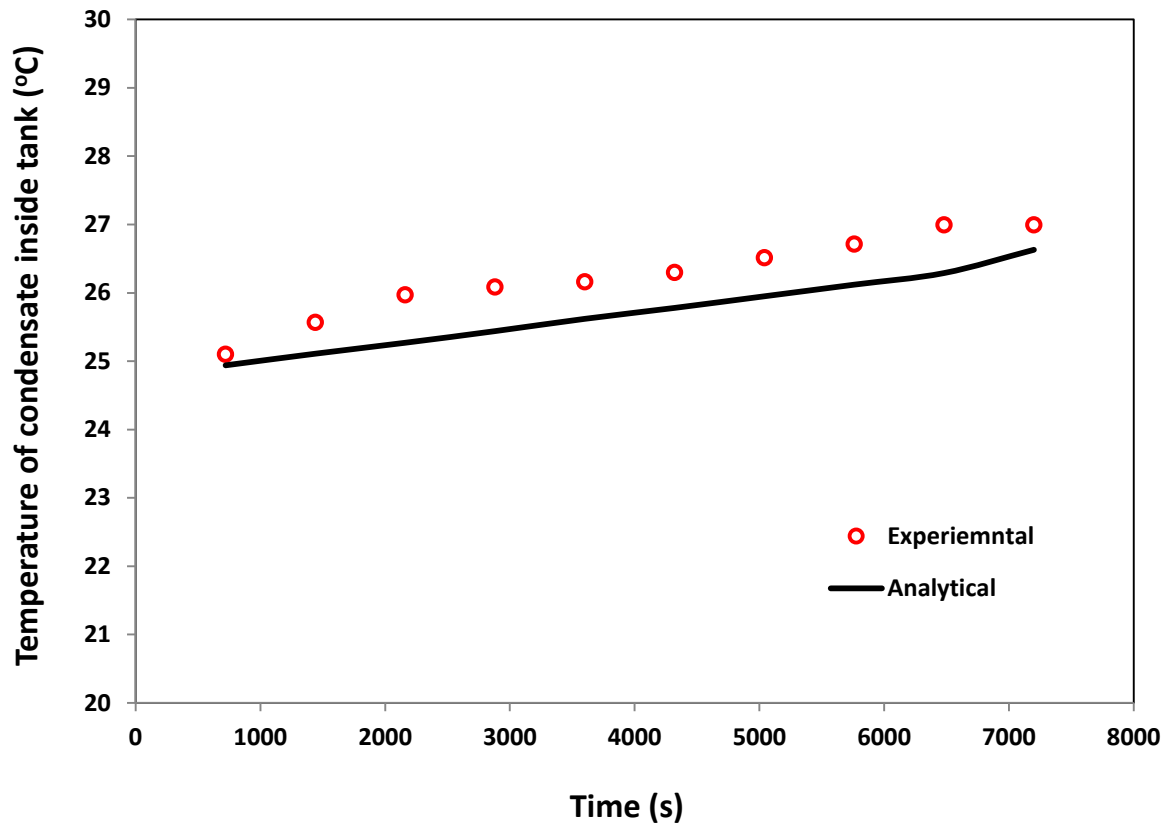
Figure 6.14 Variation of condensate temperature the tank with time for severest weather conditions- Option 'A'.
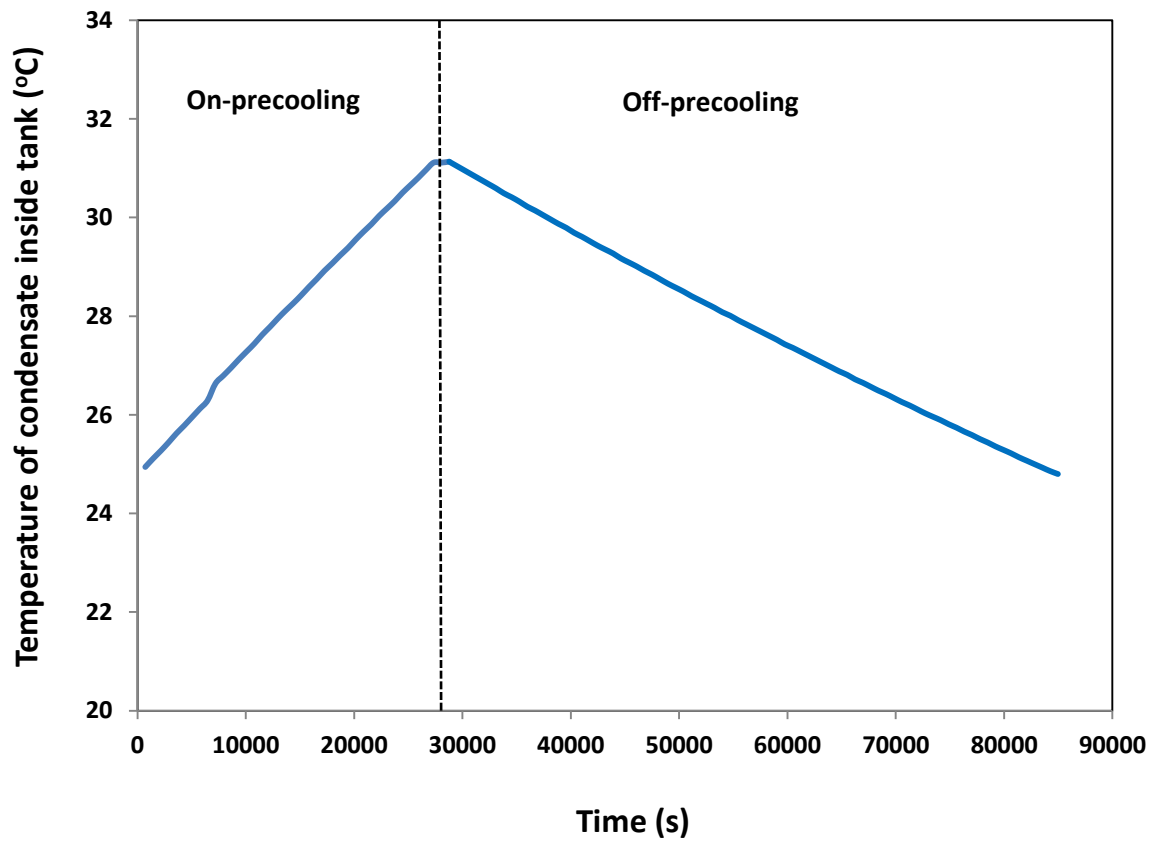
Figure 6.15 Variation of condensate temperature inside tank for complete day during on and off- periods: analytical study.

The average values of the performance parameters and comparison of analytical with the experimental results are presented in Table 6.7. It is clear that the modified system has significant advantage over the base system. It can be observed from the table that the analytical results are in good agreement with the experimental results with minimum and maximum errors of 0.12% and 5.12% respectively which are within reasonable level.

Table 6.7 Summary of results for evaporator air precooling for severest weather conditions – Option 'A'

| Quantity	Comparison of analytical with experimental results for option 'A'					
	Base system			Modified system- option 'A'		
	Experimental	Analytical	Difference (%)	Experimental	Analytical	Difference (%)
COP	3.06	3.09	-0.88	4.01	3.80	5.12
$\dot{W}_c$ (kW)	2.56	2.54	0.94	2.43	2.43	0.12
η_{II}	0.09	0.10	-3.20	0.12	0.11	4.22
$T_{a,ev,e}(^oC)$	22.7	22.4	1.40	20.1	20.0	0.71

6.2.1.b   Experimental Results for Intermediate Evaporator Inlet Air

Conditions: Effects of Air Mass Flow Rate – Option 'A'

In most of residential air conditioning applications, the room air is usually circulated continuously through the cooling system while maintaining the room to the desired comfort level. In this kind of application, the room air absorbed heat energy in the form of sensible and latent from the occupants. After the air is circulated through the evaporator, the heat energy is removed and the cycle continues. In this application, the evaporator inlet air temperature is usually lower than the outdoor air temperature. The second category of experiment in this study is basically conducted at typical evaporator

inlet air conditions similar to the re-circulated air type as described above. Experiments are performed at different mass flow rates of air entering the evaporator. The mass flow rates of air are obtained from the measured air velocities, humidity and temperature across the evaporator using the cross-sectional area of the evaporator exit. For each air flow rate, the system is run for several minutes without the air precooling to get a baseline data and the data was saved at every second. The evaporator inlet air conditions are set at $30.5 - 31.5^{o}$C temperature and $39 - 41\%$ relative humidity in the climate chamber. These values are chosen based on ARI standard rating conditions of a forced-circulation air cooling coil [71]. The ARI rating conditions are: evaporator entering air dry-bulb temperature $18 - 38^{o}$C, entering air wet-bulb temperature $16 - 29^{o}$C and air face velocity in the range of $1 - 4$ m/s. Immediately after the baseline readings are obtained, experiments are repeated for each air mass flow rate at three sets of ΔT in order to investigate the effect of decreasing the air temperature before entering the evaporator coil. The parameter ΔT is the air temperature difference across the precooler. The reason for the immediate start of the second experiment is in order to minimize the effect of ambient air temperature variation on the system which is out of control during the experiments.

Variation of cooling effect of the system as a function of air mass flow rate at different ΔT is shown in Fig. 6.16. The cooling effect increases with increase in the mass flow rate of air. This increase is expected because the cooling effect is proportional to the air flow rate as indicated from the energy balance across the evaporator, Eq. (3.1). The figure also illustrates the fact that as the air temperature before entering the evaporator is lowered, the cooling effect increases. It is to be noted that the air temperature and humidity
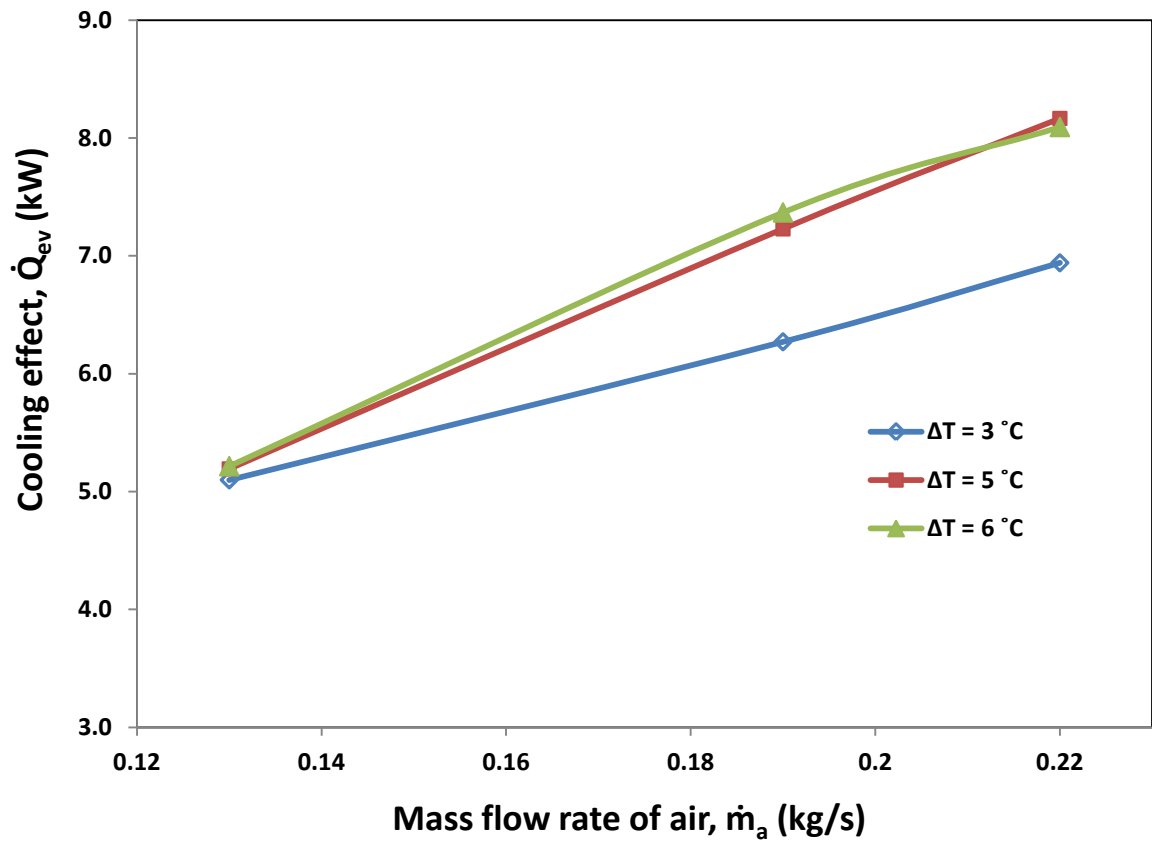
Figure 6.16 Variation of cooling effect with air mass flow rate at different ∆T - Option 'A'.

before the precooler are used in obtaining the cooling effect. Variation of compressor power with mass flow rate of air at different ΔT is presented in Fig. 6.17. As expected, the compressor power increases as the air flow rate increases because increasing the air flow rate means more load on the system as mentioned earlier. However, air precooling before the evaporator lowers the compressor power requirement as shown in the figure at different ΔT. By comparing Fig. 6.16 and 6.17, it can be observed that the increase in cooling effect with air mass flow rate is more significant than the corresponding increase in compressor power requirement. This behaviour leads to significant increase in COP as shown in Fig. 6.18. Variation of the second law efficiency with air mass flow rate is presented in Fig. 6.19. The second law efficiency is nearly constant between the mass flow rates of 0.13 and 0.19 kg/s. It is observed that the variation pattern of the second law efficiency is some how different from the other parameters. This is because of the dependency of the second law efficiency on many parameters. Higher efficiency is also noted at higher ΔT.

The average values of the performance parameters over the period of experiments for each set of air mass flow rate and ΔT are summarized in Table 6.8. The data presented in the table are the average values taken over the period of each experiment. Average percentage increase/decrease of performance parameters for air flow rate of 0.13 kg/s are shown in Table 6.9.

The overall benefits achieved by precooling the air before entering the evaporator using condensate are the reduction in power consumption, the increase in cooling effect, COP, and second law efficiency of the system.
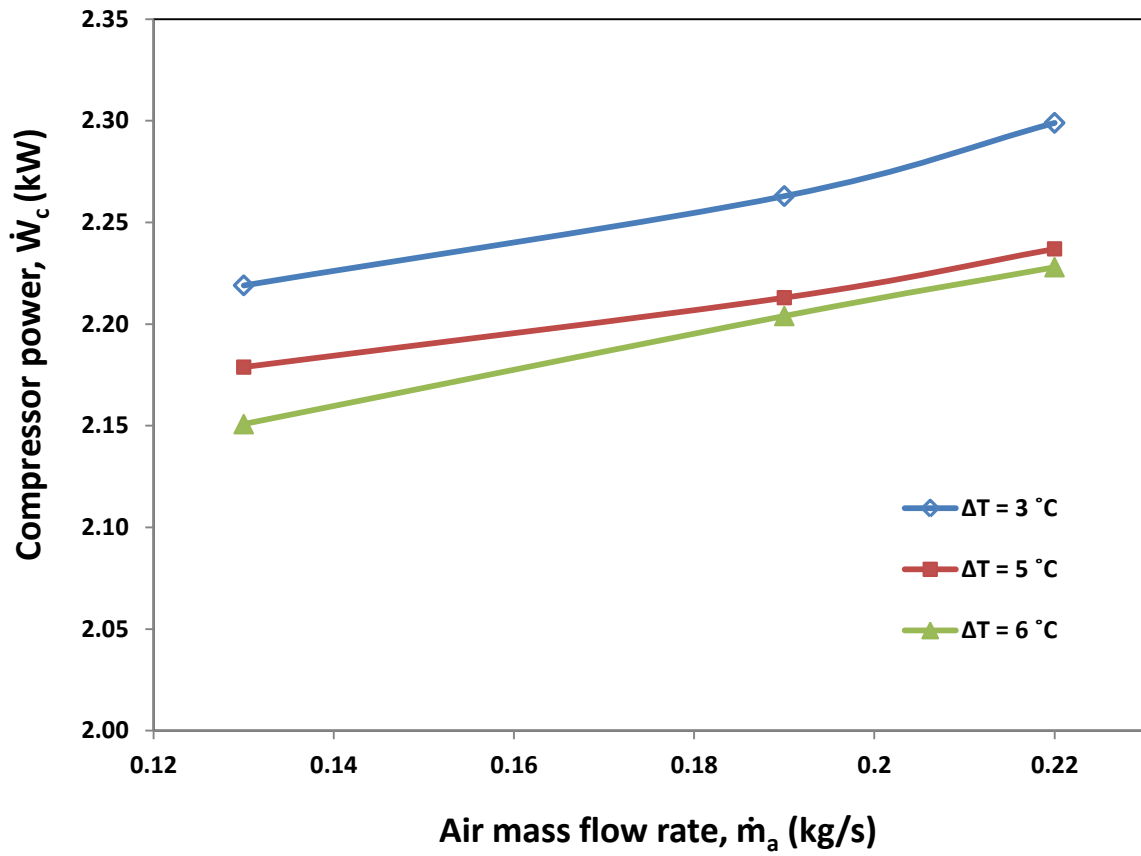
Figure 6.17 Variation of compressor power with air mass flow rate at different ΔT - Option 'A'.
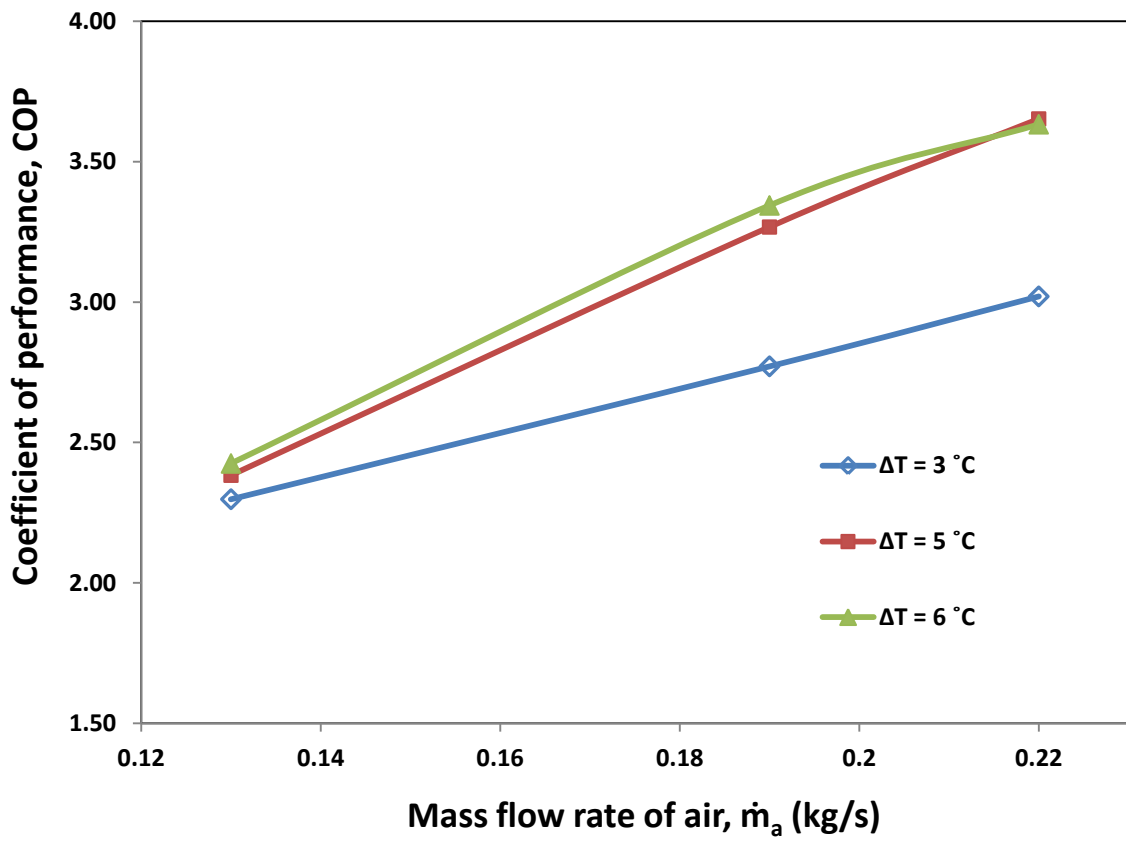
Figure 6.18 Variation of COP with air mass flow rate at different ∆T - Option 'A'.
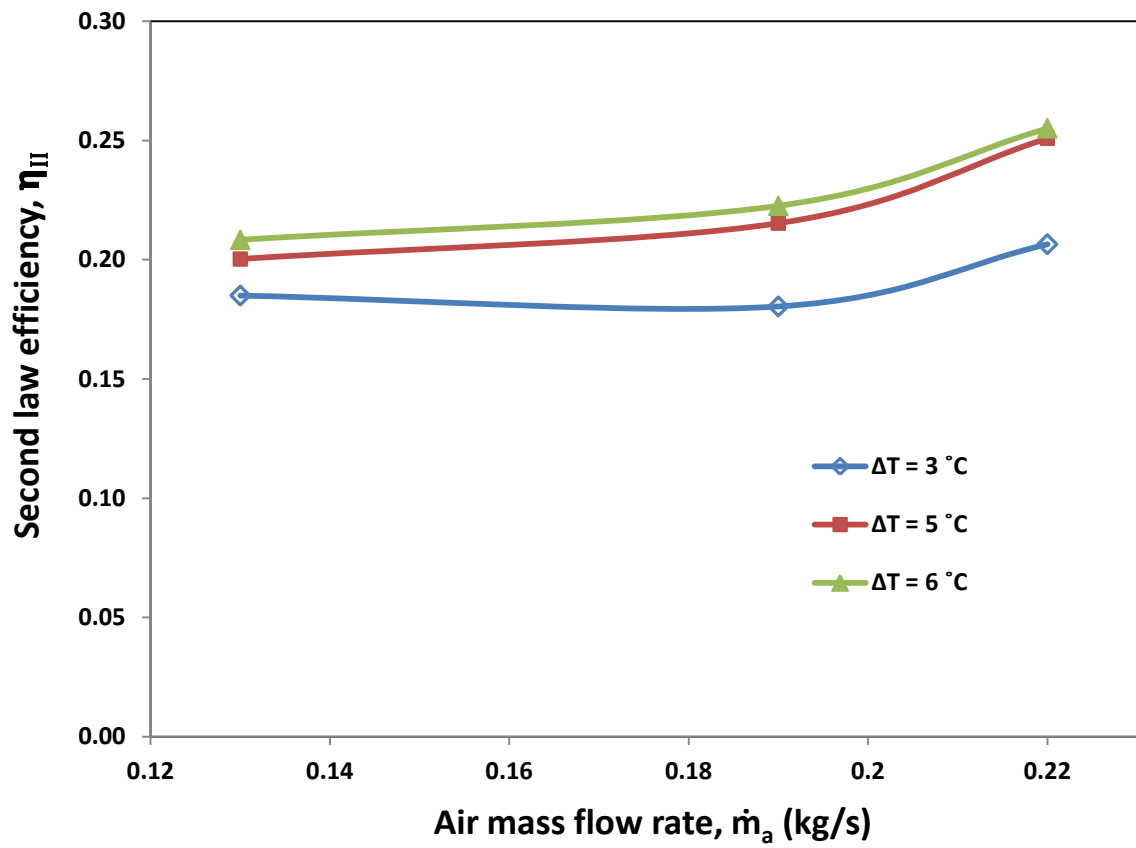
Figure 6.19 Variation of second law efficiency with air mass flow rate at different ΔT - Option 'A'.

Table 6.8 Summary of experimental results for evaporator air precooling for intermediate evaporator inlet air conditions– Option 'A'.

$\dot{m}_a$ (kg/s)	Parameter	Base system	Modified system: option 'A'		
			$\Delta T = 3\ ^oC$	$\Delta T = 5\ ^oC$	$\Delta T = 6\ ^oC$
0.13	$\dot{Q}_{ev}$ (kW)	4.74	5.10	5.19	5.22
	COP	2.10	2.30	2.38	2.43
	EER	7.17	7.84	8.13	8.27
	$\dot{W}_c$ (kW)	2.25	2.22	2.18	2.15
	η_{II}	0.16	0.18	0.20	0.21
0.19	$\dot{Q}_{ev}$	5.08	6.27	7.23	7.37
	COP	2.18	2.77	3.27	3.34
	EER	7.43	9.45	11.15	11.41
	$\dot{W}_c$ (kW)	2.33	2.26	2.21	2.20
	η_{II}	0.13	0.18	0.22	0.22
0.22	$\dot{Q}_{ev}$	5.69	6.94	8.17	8.09
	COP	2.45	3.02	3.65	3.63
	EER	8.36	10.31	12.46	12.40
	$\dot{W}_c$ (kW)	2.32	2.30	2.24	2.23
	η_{II}	0.16	0.21	0.25	0.26

Table 6.9 Average percentage reduction/increase of performance parameters for air mass flow rate of 0.13 kg/s - Option 'A'.

ΔT (^oC)	Increase in $\dot{Q}_{ev}$/EER (%)	Reduction in $\dot{W}_c$ (%)	Increase in COP (%)	Increase in η_{II} (%)
3	7.7	1.5	9.4	12.8
5	9.7	3.3	13.4	22.1
6	10.2	4.6	15.4	27.0

6.2.2. Experimental Results for Condenser Air Precooling - Option 'B'

Two sets of experiments are performed in this option. The first experiment is conducted at the severest weather conditions like in the case of option 'A'. The second experiment is carried out at intermediate conditions of the air entering the evaporator for several hours.

6.2.2.a Experimental Results for Severest Weather Conditions – Option 'B'

Experimental results for condenser air precooling option are presented in this section. The experimental conditions and procedure presented in section 6.2.1.a are also used in this option. The first experiment is the baseline, without operating the air precooler and the second experiment includes the precooler and comparative analysis between the two data is performed.

Variations of precooler inlet condensate temperature and the amount of precooling, ΔT with experimental time are shown in Fig. 6.20. It is observed that the precooler inlet condensate temperature increases over time and this is because the condensate is re-circulated back to the tank during the experiment. The increase in the precooler inlet condensate temperature causes ΔT to decrease over time, but the decrease is not that significant at the end of the experiment as shown in the figure.

Comparisons of the suction and discharge pressures obtained for the base system and the modified system are shown in Fig. 6.21. It is observed that the suction pressures from the two experiments are almost the same, but the real effect of air precooling before entering the condenser is noticed at the discharger pressures. The reduction in condenser inlet air temperature by condensate causes the compressor discharge pressure to decrease by about 5.2 % on average.
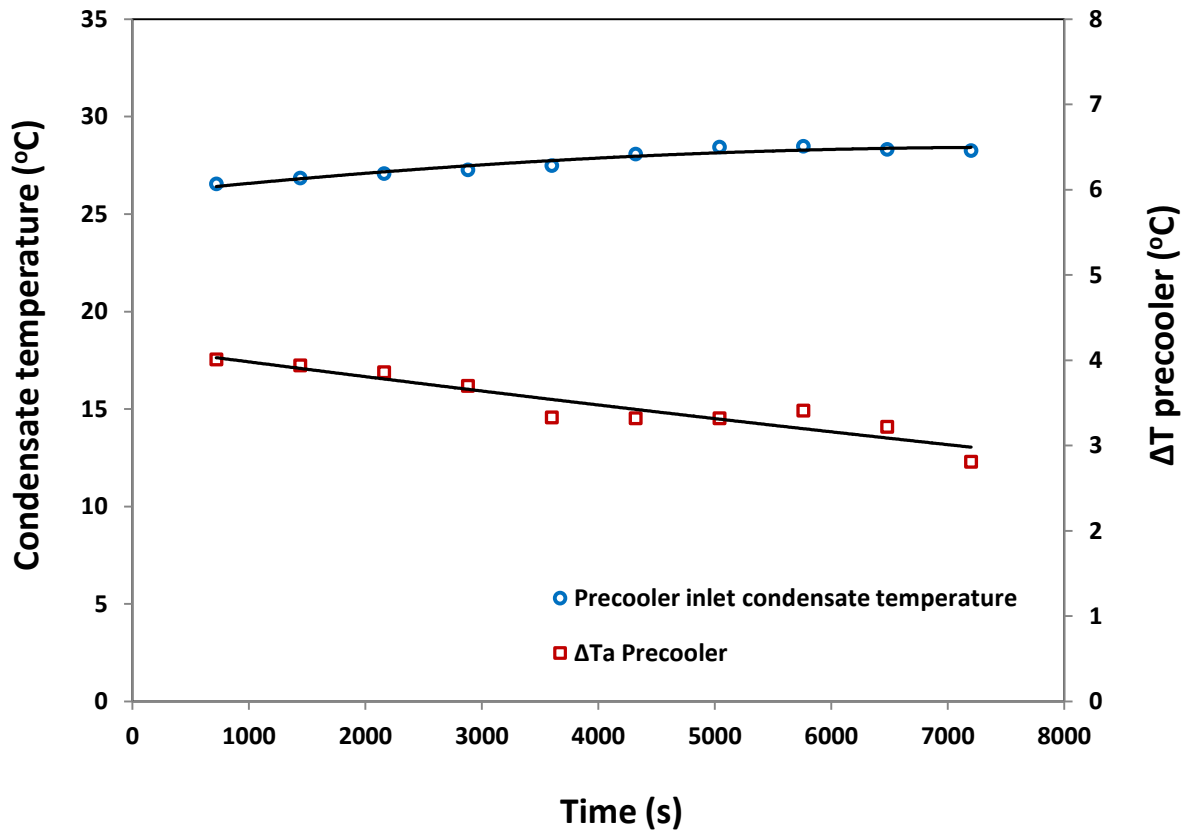
Figure 6.20 Variation of condensate inlet temperature and ΔT for severest weather conditions - Option 'B'.
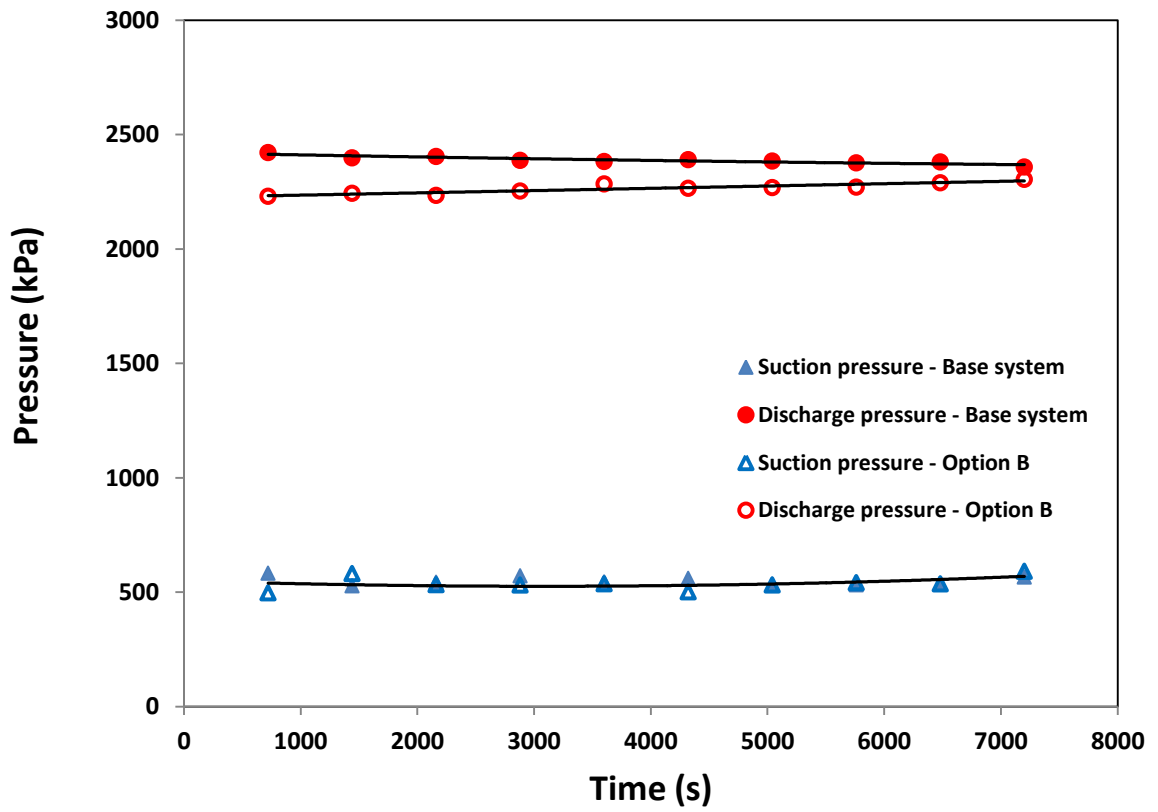
Figure 6.21 Comparison of suction and discharge pressures of the base system with option 'B' for severest weather conditions.

The decrease in compressor discharge pressure consequently leads to decrease in compressor power consumption by 4.8% on average as indicated in Fig 6.22. The compressor power of the modified system with option 'B' slightly increases over time. This increase is due to the increase in precooler inlet condensate temperature as indicated in Fig. 6.20. By lowering the discharge pressure, the compressor's life expectancy can be improved. It is noticed from Fig. 6.23 that the evaporator exit air temperature of the modified system is decreased by about 10% and this is due to lower evaporating temperature during the precooling option. Due to lower evaporator exit air temperature, the cooling effect is increased to about 15.2% as shown in Fig. 6.24. Reduction in power consumption and the corresponding increase in cooling effect resulted in significant increase in COP of about 21% as depicted in Fig. 6.25. Comparison of the second law efficiency obtained for the base system with the modified system is presented in Fig 6.26. A significant increase of about 24% in the second law efficiency is observed when the air entering the condenser is lowered. The increase in the second law efficiency is due to the decrease in evaporator exit air temperature and the corresponding increase in COP. The average value of precooler effectiveness obtained from the results is 0.41. Summary of the experimental results is presented in Table 6.10.

6.2.2.b   Experimental Results for Intermediate Evaporator Inlet Air Conditions – Option 'B'.

Experiments are also conducted for option 'B' at other conditions of air rather than the severest weather conditions. Two sets of experiments are conducted for the duration of about six hours in order to know how long the air precooling will last before the
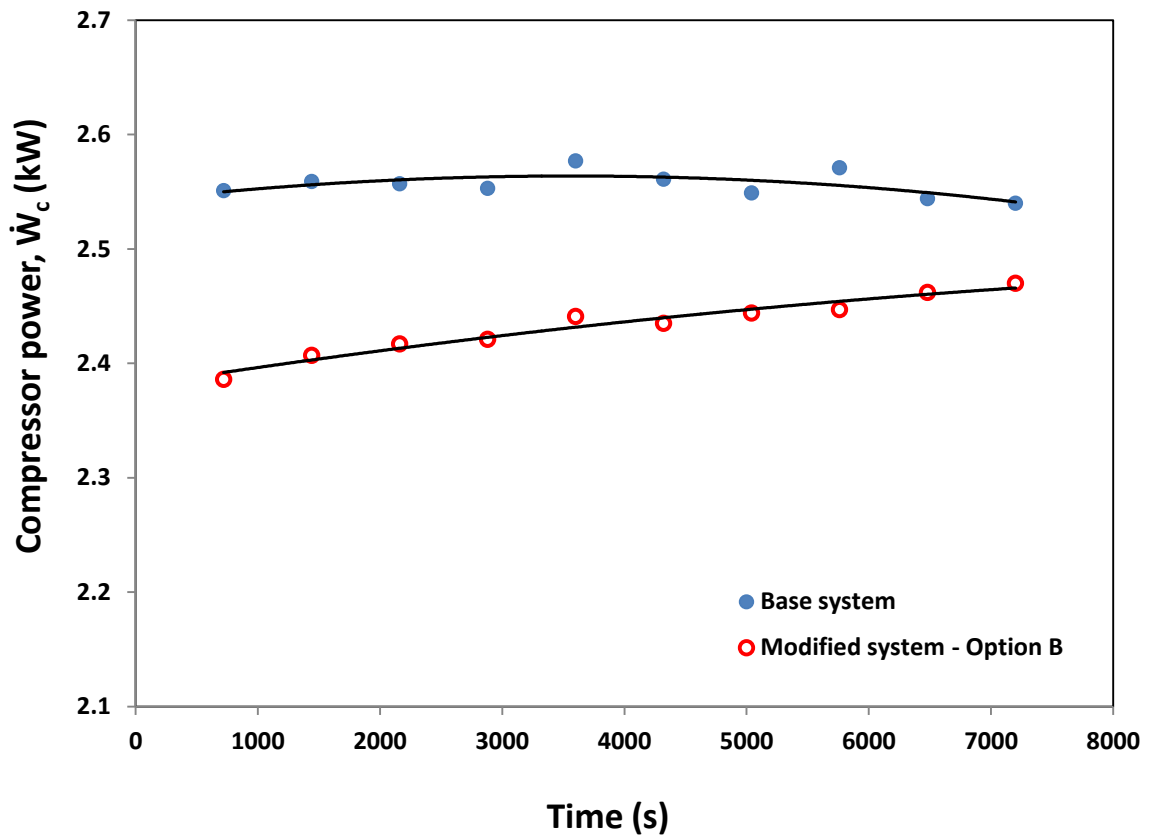
Figure 6.22 Comparison of compressor power of base system with option 'B' for severest weather conditions.
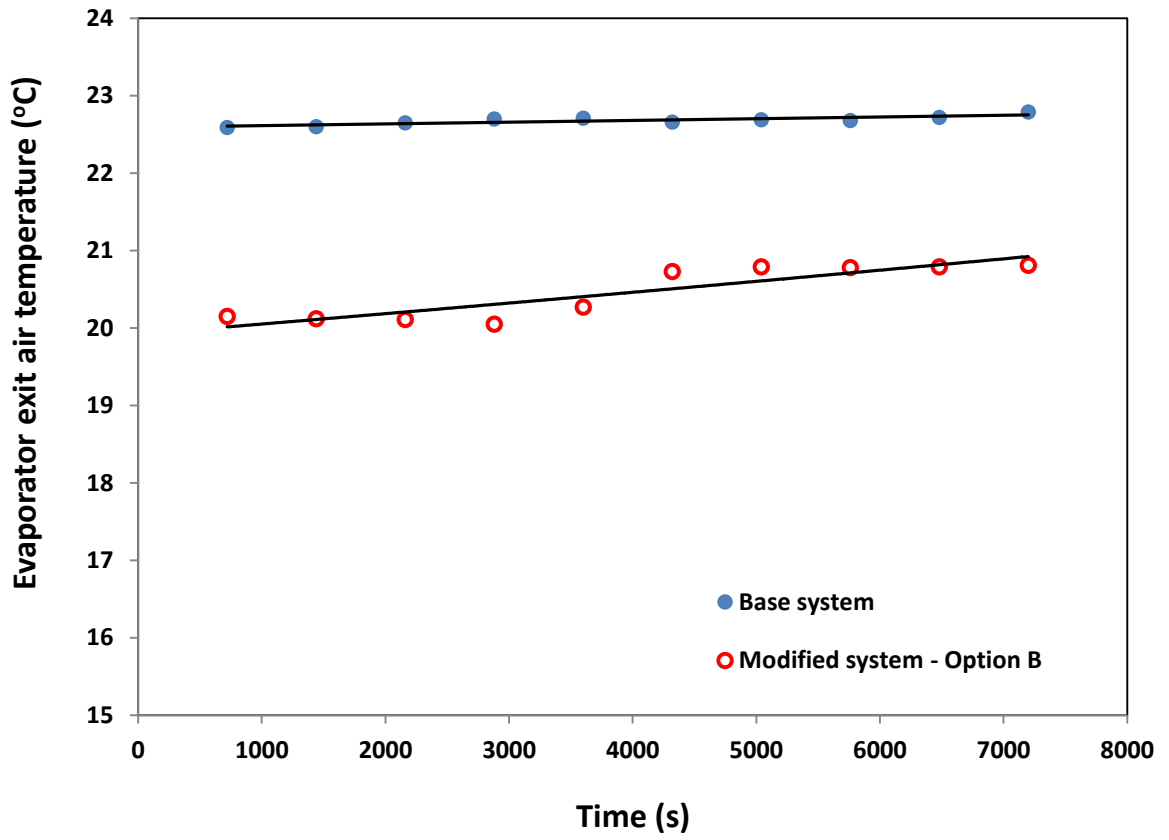
Figure 6.23 Comparison of evaporator exit air temperature of base system with option 'B' for severest weather conditions.
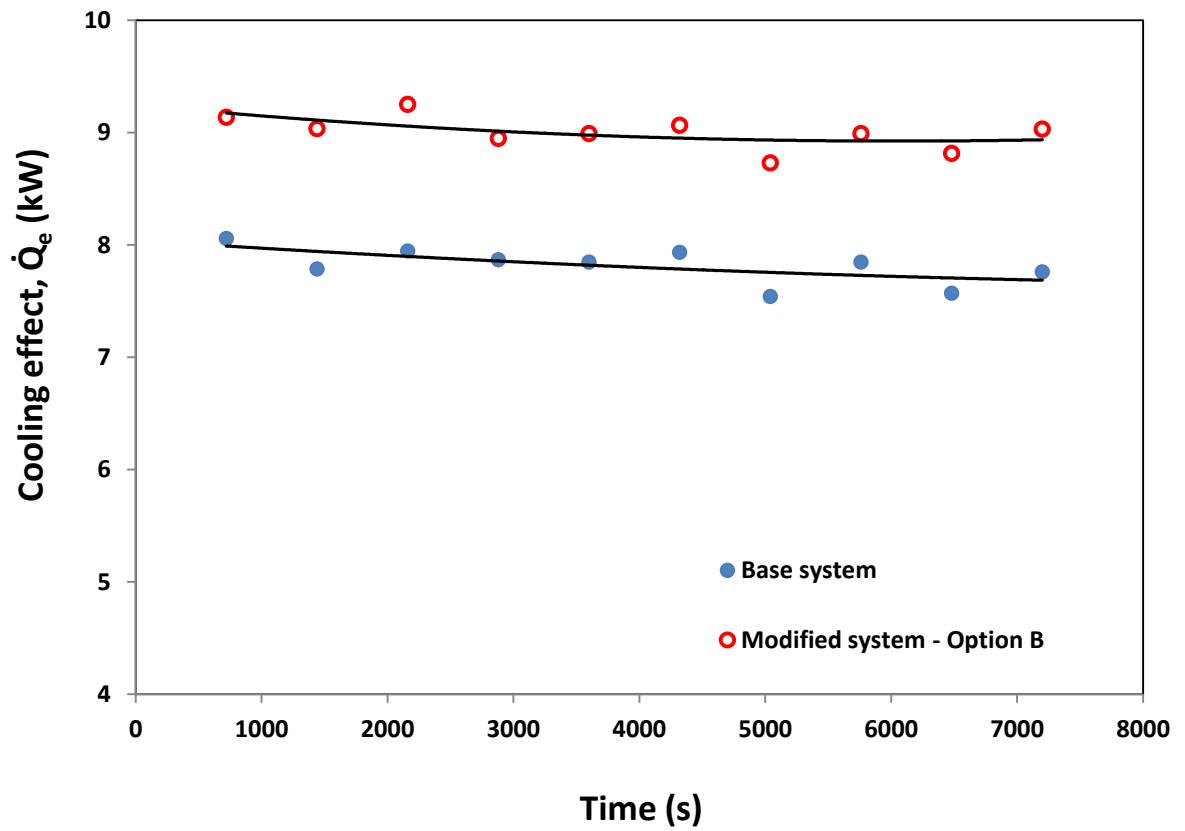
Figure 6.24 Comparison of cooling effect of base system with option 'B' for severest weather conditions.
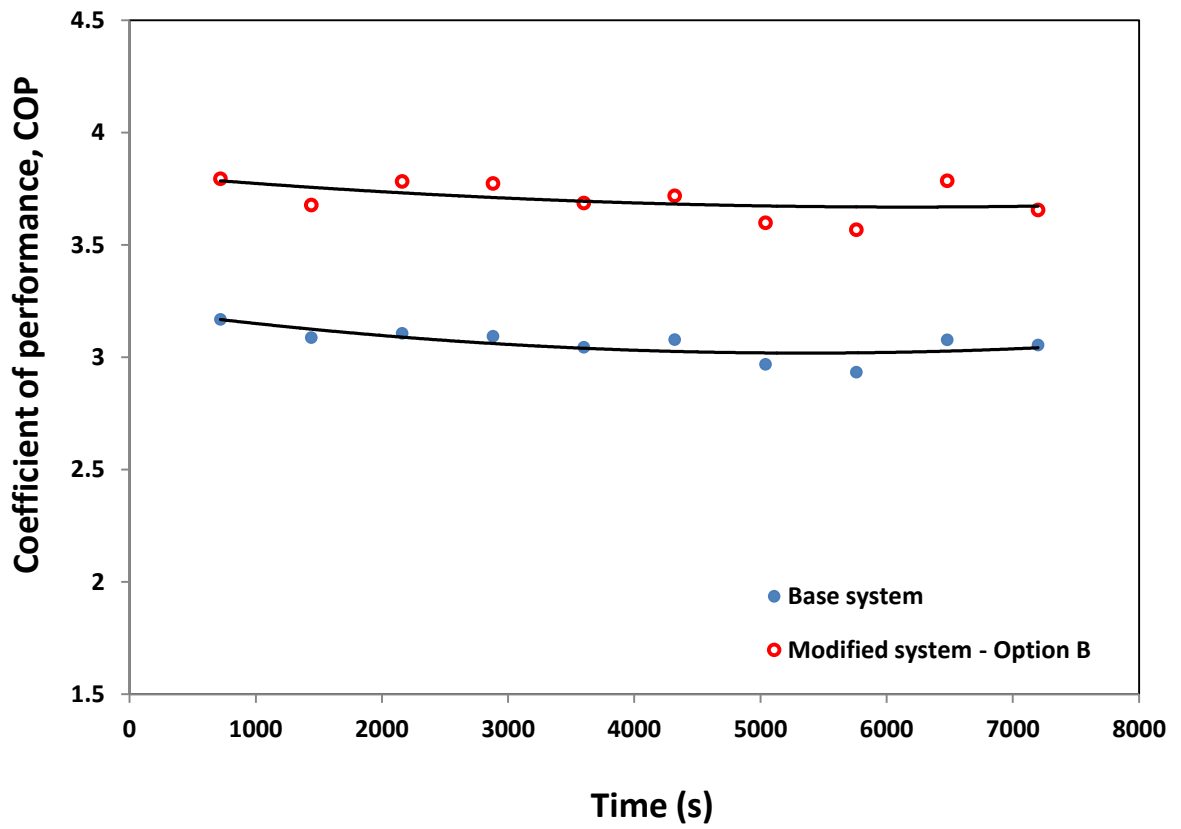
Figure 6.25 Comparison of COP of base system with option 'B' for severest weather conditions.
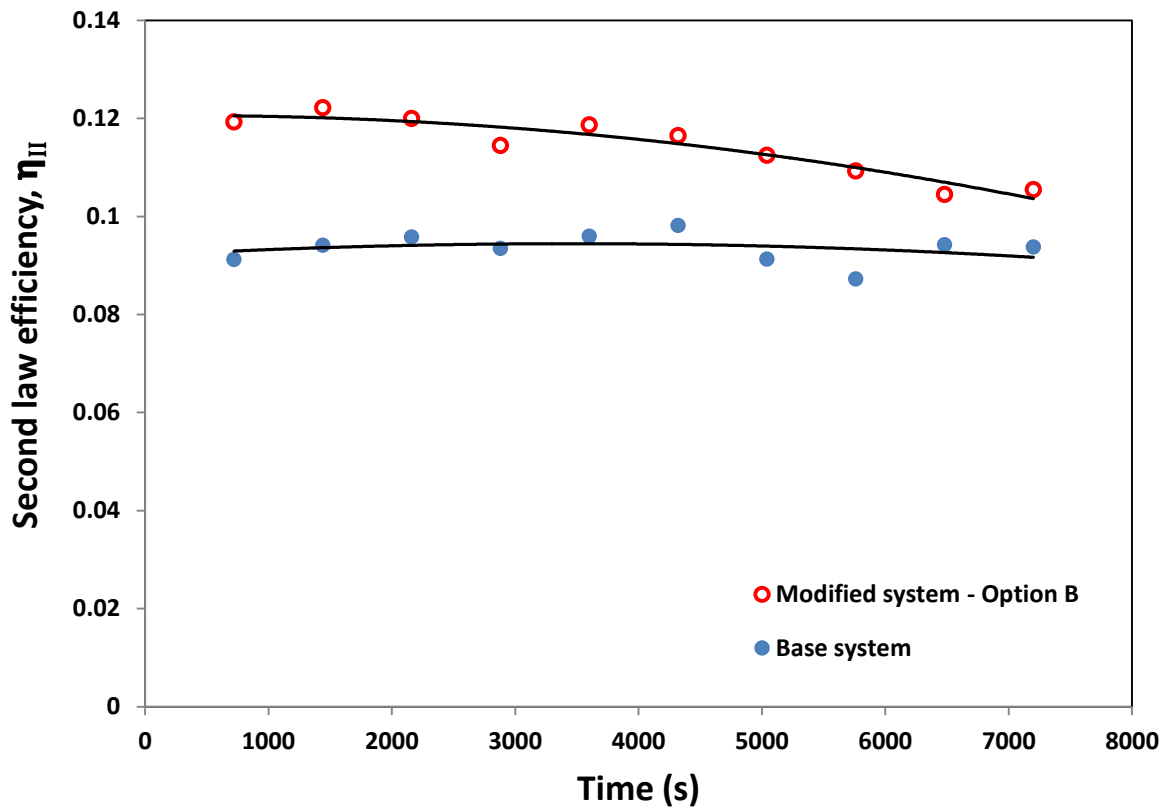
Figure 6.26 Comparison of second law efficiency of base system with option 'B' for severest weather conditions.

Table 6.10 Average values of improvements of modified system over the base system – Option 'B'.

Parameter	Base system	Modified system - option B	Improvement
$\dot{Q}_{ev}$ (kW)	7.84	9.04	15.3 % increase
COP	3.06	3.71	21.1 % increase
$\dot{W}_c$ (kW)	2.56	2.44	4.8 % decrease
η_{II}	0.09	0.12	23.5 % increase

circulated condensate become heated so as to justify the feasibility of the precooling technique using condensate. For this reason, the two experiments are conducted during high ambient temperatures between 41 and 45 $^{\circ}$C. The first experiment is carried out as the baseline, without operating the precooler and the second experiment includes the precooler. During the two experiments, the data was recorded at every minute. Using the available weather forecast, two consecutive days of similar climate conditions are selected for running the experiments. The performance parameters obtained from the base system and those from modified system with option 'B' are then compared. The experimental conditions used during the two experiments are given in Table 6.11.

Variations of air and condensate temperatures across the precooler with experimental time are shown in Fig. 6.27. The difference of precooler inlet and outlet air temperature represents the amount of air precooling achieved. It is observed from Fig. 6.27 that the air temperature difference across the precooler decreases with increase in condensate inlet temperature.

Table 6.11 Experimental conditions for intermediate evaporator inlet air conditions - Option 'B'.

Parameter	Values
Evaporator entering air temperature	27 - 29 $^{\circ}$C
Evaporator entering air relative humidity	40 – 43 %
Volumetric flow rate of air to the evaporator	0.14 m^3/s
Ambient air temperature	40 - 46 $^{\circ}$C
Initial condensate temperature at the precooler inlet	25 $^{\circ}$C
Mass flow rate of condensate through the precooler	0.18 kg/s
Volume of condensate in the tank	0.9 m^3
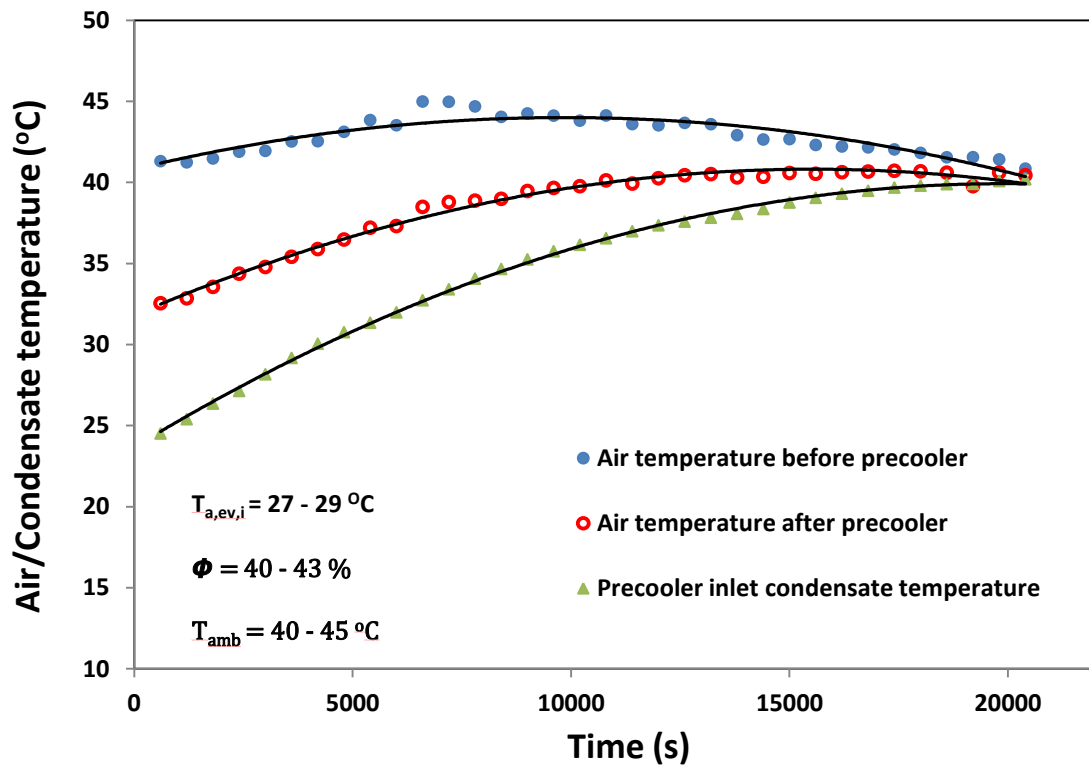
Figure 6.27 Temperature variations across precooler - Option 'B'.

It is interesting to note that the condensate temperature remained effective for air precooling before the condenser until about six hours when the air temperatures at the precooler inlet and exit coincide. The precooler effectiveness in this application is found to be about 0.59. The six hours precooling of condenser inlet air using condensate is quite great in minimizing energy consumption by the VCAC systems and hence the technique can be applied during the peak period of high ambient temperatures.

The change in condenser inlet air temperature had a direct effect on the compressor discharge pressure. Comparison of compressor discharge pressure between the base system and the modified system is shown in Fig 6.28. A significant decrease in discharge pressure is observed for the modified system with option 'B'. The decrease in the discharge pressure is as a result of lowering the condenser inlet air temperature by condensate. It is noted that the discharge pressure of option 'B' increases with time and this is due to the increase in condensate temperature. The decrease in the discharge pressure for the modified system with option 'B' resulted in the decrease in discharge temperature as shown in Fig. 6.29. The resulting advantage of lower discharge pressure and temperature due to decrease in condenser air temperature is decrease in compressor power consumption. Fig. 6.30 shows the comparison of compressor power obtained from the base system and the modified system with option 'B'. The percentage decrease in the compressor power is about 10% at the beginning of the precooling operation and then gradually decreases due to increase in condensate temperature. The average percentage decrease in compressor power during the period of experiment is about 6.7%.

Comparison of COP of the base system with the modified system of option 'B' is shown in Fig. 6.31. It is observed that the COP has increased by about 40% at the beginning of
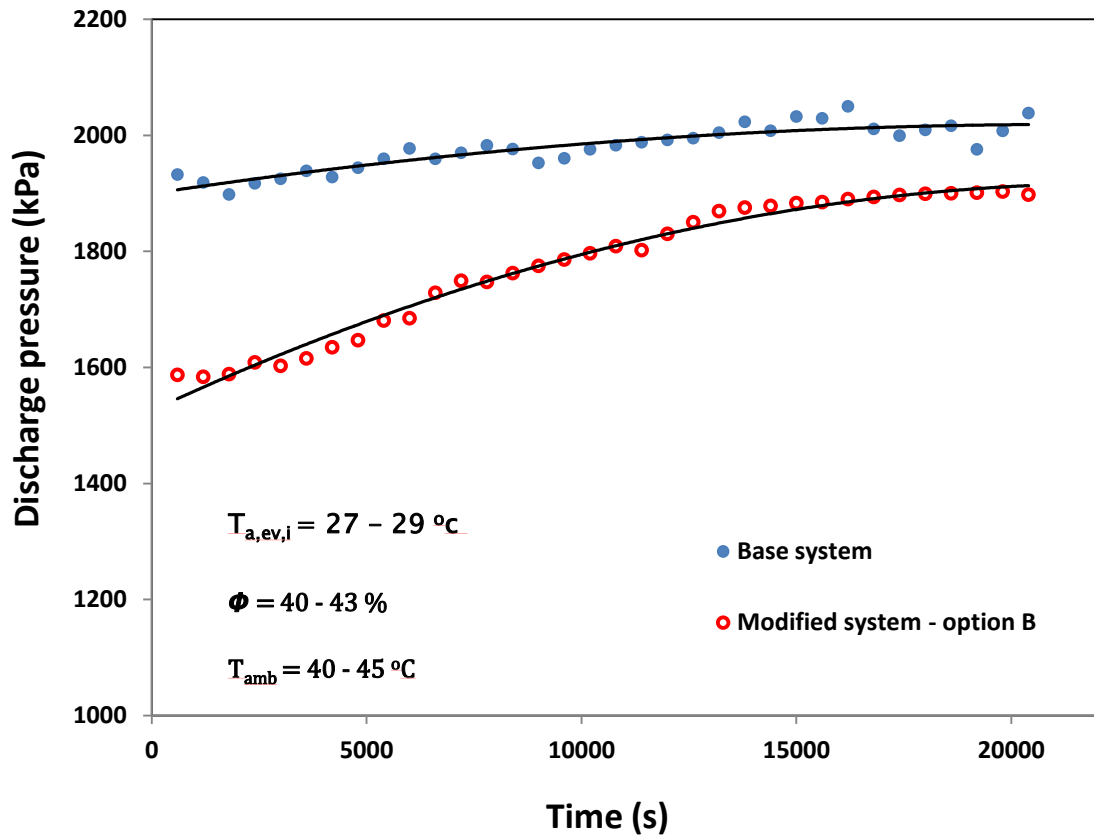
Figure 6.28 Comparison of compressor discharge pressure of base system with modified system - Option 'B'.
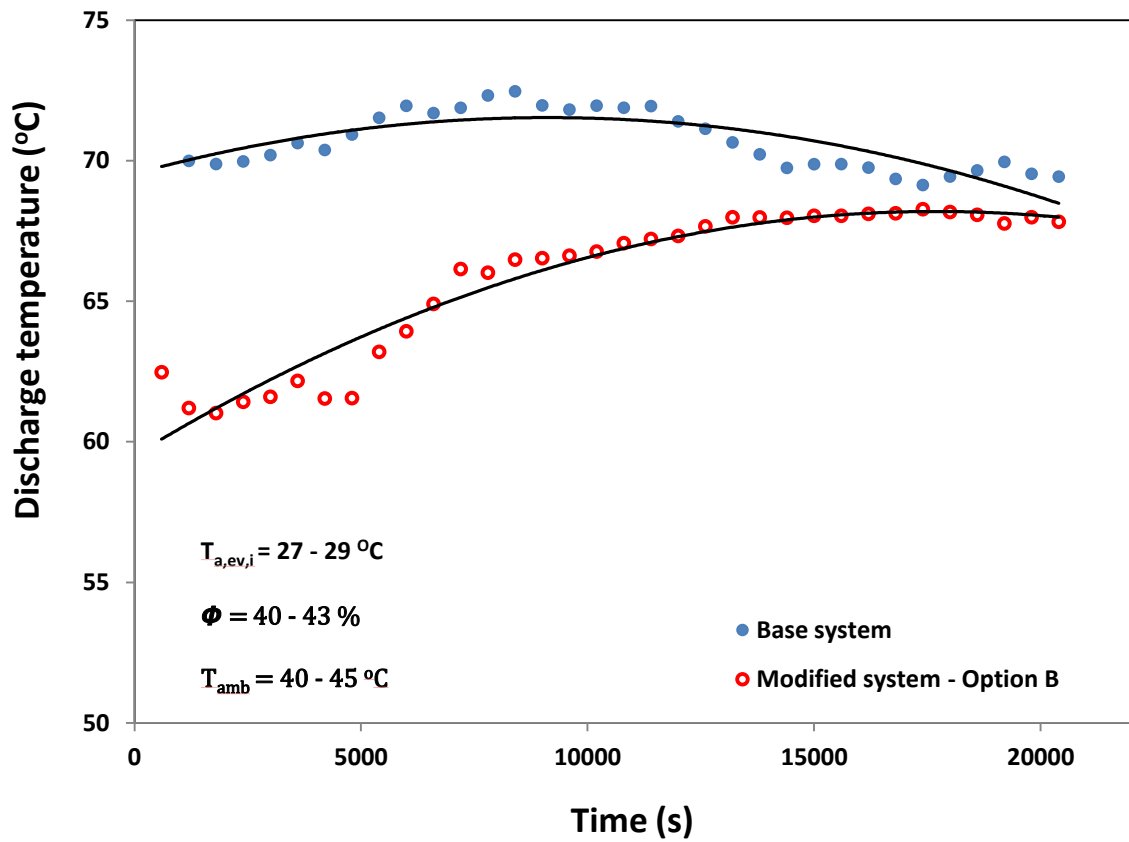
Figure 6.29 Comparison of compressor discharge temperature of base system with modified system - Option 'B'.
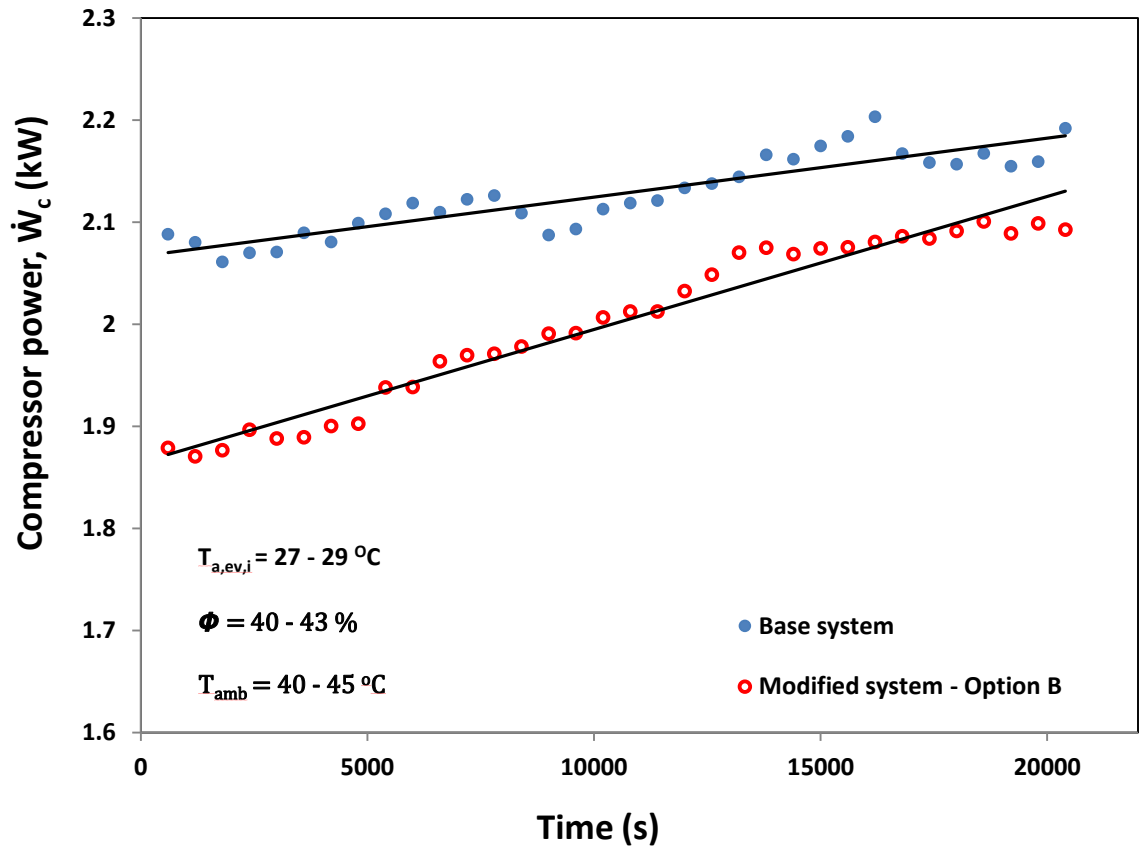
Figure 6.30 Comparison of compressor power consumption of base system with modified system - Option 'B'.
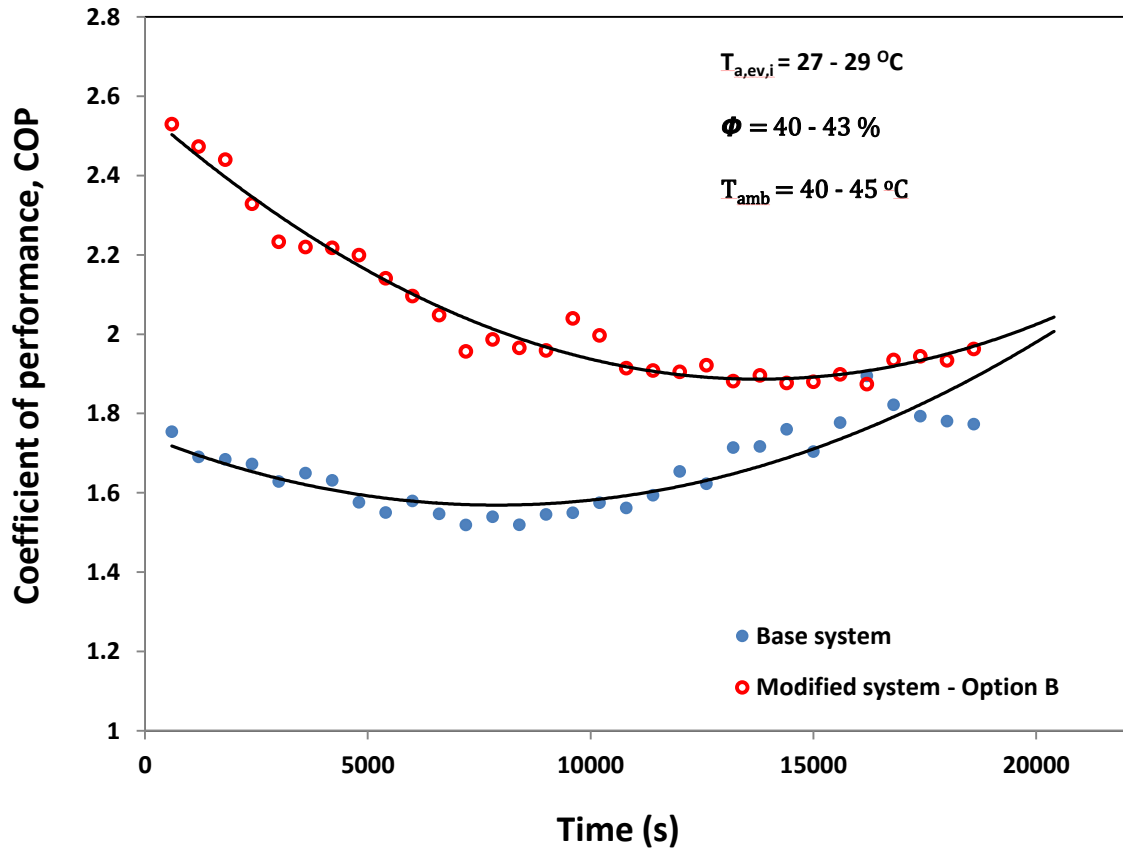
Figure 6.31 Comparison of COP of base system with modified system - Option 'B'.

the air precooling. The average percentage increase in COP during the experimental period is 27.7% when the air entering the condenser is precooled. The increase in COP is as a result of the decrease in compressor power consumption. Fig 6.32 shows the comparison of second law efficiency of the base system and the modified system with option 'B'. It can be observed that the efficiency is improved by about 27.2% on average when the condenser inlet air temperature is lowered by the condensate.
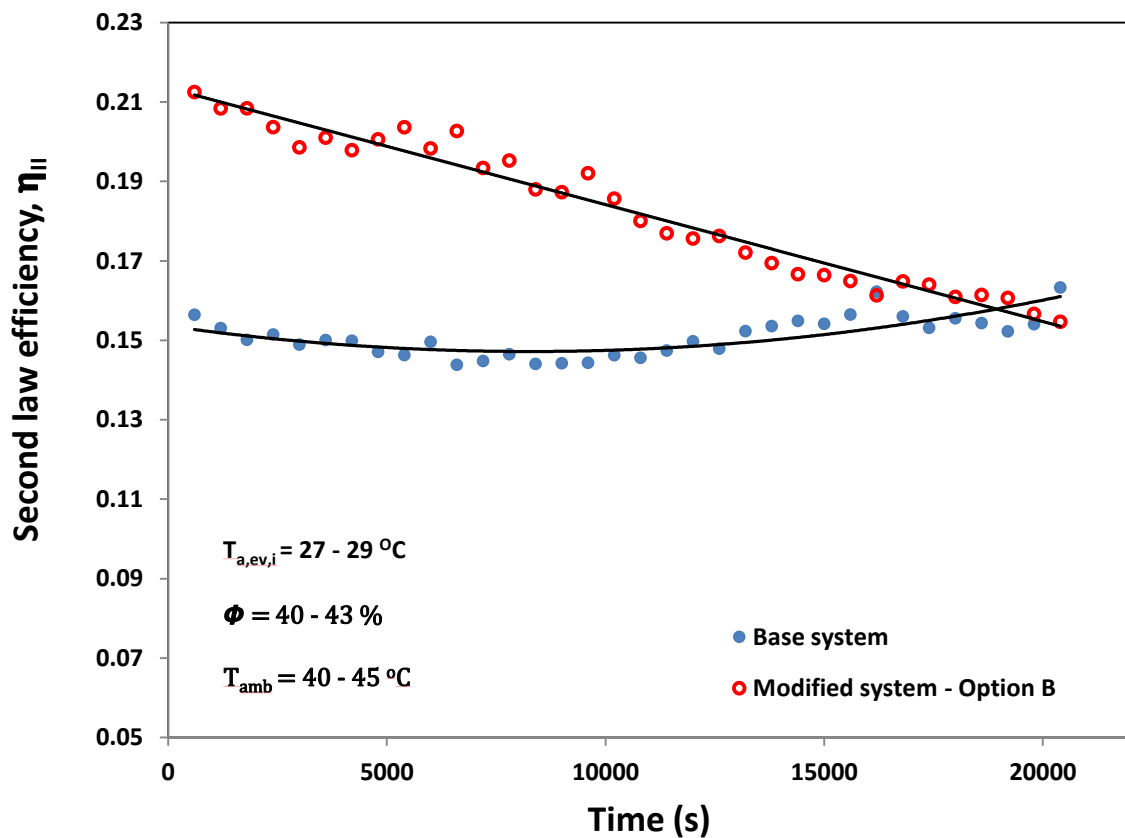
Figure 6.32 Comparison of second law efficiency of base system with modified system - Option 'B'.

6.2.3. Experimental Results for Refrigerant Subcooling – Option 'C'

The purpose of subcooling is to lower the temperature of the high pressure refrigerant after exiting the condenser in order to improve the system performance. This technique is essential in providing enough cooling to the refrigerant so that it becomes completely liquid before entering the expansion valve which provides smooth expansion of the refrigerant at the expansion valve. It is expected that the efficiency of the system will be improved by subcooling the refrigerant. Experimental results for refrigerant subcooling option are presented in this section. The same experimental conditions and procedure presented in section 6.2.1.a are used in this option. The first experiment is the baseline, without operating the subcooler and the second experiment includes the subcooling.

Variations of refrigerant temperatures at the inlet and exit of the subcooler as well as the subcooler effectiveness are shown in Fig. 6.33. It is noted that about 14 $^{\circ}$C subcooling is achieved on average and this is due to the high effectiveness of the subcooler which is around 0.7. The reduction in refrigerant temperature before expansion by subcooling had a direct effect on the system's operating temperature and pressures, and hence the power consumption and cooling effect. Comparison of compressor discharge pressure of the base system with the modified system of option 'C' is shown in Fig. 6.34. An appreciable decrease in the discharge pressure is observed during the subcooling experiment. Since the discharge pressure for option 'C' is decreased, the corresponding discharge temperature is expected to decrease. The corresponding compressor discharge temperature drop can be seen from the comparison of the discharge temperature for the base system with the modified system of option 'C' presented in Fig. 6.35. About 23% reduction in the discharge pressure is noted by subcooling. The advantage of lower
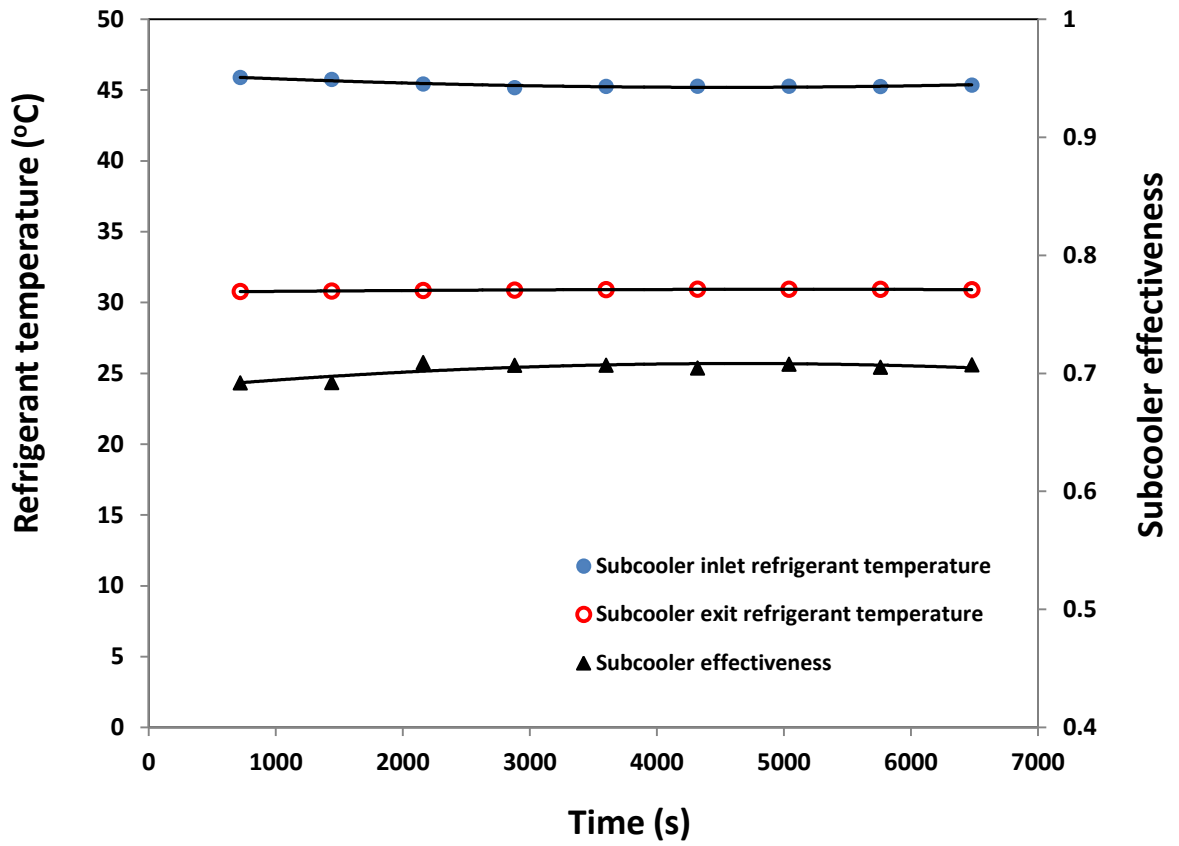
Figure 6.33 Variations of refrigerant temperatures across subcooler and subcooler effectiveness for severest weather conditions – Option 'C'.
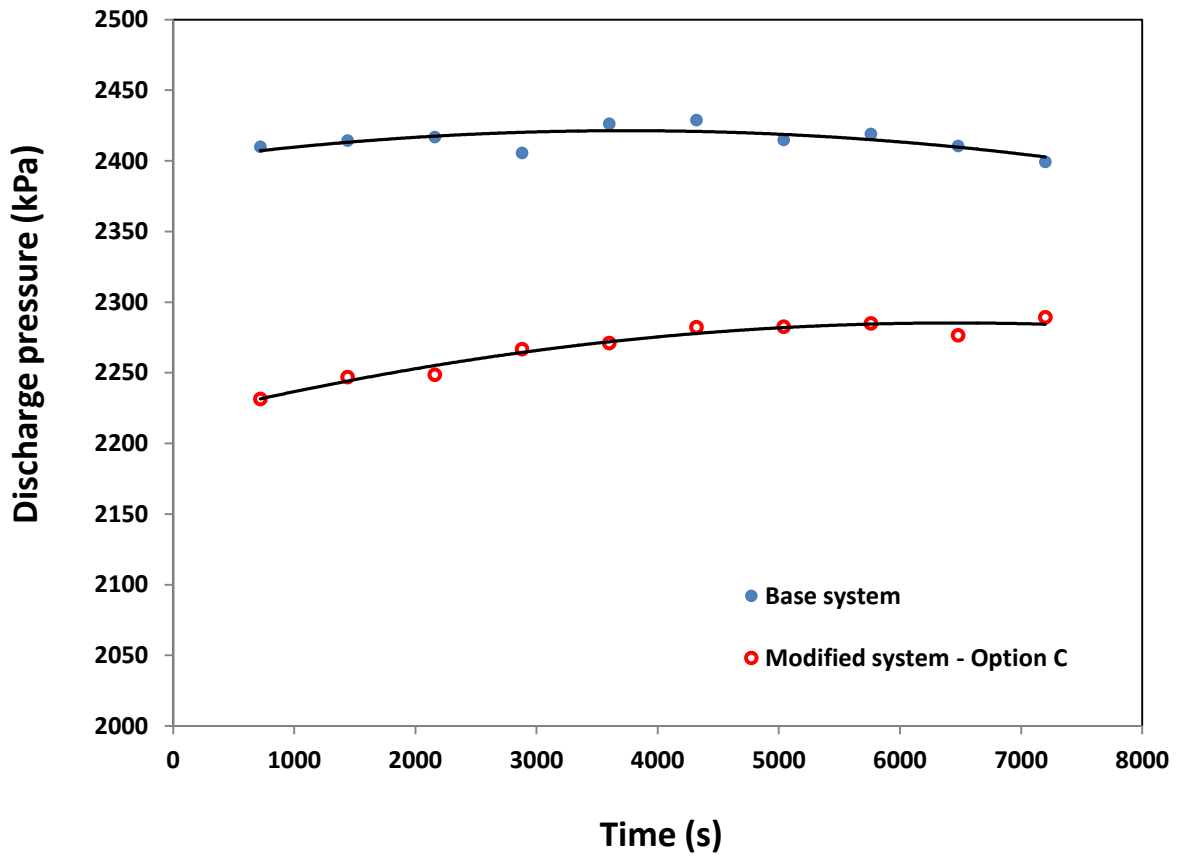
Figure 6.34 Comparison of compressor discharge pressure of the base system with option 'C' for severest weather conditions.
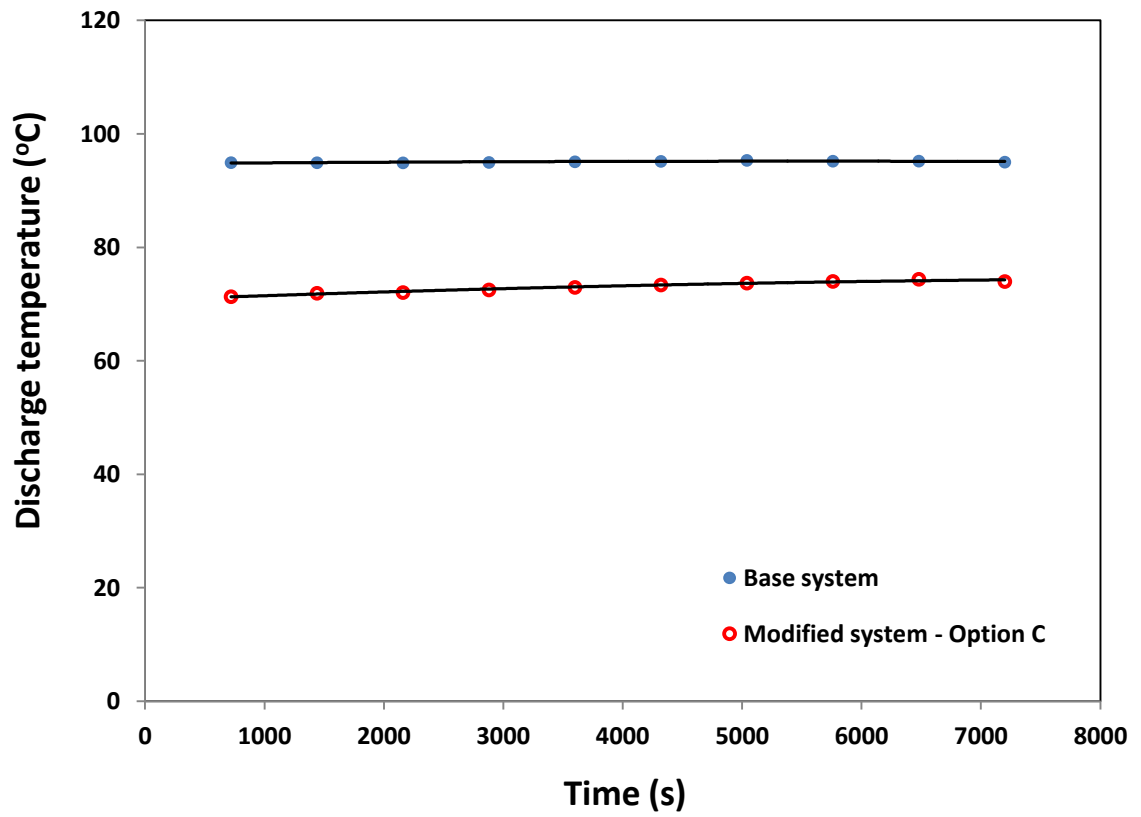
Figure 6.35 Comparison of compressor discharge temperature of base system with option 'C' for severest weather conditions.

discharge temperature is that there will be less strain on the compressor and hence a longer compressor's life expectancy is possible. Fig. 6.36 shows the decrease in compressor power consumption of about 3.7% and this is as a result of lower compressor discharge pressure and temperature due to refrigerant subcooling. It is observed from the figure that the compressor power for the modified system with option 'C' increase sharply. This increase in compressor power is due to the increase in subcooler inlet condensate temperature with time which reduces the amount of subcooling as seen in Fig. 6.37. The evaporator exit air temperature is also decreased as a result of lower evaporating temperature due to subcooling as depicted in Figs. 6.38 and Fig. 6.39.

Comparison of cooling effect of base system with option 'C' is shown in Fig. 6.40 and about 25.6% increase in the cooling effect due to subcooling is observed. The increase in the cooling effect is attributed to the lower evaporating temperature and hence the evaporator exit air temperature. The improvement of cooling effect due to subcooling and the corresponding decrease in compressor power consumption resulted in significant increase in COP, and hence an increase in second law efficiency as noted in Figs. 6.41 and 6.42.

6.3. Comparison of Experimental Results for Options 'A', 'B' and 'C'

Experiments conducted at the severest weather conditions for the three options are carried out at the same experimental conditions and for this reason the results are compared. Significant reduction in compressor power consumption is noted for all the three options as shown in Table 6.12. But the reduction in power is higher for option 'A', followed by
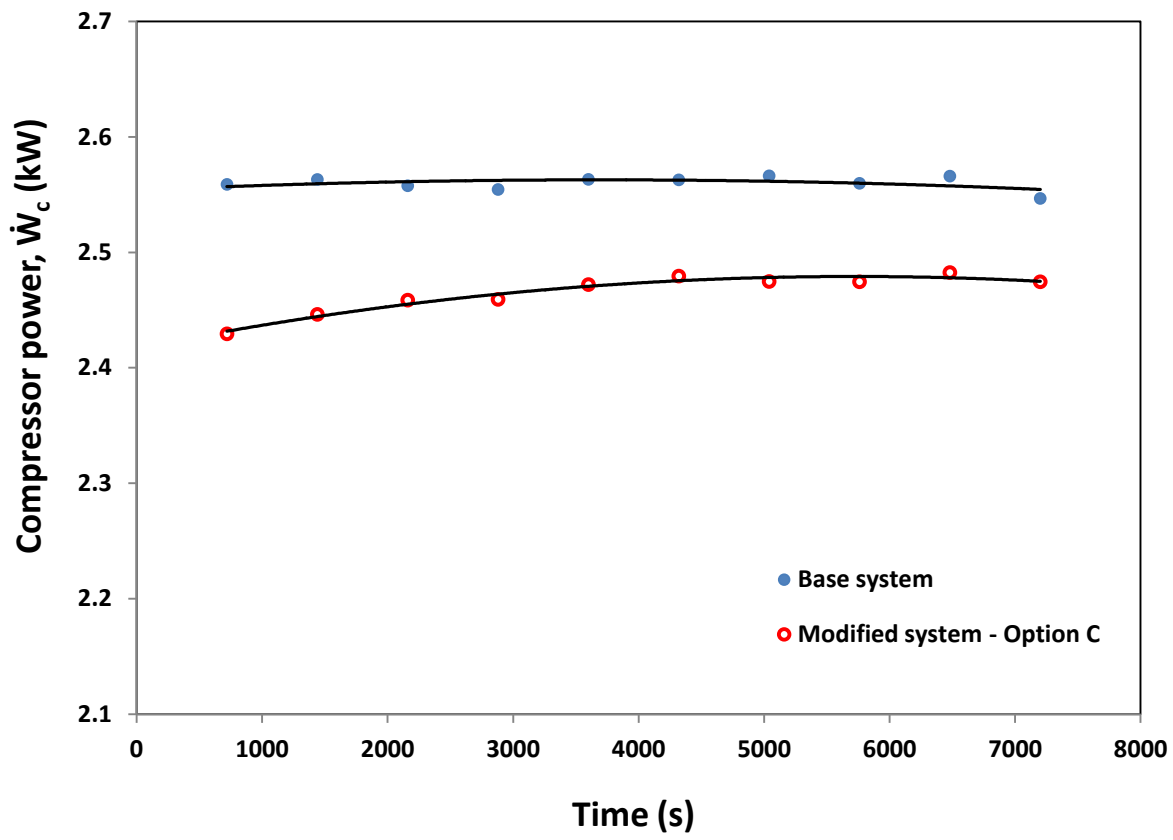
Figure 6.36 Comparison of compressor power consumption of base system with option 'C' for severest weather conditions.
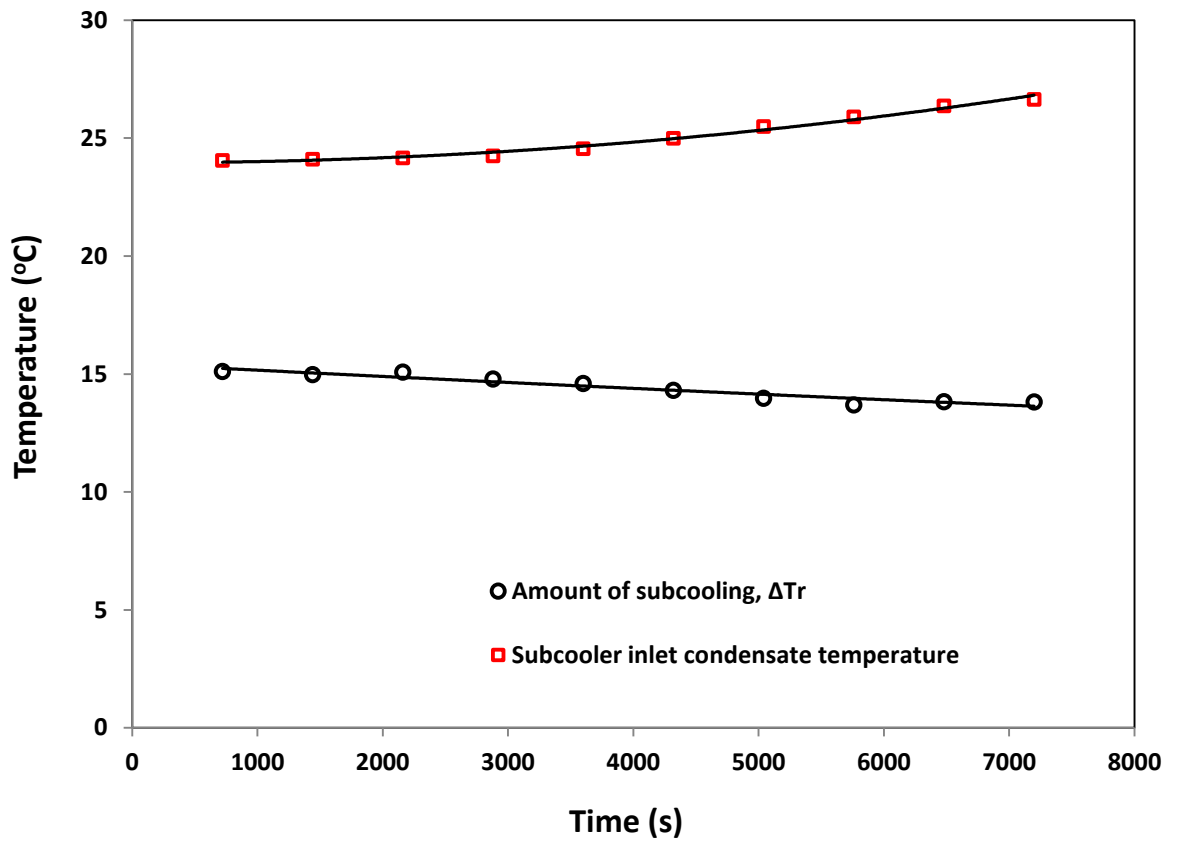
Figure 6.37 Variation of subcooler inlet condensate temperature and amount of subcooling for severest weather conditions - Option 'C'.
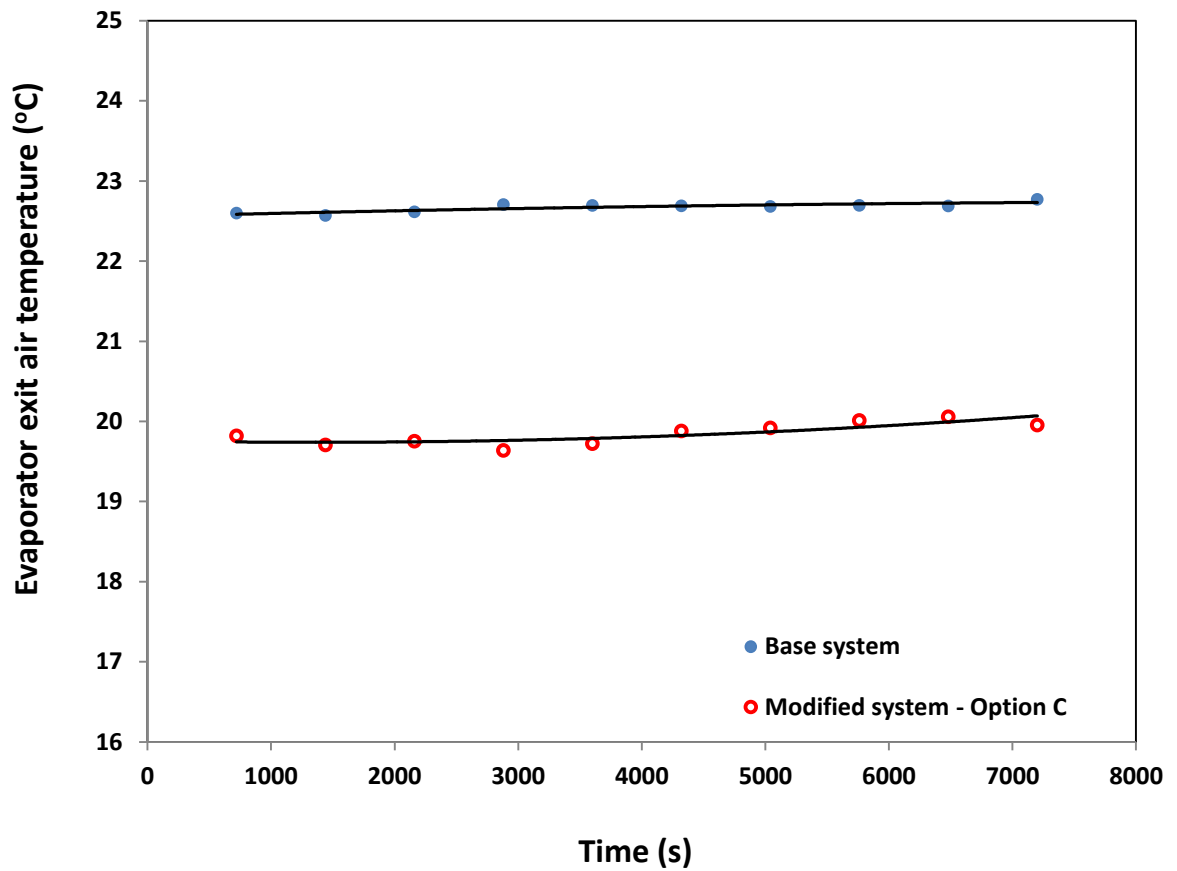
Figure 6.38 Comparison of evaporator exit air temperature of base system with option 'C' for severest weather conditions.
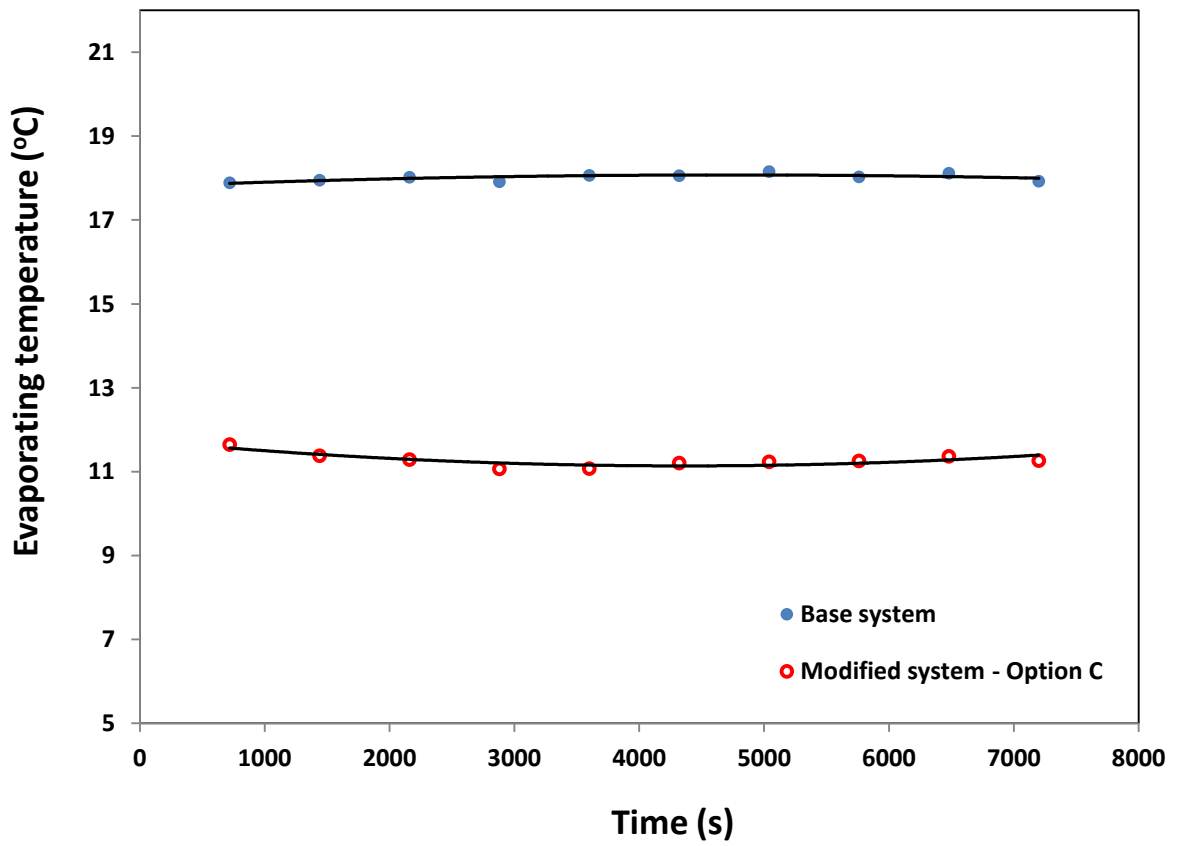
Figure 6.39 Comparison of evaporating temperature of base system with option 'C' for severest weather conditions.
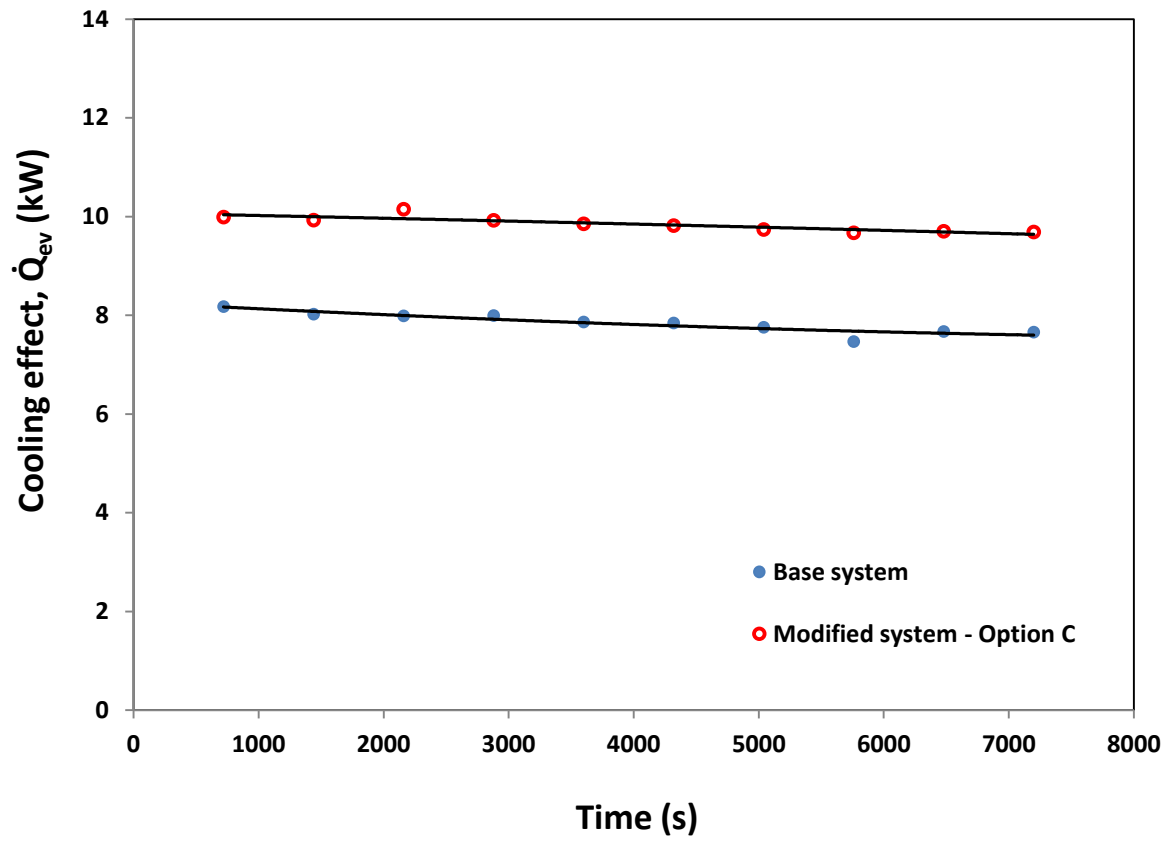
Figure 6.40 Comparison of cooling effect of base system with option 'C' for severest weather conditions.
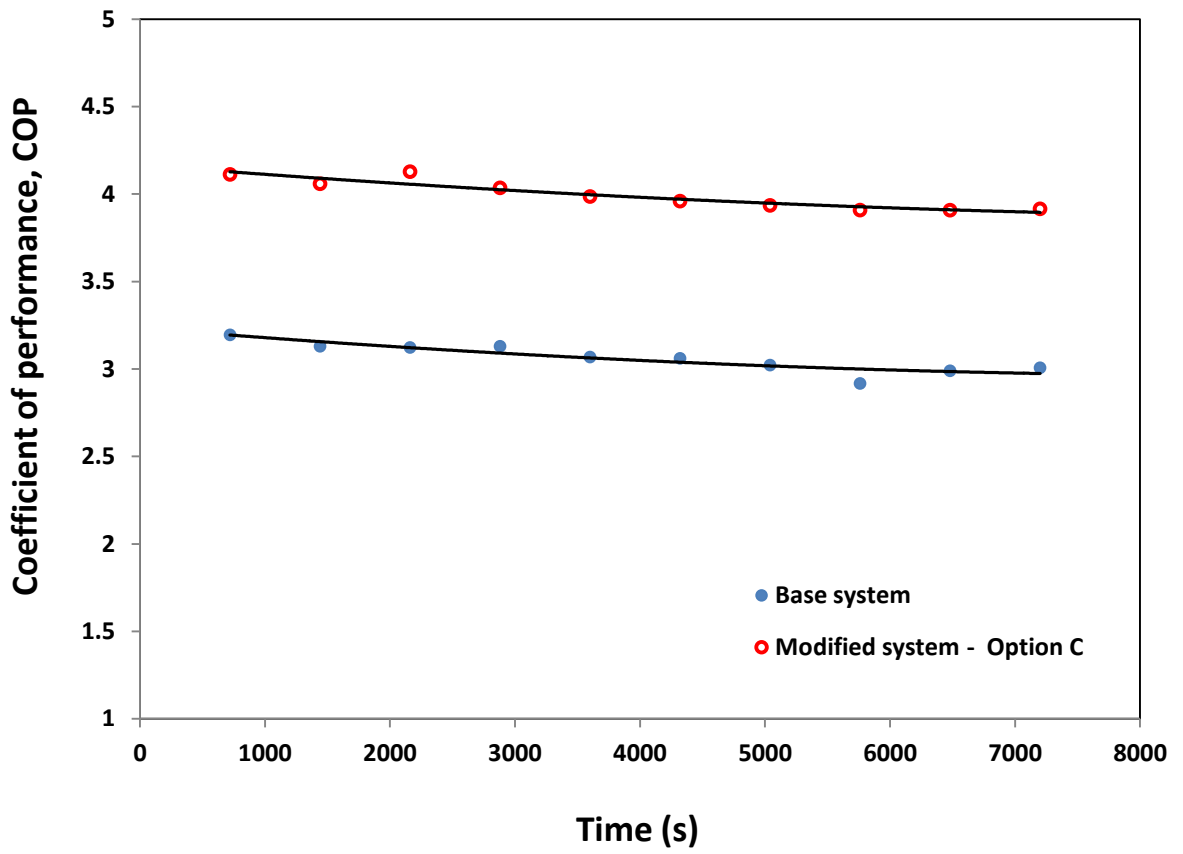
Figure 6.41 Comparison of COP of base system with option 'C' for severest weather conditions.
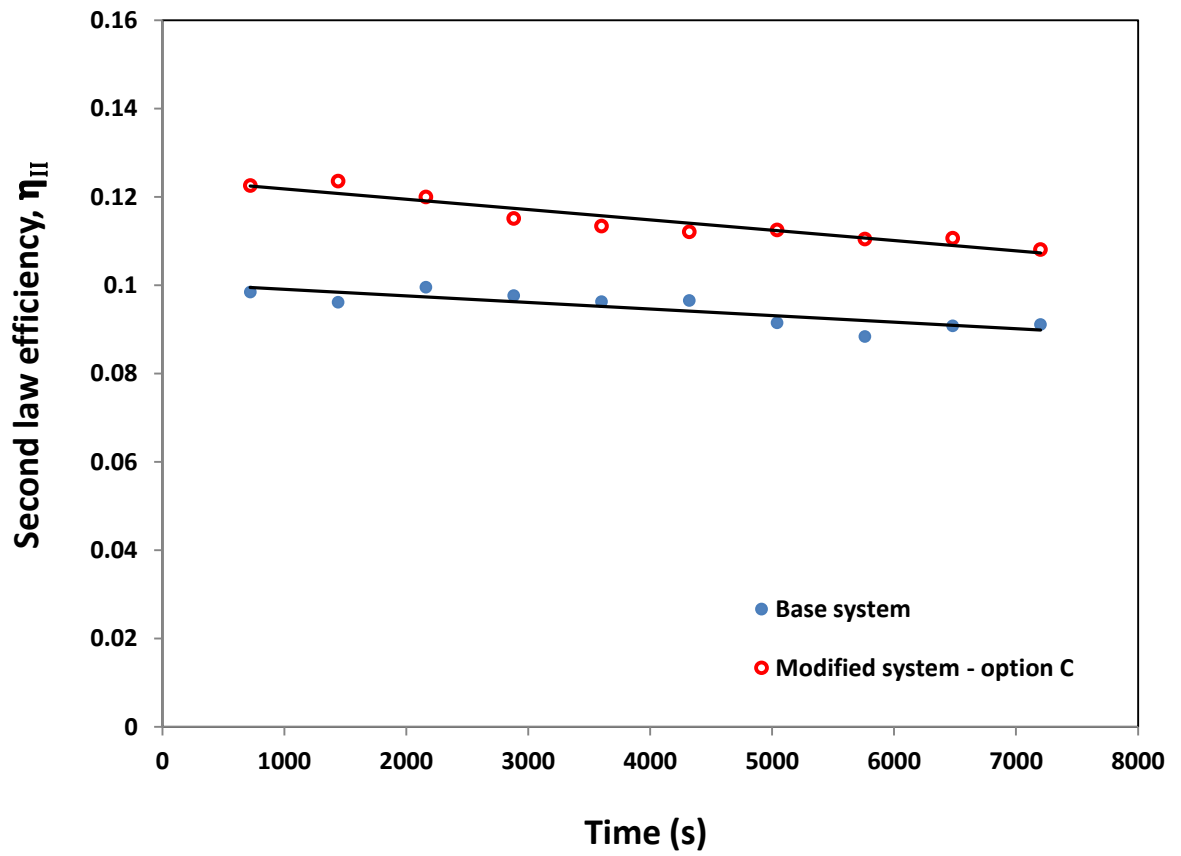
Figure 6.42 Comparison of second law efficiency of base system with option 'C' for severest weather conditions.

Table 6.12 Comparison of experimental results of base system with the modified system for severest weather conditions.

Quantity	Average Values			
		Modified system		
	Base system	Option 'A'	Option 'B'	Option 'C'
COP	3.06	4.01	3.71	4.00
Q_{ev} (kW)	7.84	9.74	9.05	9.85
$\dot{W}_c$ (kW)	2.56	2.43	2.44	2.47
η_{II}	0.095	0.118	0.117	0.115
$T_{a,ev,e}$ (^oC)	22.7	20.1	20.3	19.9
$\dot{m}_c$ (kg/h)	7.2	6.9	7.4	7.6

Table 6.13 Improvement of the modified system over the base system.

	Coefficient of performance, COP	Second law efficiency, η_{II}	Compressor power, $\dot{W}_c$
Option 'A'	30.94 % increase	24.84 % increase	5.08 % decrease
Option 'B'	21.11 % increase	23.51 % increase	4.82 % decrease
Option 'C'	30.42 % increase	21.53 % increase	3.70 % decrease

option 'B', then option 'C'. Comparing the COP for the base system with the modified system, it can be noted that the COP of the modified system with option 'A' is higher. The second law efficiency which describes the actual performance of the system is found to be highest for option 'A', followed by option 'B' then option 'C'. This means that the thermodynamics imperfections are more in option 'C' set-up. However, the efficiency of the system with option 'C' is still better than that for the base system.

The rate of condensate extraction from the system during the four experiments is also compared as shown in the table. The rate of condensate extraction for experiment with option 'A' is found to be almost the same with that obtained from the base system experiment. The rates of condensate extraction for the system with options 'B' and 'C' are also almost the same with that for the base system with 3% and 5% higher, respectively. The overall assessment of the three options is that option 'A' gives better system performance improvement followed by option 'B', then option 'C'.

It is to be noted that the power consumed by the condensate pump is not considered in all the analyses since the power input of auxiliary equipment per ton of cooling is generally low for large air conditioning systems [72].

CHAPTER 7

UNCERTAINTY AND ERROR ANALYSES

No physical quantity can be measured with perfect certainty. There are always errors in measurements. A method of estimating uncertainty in experimental results is presented in [73] and the method is applied in this thesis. In the present study, the temperatures, pressures, relative humidity, mass flow rate of air and compressor current are measured using the instruments mentioned in section 5.6 with respective instruments errors.

Uncertainties of calculated parameters such as cooling effect, COP, and second law efficiency are calculated on the basis of the uncertainties in the measured parameters. Uncertainties due to instrument errors are already given in section 5.6 and the uncertainty due to random error $\delta_{r,e}$ of any quantity is determined using the standard deviation of the mean as:

$$\delta_{r,e} = \left[\frac{\sum_{i=1}^{N}(x_i-\tilde{x})^2}{N(N-1)}\right]^{1/2} \tag{7.1}$$

Where N is the number of measurements and $\tilde{x}$ is the arithmetic mean of each reading which is given as:

$$\tilde{x} = \frac{1}{N}\sum_{i=1}^{N} x_i \tag{7.2}$$

The coefficient of determination that correlates analytical results with experimental data

is expressed as:

$$r^2 = \frac{[N \sum x_i y_i - (\sum x_i)(\sum y_i)]^2}{[N \sum x_i^2 - (\sum x_i)^2][N \sum y_i^2 - (\sum y_i)^2]} \qquad (7.3)$$

For any result R given as a function of independent variables $x_1, x_2, x_3 \ldots\ldots x_n$. Thus,

$$R = f(x_1, x_2, x_3, \ldots\ldots\ldots\ldots x_n) \qquad (7.4)$$

Consider δ_R to be the uncertainty in the calculated result, and $\delta_1, \delta_2, \delta_3, \ldots\ldots \delta_n$ be the uncertainties in the independent variables, then the uncertainty in the calculated result is given as:

$$\delta_R = \left[\left(\frac{\partial R}{\partial x_1} \delta_1 \right)^2 + \left(\frac{\partial R}{\partial x_2} \delta_2 \right)^2 + \ldots + \left(\frac{\partial R}{\partial x_{1n}} \delta_n \right)^2 \right]^{1/2} \qquad (7.5)$$

7.1.   Uncertainty Analysis of the Experimental Results

The cooling effect of the system $\dot{Q}_{ev}$ is a function of air mass flow rate and enthalpy difference across the evaporator as shown in chapter 3. Reference to Eq. (7.5), uncertainty in the cooling effect is determined as:

$$\delta_{\dot{Q}_{ev}} = \left[\left(\frac{\partial \dot{Q}_{ev}}{\partial \dot{m}_a} \delta_{\dot{m}_a} \right)^2 + \left(\frac{\partial \dot{Q}_{ev}}{\partial h_{a,ev,i}} \delta_{h_{a,ev,i}} \right)^2 + \left(\frac{\partial \dot{Q}_{ev}}{\partial h_{a,ev,e}} \delta_{h_{a,ev,e}} \right)^2 \right]^{1/2} \qquad (7.6)$$

The enthalpy of the air is a function of temperature and humidity and is given as:

$$h = T + \frac{0.622 \emptyset P_g}{P - \emptyset P_g} (2501.3 + 1.86T) \qquad (7.7)$$

where P_g is the saturated vapor pressure determined at T.

From Eq. (7.7),

$$\frac{\partial h}{\partial T} = 1 + \frac{1.1569 \emptyset P_g}{P - \emptyset P_g} \tag{7.8}$$

$$\frac{\partial h}{\partial \emptyset} = \frac{0.622 P_g (2501.3 + 1.86T)(P - \emptyset P_g + \emptyset)}{(P - \emptyset P_g)^2} \tag{7.9}$$

and therefore,

$$\delta_h = \left[\left(\frac{\partial h}{\partial T} \delta_T \right)^2 + \left(\frac{\partial h}{\partial \emptyset} \delta_\emptyset \right)^2 \right]^{1/2} \tag{7.10}$$

The compressor power consumption is obtained from the measured current with voltage source of 220 V. In this case, the compressor power is a function of current only and the uncertainty in the power is:

$$\delta_{\dot{W}_c} = \left(\frac{\partial \dot{W}_c}{\partial I} \delta_I \right) \tag{7.11}$$

Uncertainties in *COP* and *COP_{max}* are calculated, respectively, as:

$$\delta_{COP} = \left[\left(\frac{\partial COP}{\partial \dot{Q}_{ev}} \delta_{\dot{Q}_{ev}} \right)^2 + \left(\frac{\partial COP}{\partial \dot{W}_c} \delta_{\dot{W}_c} \right)^2 \right]^{1/2} \tag{7.12}$$

$$\delta_{COP_{max}} = \left[\left(\frac{\partial COP_{max}}{\partial T_L} \delta_{T_L} \right)^2 + \left(\frac{\partial COP_{max}}{\partial T_H} \delta_{T_H} \right)^2 \right]^{1/2} \tag{7.13}$$

where
$$\delta_{T_L} = \left[\left(\frac{\partial T_L}{\partial T_{a,ev,i}} \delta_{T_{a,ev,i}} \right)^2 + \left(\frac{\partial T_L}{\partial T_{a,ev,e}} \delta_{T_{a,ev,e}} \right)^2 \right]^{1/2} \tag{7.14}$$

The second law efficiency uncertainty is calculated as:

$$\delta_{\eta_{II}} = \left[\left(\frac{\partial \eta_{II}}{\partial COP} \delta_{COP} \right)^2 + \left(\frac{\partial \eta_{II}}{\partial COP_{max}} \delta_{COP_{max}} \right)^2 \right]^{1/2} \tag{7.15}$$

The uncertainty values of the experimental data for the base system and options 'A', 'B' and 'C' at severest weather conditions are calculated using the above procedure and is given in Tables 7.1 to 7.4.

7.2.   Error Analysis of Analytical Results

In order to investigate how well the predicted condensate obtained by the analytical model fits the experimental extracted condensate, the two data sets are compared using the statistical relations presented earlier. The analytical and experimental results of daily condensate extraction rates are plotted against each other and the coefficients of determination, r^2 are displayed for the month of June through September in Figs. 7.1 - 7.4, respectively. The correlation equations are also shown in the figure. The figures indicate that there is good agreement between the analytical and experimental results.

Table 7.1 Uncertainty values of experimental results: Base system.

Description	Average Value	Total Uncertainty Value	Total Uncertainty (%)
Base system			
Measured parameters			
Evaporator inlet air temperature, ^{o}C	36.06	±0.20	±0.55
Evaporator exit air temperature, ^{o}C	22.67	±0.21	±0.93
Evaporator inlet air relative humidity	0.78	±0.0263	±3.37
Evaporator exit air relative humidity	0.94	±0.0256	±2.72
Condenser inlet air temperature, ^{o}C	38.18	±0.23	±0.60
Compressor electric current, A	11.64	±0.24	±2.04
Suction pressure, kPa	578.9	±4.16	±0.72
Discharge pressure, kPa	2416	±7.18	±0.30
Calculated parameters			
Mass flow rate of air, kg/s	0.159	±0.00318	±2
Cooling effect, kW	7.84	±0.49	±6.25
Compressor power, kW	2.56	±0.052	±2.03
Coefficient of performance COP	3.064	±0.2	±6.56
Second law efficiency	0.0946	±0.0068	±7.2

Table 7.2 Uncertainty values of experimental results: Option 'A'.

Description	Average Value	Total Uncertainty Value	Total Uncertainty (%)
Option 'A'			
Measured parameters			
Evaporator inlet air temperature, ^{o}C	36.12	±0.22	±0.61
Evaporator exit air temperature, ^{o}C	20.1	±0.22	±1.09
Evaporator inlet air relative humidity	0.81	±0.0261	±3.21
Evaporator exit air relative humidity	0.94	±0.0262	±2.79
Condenser inlet air temperature, ^{o}C	36.16	±0.24	±0.94
Compressor electric current, A	11.04	±0.23	±2.08
Suction pressure, kPa	521.5	±4.23	±0.81
Discharge pressure, kPa	2240	±7.85	±0.35
Calculated parameters			
Mass flow rate of air, kg/s	0.159	±0.00318	±2
Cooling effect, kW	9.74	±0.49	±5.03
Compressor power, kW	2.43	±0.0504	±2.07
Coefficient of performance COP	4.01	±0.2	±4.98
Second law efficiency	0.118	±0.007	±5.94

Table 7.3 Uncertainty values of experimental results: Option 'B'.

Description	Average Value	Total Uncertainty Value	Total Uncertainty (%)
Option 'B'			
Measured parameters			
Evaporator inlet air temperature, ^{o}C	36.02	±0.24	±0.67
Evaporator exit air temperature, ^{o}C	20.34	±0.24	±1.18
Evaporator inlet air relative humidity	0.79	±0.0263	±3.33
Evaporator exit air relative humidity	0.95	±0.0259	±2.73
Condenser inlet air temperature, ^{o}C	36.9	±0.24	±0.65
Compressor electric current	11.07	±0.23	±2.08
Suction pressure, kPa	540.2	±3.92	±0.73
Discharge pressure kPa	2261	±8.13	±0.34
Calculated parameters			
Mass flow rate of air, kg/s	0.159	±0.00318	±2
Cooling effect, kW	9.04	±0.48	±5.31
Compressor power, kW	2.44	±0.0513	±2.1
Coefficient of performance COP	3.71	±0.21	±5.66
Second law efficiency	0.117	±0.0075	±6.41

Table 7.4 Uncertainty values of experimental results: Option 'C'.

Description	Average Value	Total Uncertainty Value	Total Uncertainty (%)
Option 'C'			
Measured parameters			
Evaporator inlet air temperature, ^{o}C	36.24	±0.208	±0.57
Evaporator exit air temperature, ^{o}C	19.85	±0.21	±1.06
Evaporator inlet air relative humidity	0.79	±0.0261	±3.30
Evaporator exit air relative humidity	0.91	±0.0257	±2.82
Condenser inlet air temperature, ^{o}C	35.86	±0.23	±0.64
Compressor electric current	11.2	±0.23	±2.05
Suction pressure, kPa	554.1	±4.45	±0.80
Discharge pressure, kPa	2266	±8.27	±0.36
Calculated parameters			
Mass flow rate of air, kg/s	0.159	±0.00318	±2
Cooling effect, kW	9.85	±0.49	±4.97
Compressor power, kW	2.47	±0.0512	±2.1
Coefficient of performance COP	3.99	±0.2	±5.01
Second law efficiency	0.115	±0.0068	±5.91

134
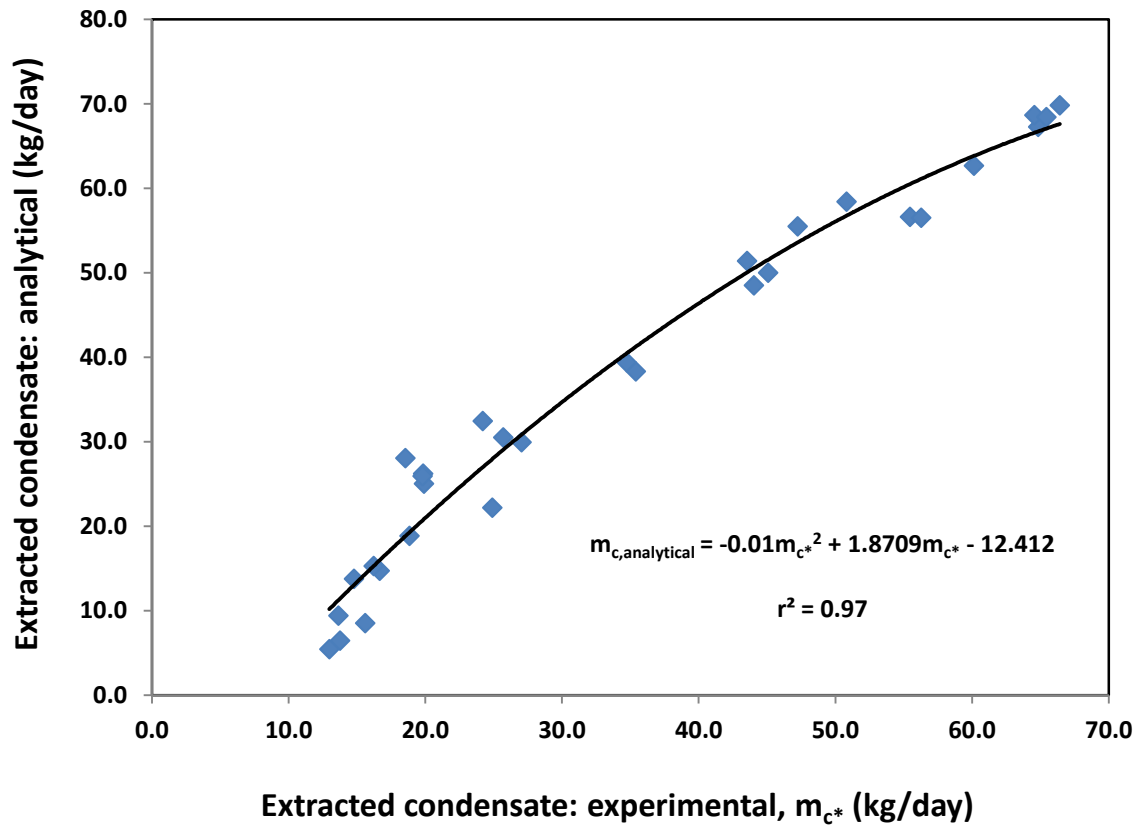
Figure 7.1 Polynomial curve fitting of the analytical versus experimental condensate extracted in June.

The equation shown on the figure:

$$m_{c,analytical} = -0.01m_{c*}^2 + 1.8709m_{c*} - 12.412$$

$$r^2 = 0.97$$
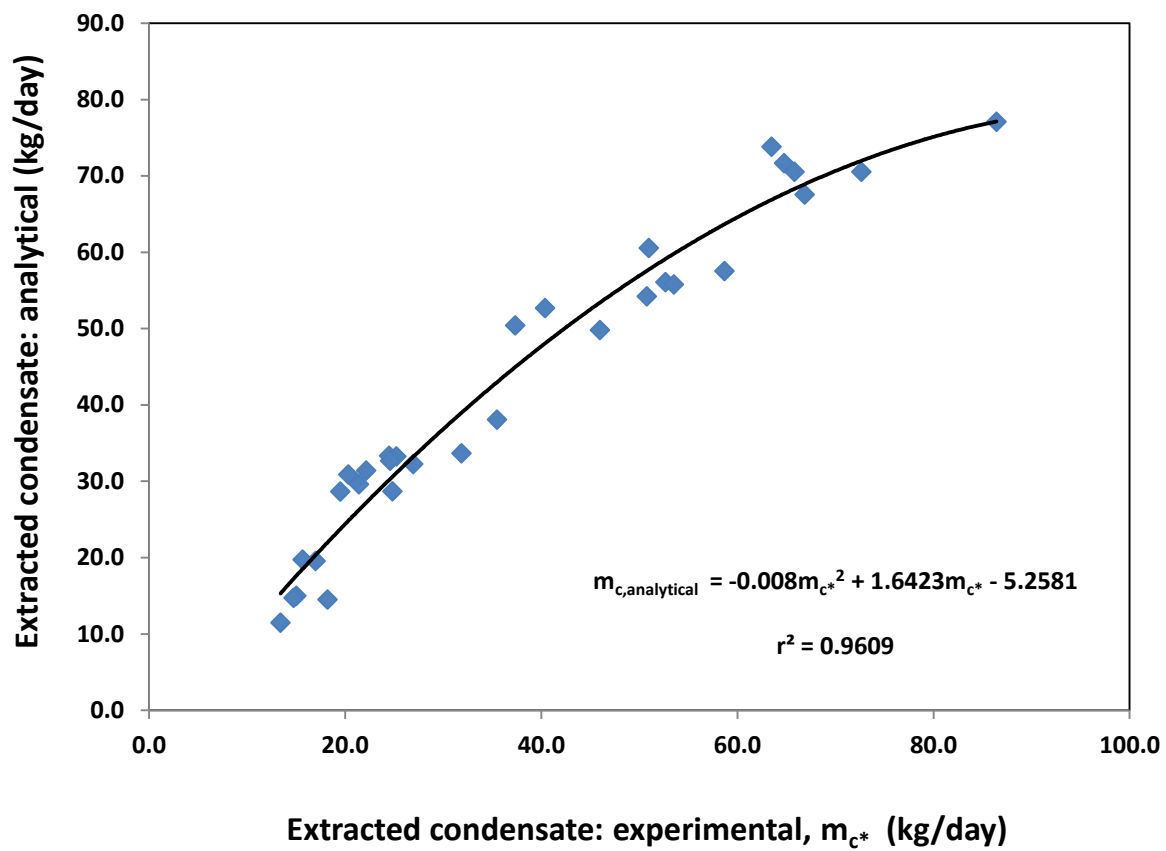
Figure 7.2 Polynomial curve fitting of the analytical versus experimental condensate extracted in July.
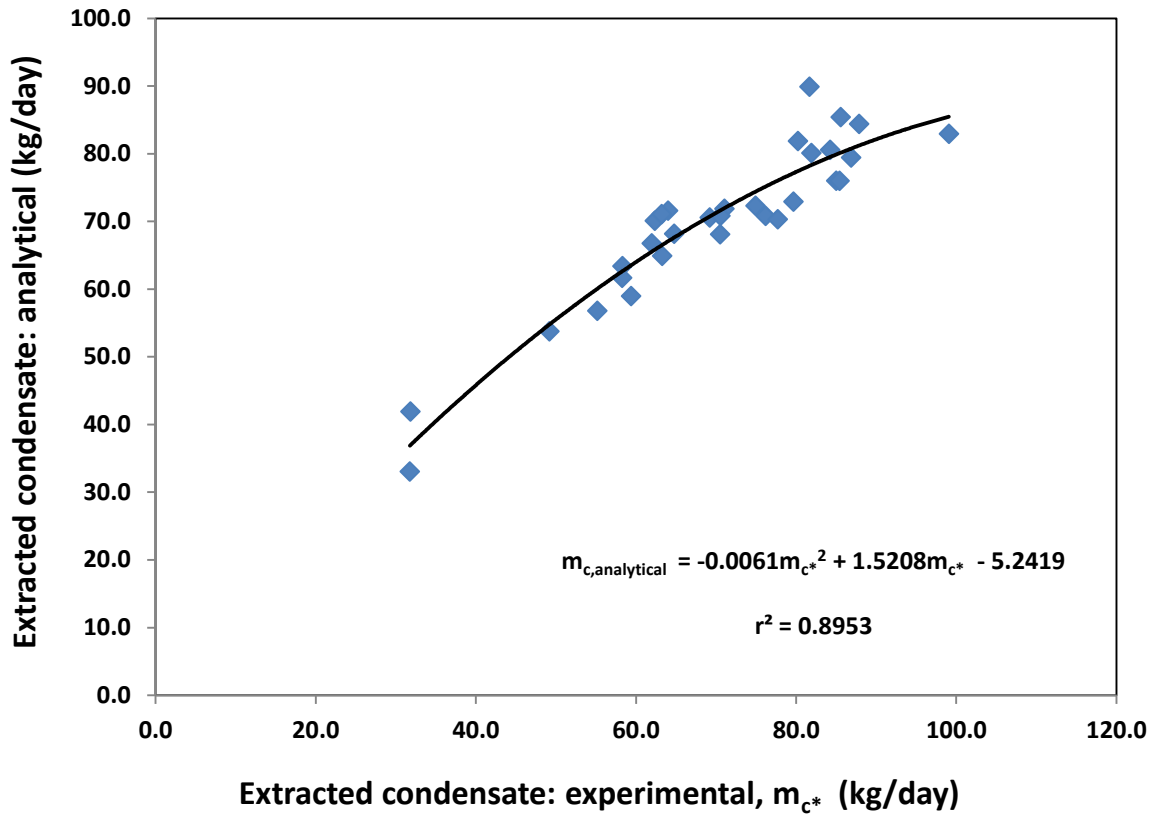
Figure 7.3 Polynomial curve fitting of the analytical versus experimental condensate extracted in August.
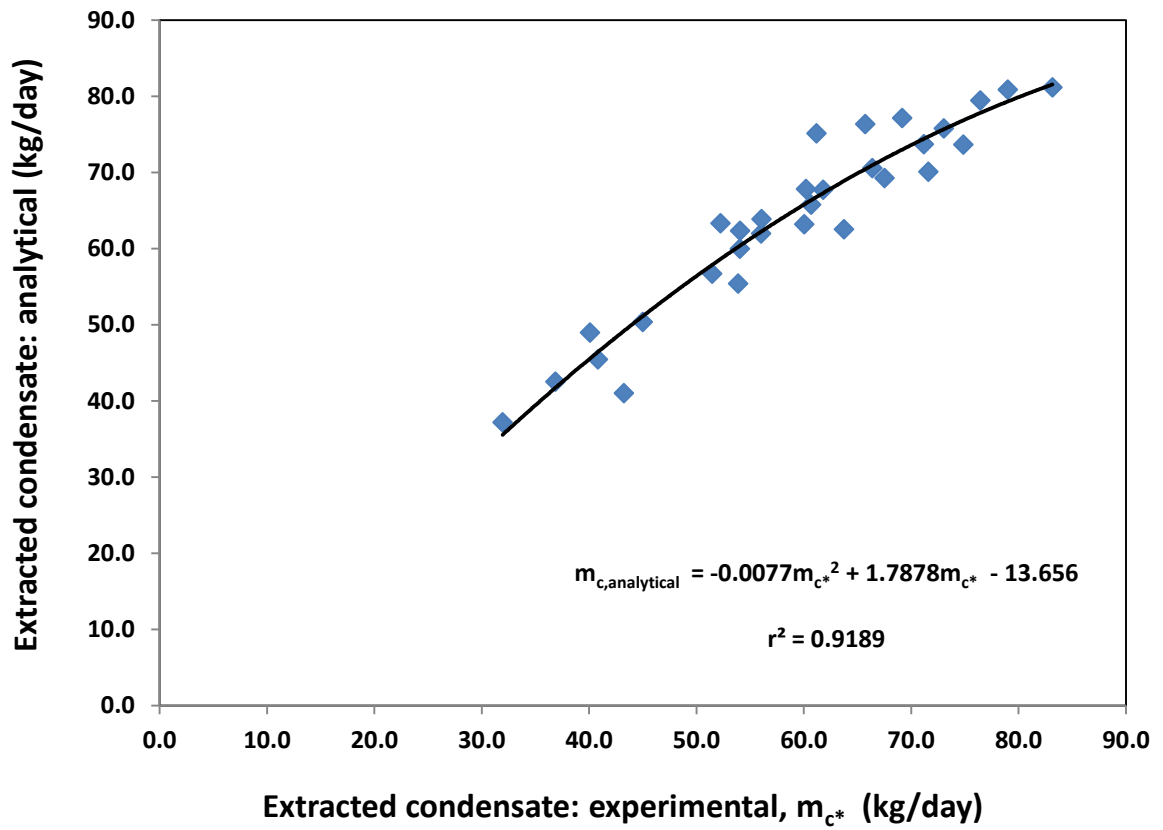
Figure 7.4 Polynomial curve fitting of the analytical versus experimental condensate extracted in September.

The equation shown on the figure:

$$m_{c,analytical} = -0.0077 m_{c*}^2 + 1.7878 m_{c*} - 13.656$$

$$r^2 = 0.9189$$

Axis labels: y-axis: Extracted condensate: analytical (kg/day); x-axis: Extracted condensate: experimental, m_{c*} (kg/day)

CHAPTER 8

CONCLUSIONS

Performance evaluation of a vapor compression air conditioning (VCAC) system and condensate extraction from the system has been carried out successfully in this thesis. The rate of condensate extraction from the VCAC system is evaluated experimentally and analytically using actual climate data of Dhahran, Saudi Arabia and substantial amount is obtained. Chemical analysis on the collected condensate is also carried out to determine its quality. Also, experimental and analytical studies are carried out to evaluate the performance of the base VCAC system and the results are compared with the performance after the system modification. Modification on the system involves: option 'A' – a precooler is added for precooling air stream before entering the evaporator, option 'B'- another precooler is incorporated in the system for precooling the air entering the condenser; and option 'C' - a subcooler is added for refrigerant subcooling after exiting the condenser. All the three options are studied using the collected condensate from the system.

Experiments are conducted at severest weather conditions for Dhahran area on the base system and the modified system and at some other conditions for verification. The severest weather conditions are 36°C dry-bulb temperature and 80% relative humidity determined from the climate data using the maximum enthalpy condition of the air. Comparative analyses between the base system and modified system with the three

different options are presented. The derived conclusions on the overall study are discussed in the following sections:

8.1. Condensate Extraction from the VCAC System

The following conclusions are derived for condensate collection from the base air conditioning system:

i. The rate of condensate extraction from the VCAC system is influenced mainly by the air relative humidity and dry-bulb temperature, but the humidity influence is more significant.

ii. The amount of condensate captured in Dhahran from the 1.5 ton VCAC system for the months of June, July, August and September are 1036, 1181, 2173 and 1781 kg, respectively, and these amounts are obtained experimentally on hourly basis. Analytical results of condensate extraction obtained from hourly calculations using the actual climate data of Dhahran are found to be in good agreement with the experimental results with correlation coefficient of the results above 90%.

iii. The large amount of condensate obtained in Dhahran during the summer months signifies that the condensate is enough for the air precooling and subcooling. In general, regions with similar climate conditions can use this concept.

iv. Condensate chemical analysis reveals that the condensate can be used as drinking water after undergoing the required microbial processes.

v. It can also be used to improve the performance of air conditioning systems and other applications such as cooling tower make up water and irrigation. In addition, the air

conditioners condensate can be used to supplement the domestic water supply and reduce the harmful environmental effect caused by condensate spillage.

8.2.   Evaporator Inlet Air Precooling - Option 'A'

The following conclusions are derived from the comparative study between the base system and the modified system with air precooling before entering the evaporator:

i. The compressor power consumption is decreased by about 5% on average as a result of the decrease in discharge pressure when the air temperature entering the evaporator is lowered by about $5.7^{o}C$ through the precooler for experiments conducted at severest weather conditions.

ii. The coefficient of performance, COP is increased by about 31% and the second law efficiency by 24.85% on average. The condensate temperature inside the tank during the experiment is raised approximately by $3^{o}C$. This is a clear indication that the precooling technique will last long before the condensate that is passing from the tank through the precooler is warmed.

iii. Analytical results are compared with the experimental results for severest weather conditions and they are in good agreement with maximum error of about 5%.

iv. The rate of condensate extraction for experiment with option 'A' is found to be almost the same with that obtained from the base system experiment.

v. The effect of air mass flow rate through the evaporator is also investigated for different temperature difference (ΔT) cross the precooler of option 'A'. The increase in air flow rate increases the cooling effect, COP and the compressor power consumption. The average increase in COP and second law efficiency at $\Delta T = 3^{o}C$ are 9.4 and 12.8% respectively, and the corresponding reduction in compressor power is

1.5% when compared with base system, at air mass flow rate of 0.13kg/s. The increase in COP and second law efficiency are 15.4 and 27% respectively while the corresponding reduction in compressor power is about 4.6% at $\Delta T = 6^{\circ}C$.

8.3. Condenser Inlet Air Precooling - Option 'B'

The following conclusions are derived from the comparative study between the base system and the modified system with air precooling before entering the condenser.

i. Lowering the air temperature before entering the condenser by about 3.5 $^{\circ}C$ resulted in lower compressor discharge pressure, hence lower compressor power during the experiments conducted for severest weather conditions. The average decrease in compressor power is about 4.82% on average.

ii. Due to condenser air precooling, the cooling effect is also increased and the combined effect of the increase in cooling effect and decrease in compressor power resulted in increase in the COP of about 21.11% and second law efficiency of 23.51% on average. The rate of condensate extraction during option 'B' experiment is almost the same with that obtained from the base system with about 3% higher.

iii. Other Experiments are also carried out for option 'B' for several hours in order to justify the feasibility of applying the air precooling technique using condensate. The volume of condensate used during the precooling and the initial condensate temperature before the precooling are 0.9 m^3 and 25$^{\circ}C$, respectively.

iv. During the precooling of condenser inlet air by the condensate, the temperature of the condensate remained effective in lowering the air temperature until about six hours when the air temperatures at the precooler inlet and exit coincide. The average

percentage decrease in compressor power as a result of the air precooling before the condenser is found to be 6.7%, increase in COP and second law efficiency of 27.7 and 27.2% respectively.

v. The six hours precooling of condenser inlet air using condensate is quite great in minimizing the energy consumption by VCAC systems and improving their performance. Hence, the technique can be applied to the existing VCAC systems during the period of high ambient temperatures.

8.4. Refrigerant Subcooling - Option 'C'

The following conclusions are derived from the comparative study between the base system and the modified system with refrigerant subcooling downstream of the condenser.

i. The compressor discharge pressure and temperature are reduced significantly as a result of subcooling the refrigerant before expansion and this lead to the decrease in compressor power consumption by about 3.7% on average.

ii. The positive effects of refrigerant subcooling to the system performance are the increase in COP by about 30.4% and second law efficiency by 21.5% on average.

iii. The rate of condensate extraction of condensate extraction during option 'C' experiment is about 5% higher than that obtained from the base system.

8.5. Overall Conclusions for the Three Options

The following overall conclusions are derived from the comparative study between the base system and the modified system with the three individual options.

i. The performance of the modified VCAC system has advantages over the base system. Compressor discharge pressure is found to be decreased for all the three options.

ii. The technical advantage of the decrease in the discharge pressure beside lower compressor power consumption is the tendency of the compressor to have longer life due to reduced stresses on the compressor parts.

iii. The overall performance assessment of the three options is that option 'A' gives better system performance improvement followed by option 'B', then option 'C'.

8.6. Recommendations

The following are recommended for future work:

a. Insulation of the condensate-storage tank should be optimized to keep the temperature of the fresh condensate as low as possible for better use of it in this kind of application. The temperature of the fresh condensate from the evaporator is generally as low as $5^{\circ}C$.

b. Some means of cooling down the condensate after circulating it through the precoolers or subcooler should be considered so that the technique can be applied continuously during the hot-humid summer seasons.

c. For large buildings applications, the condensate storage tank should be located inside the building to minimize the heat gain from the ambient outside air.

d. Possibility of using condensate to cool the high pressure superheated refrigerant vapor after compressor and before entering the condenser should be explored in future.

e. Another study is recommended on a vapor compression chiller which is used in large buildings and produces more condensate. Thereafter, overall economic analysis of the modified system should be carried out in order to have a clear vision of adopting the concept to the existing air conditioners by manufacturers.

APPENDICES

APPENDIX A: PHOTOGRAPHS OF EXPERIMENTAL SET-UP
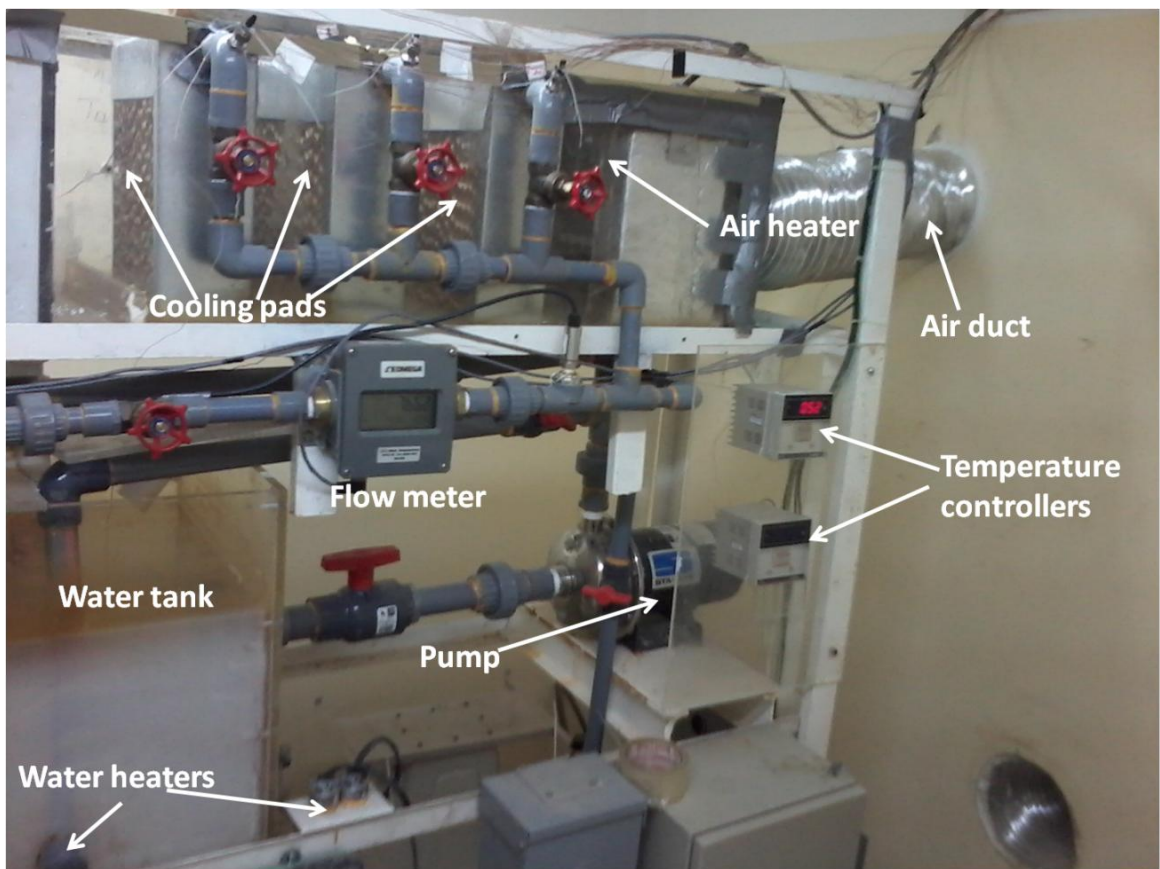
Figure A-1 Experimental set-up: the climate chamber.

Figure A-2 Photograph of the precooler for option 'A' before installation.
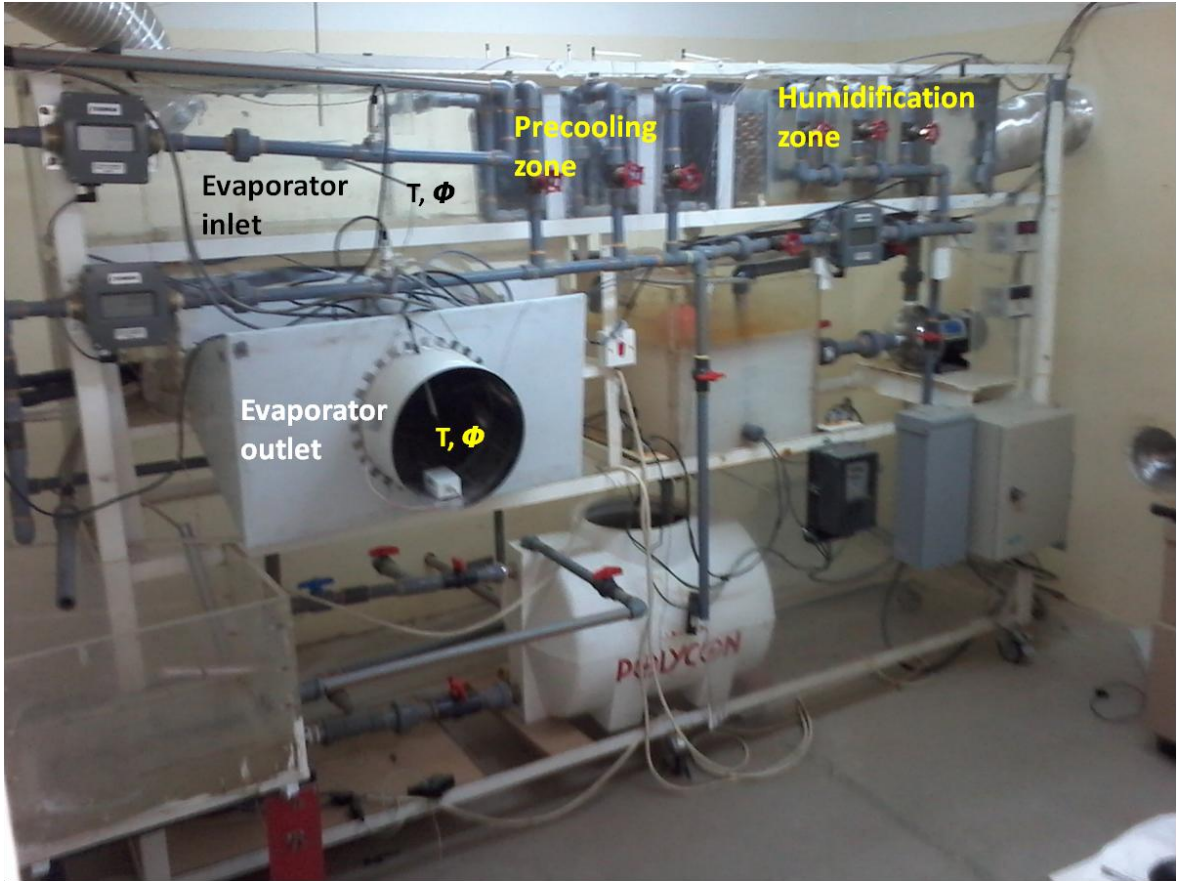
Figure A-3 Picture of experimental rig for option 'A'.
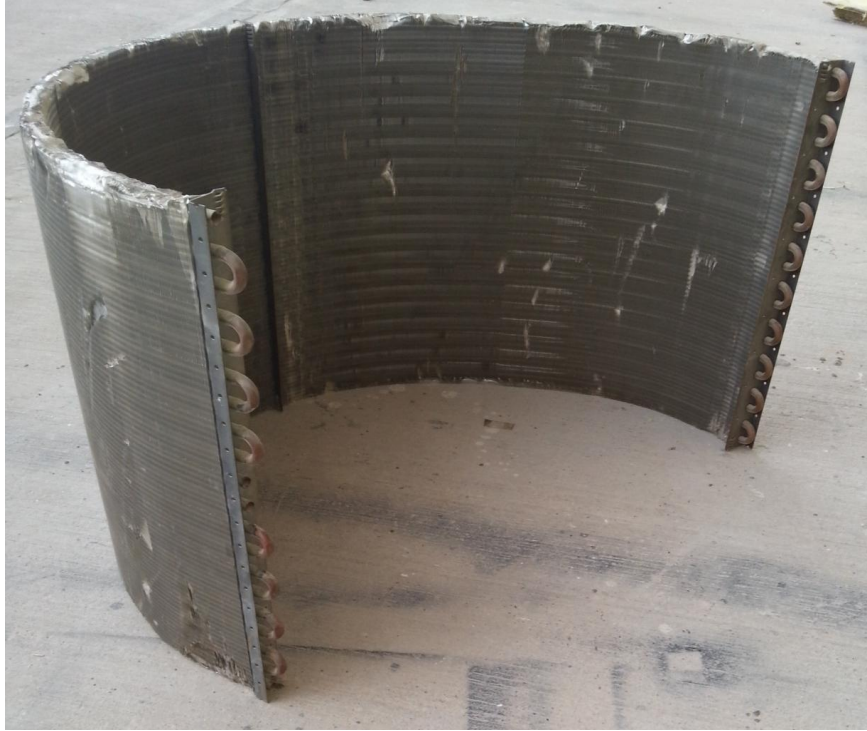
Figure A-4 Picture of precooler for condenser air precooling: option 'B'.

Figure A-5 Installation of precooler for option 'B' behind the condenser.

Figure A-6 Precooler for option 'B' after installation.
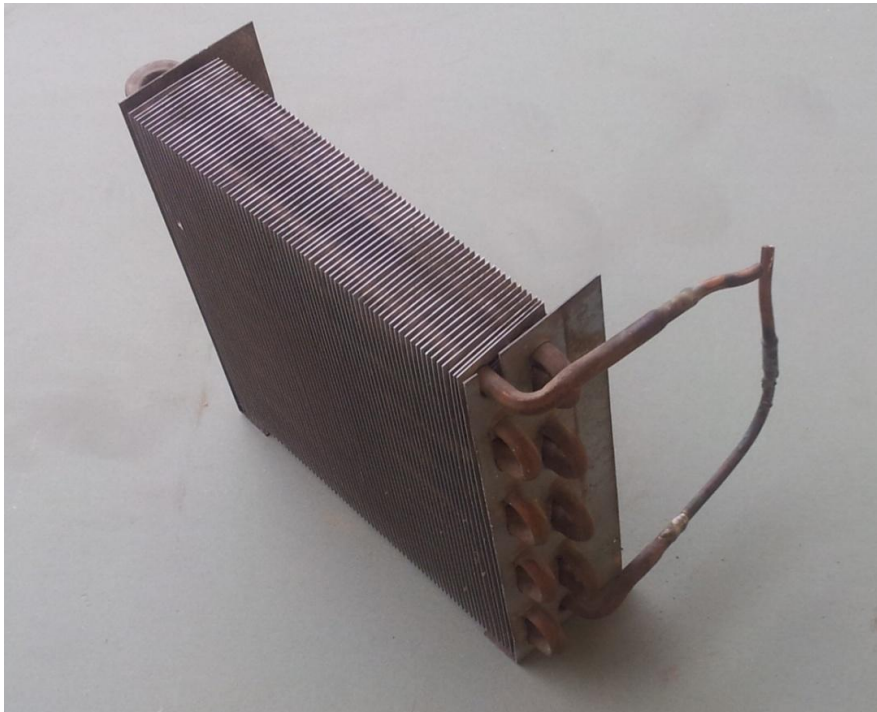
Figure A-7 Picture of subcooler for option 'C' before installation.

Figure A-8 Glassed-face picture of subcooler showing water inlet before installation.

Figure A-9 Three-D picture of subcooler showing the refrigerant inlet and outlet connections.

151

Figure A-10 Picture of the subcooler after installation.

Figure A-11 Front-face of the completed experimental set-up showing the outdoor unit and subcooler.

Figure A-12 Photograph of the experimental set-up outside the room showing the outdoor unit and condensate-storage tank.

Figure A-13 Data acquisition system that is used during the experiments.

APPENDIX B: NUMERICAL CODES
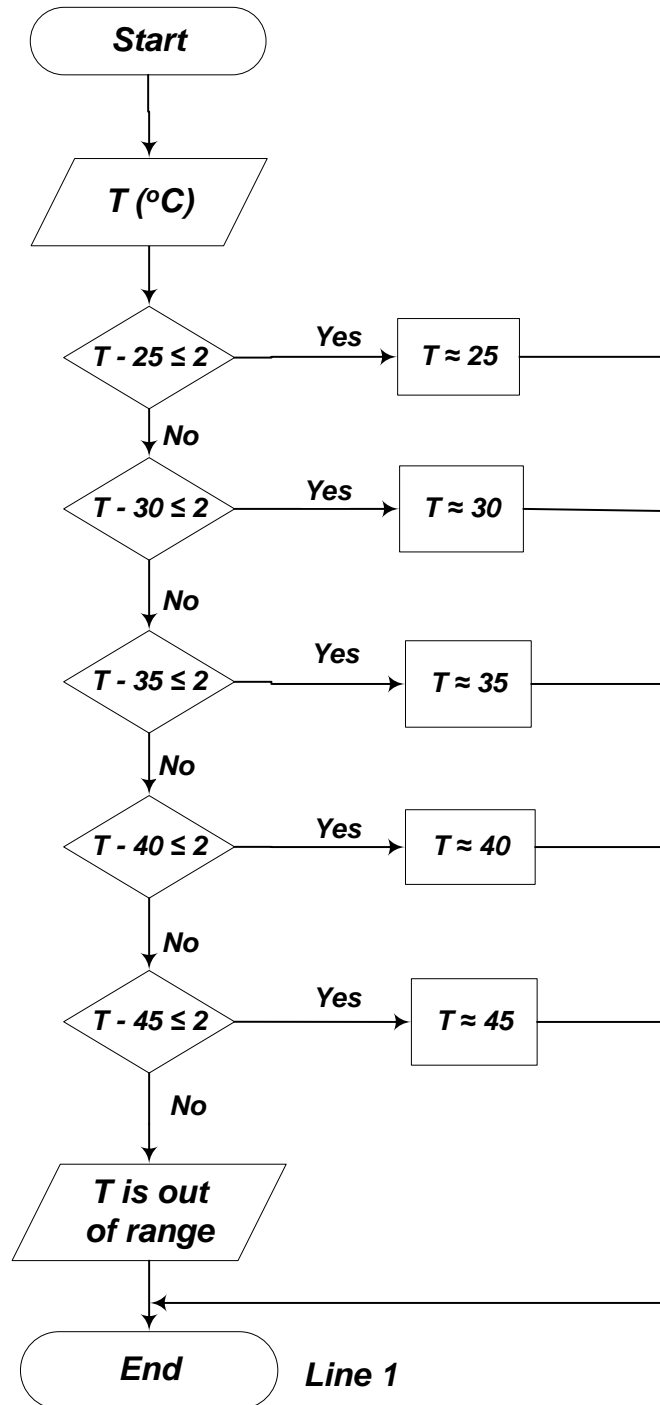
Figure B-1 Flow chart for the ambient temperature data sets.

156

Continue from line 1

Φ (%)

| Φ - 10 ≥ - 5, Φ - 10 ≤ 4 | Yes → | Φ ≈ 10 |

| Φ - 20 ≥ - 5, Φ - 20 ≤ 4 | Yes → | Φ ≈ 20 |

| Φ - 30 ≥ - 5, Φ - 30 ≤ 4 | Yes → | Φ ≈ 30 |

| Φ - 40 ≥ - 5, Φ - 40 ≤ 4 | Yes → | Φ ≈ 40 |

| Φ - 50 ≥ - 5, Φ - 50 ≤ 4 | Yes → | Φ ≈ 50 |

| Φ - 60 ≥ - 5, Φ - 60 ≤ 4 | Yes → | Φ ≈ 60 |

| Φ - 70 ≥ - 5, Φ - 70 ≤ 4 | Yes → | Φ ≈ 70 |

| Φ - 80 ≥ - 5, Φ - 80 ≤ 4 | Yes → | Φ ≈ 80 |

| Φ - 90 ≥ - 5, Φ - 90 ≤ 4 | Yes → | Φ ≈ 90 |

| Φ - 95 ≤ 5 | Yes → | Φ ≈ 95 |

Φ is out of range

End   Line 2
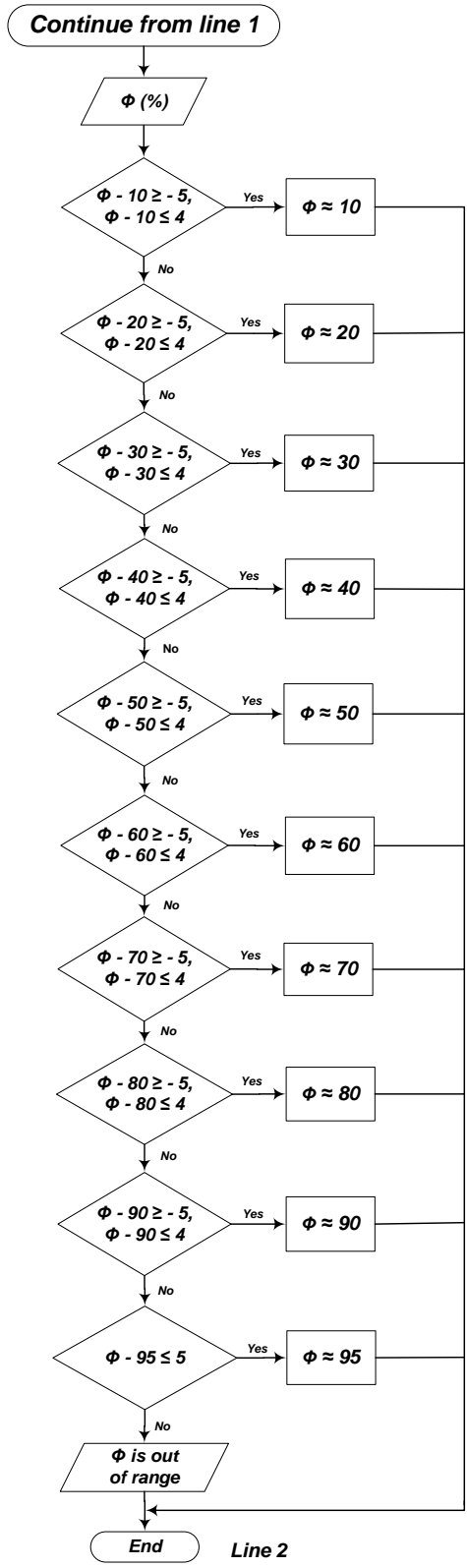
Figure B-2 Flow chart for the relative humidity data sets.

157

1. A Matlab code that approximate the climate data according to (Figs. B-1, B-2) and Table 6.1 and assign the amount of condensate obtained from experiment to the marching combination of the actual hourly temperature and relative humidity of several months.

```matlab
clc
clear all
% A = importdata('mydata.txt', ' ', 1);

% This reads in data from the excel sheet containing Temperature and
% Relative humidity in two columns
[A, headertext1] = xlsread('Augusst2013.xlsx', 'Sheet1');

n = length(A); % This returns the number of rows of data

% Creating an empty array to store the results
data = zeros ( n, 3);
data1 = zeros ( n, 3); % This array contains the conditioned data
data(:,1) = A(:,1); % storing the temperature in the first column
data(:,2) = A(:,2); % storing the relative humidity in the second
column


% This loop conditions the temperature data to the pilot values by
% approximation
for i = 1:1:n

    if abs(data(i,1) - 25)<= 2
        data1(i,1) = 25;
    elseif abs(data(i,1) - 30)<= 2
        data1(i,1) = 30;
    elseif abs(data(i,1) - 35)<= 2
        data1(i,1) = 35;
    elseif abs(data(i,1) - 40)<= 2
        data1(i,1) = 40;
    elseif abs(data(i,1) - 45)<= 3
        data1(i,1) = 45;
    else
        text1 = 'Temperature is out of range';
        disp (text1)
    end
end


% This loop conditions the Relative humidity data to the pilot values
by
% approximation
for i = 1:1:n
```

158

```matlab
        if (data(i,2) - 10)>= -5 && (data(i,2) - 10)<= 4
            data1(i,2) = 10;
        elseif (data(i,2) - 20)>= -5 && (data(i,2) - 20)<= 4
            data1(i,2) = 20;
        elseif (data(i,2) - 30)>= -5 && (data(i,2) - 30)<= 4
            data1(i,2) = 30;
        elseif (data(i,2) - 40)>= -5 && (data(i,2) - 40)<= 4
            data1(i,2) = 40;
        elseif (data(i,2) - 50)>= -5 && (data(i,2) - 50)<= 4
            data1(i,2) = 50;
        elseif (data(i,2) - 60)>= -5 && (data(i,2) - 60)<= 4
            data1(i,2) = 60;
        elseif (data(i,2) - 70)>= -5 && (data(i,2) - 70)<= 4
            data1(i,2) = 70;
        elseif (data(i,2) - 80)>= -5 && (data(i,2) - 80)<= 4
            data1(i,2) = 80;
        elseif (data(i,2) - 90)>= -5 && (data(i,2) - 90)<= 4
            data1(i,2) = 90;
        elseif (data(i,2) - 95)>= -5 && (data(i,2) - 95)<= 5
            data1(i,2) = 95;
        else
            text2 = 'Relative humidity is out of range';
            disp (text2)
        end
end


% Supply the predicted volume (Liters) of condensate into the data
array

for i = 1:1:n

    if data1(i,1)== 25
        if data1(i,2) == 40
            data(i,3)= 1.1;
        elseif data1(i,2) == 50
            data(i,3)= 1.4;
        elseif data1(i,2) == 60
            data(i,3)= 2;
        elseif data1(i,2) == 70
            data(i,3)= 2.8;
        elseif data1(i,2) == 80
            data(i,3)= 3.16;
        elseif data1(i,2) == 90
            data(i,3)= 3.48;
        elseif data1(i,2) == 95
            data(i,3)= 3.8;
        else
            data(i,3) = 0; % Zero in this case means out of range
        end

     elseif data1(i,1)== 30
        if data1(i,2) == 20
            data(i,3)= 0.6;
        elseif data1(i,2) == 30
            data(i,3)= 0.8;
```

159

```matlab
    elseif data1(i,2) == 40
        data(i,3)= 1.6;
    elseif data1(i,2) == 50
        data(i,3)= 2.5;
    elseif data1(i,2) == 60
        data(i,3)= 2.8;
    elseif data1(i,2) == 70
        data(i,3)= 3.2;
    elseif data1(i,2) == 80
        data(i,3)= 3.9;
    elseif data1(i,2) == 90
        data(i,3)= 4.4;
    elseif data1(i,2) == 95
        data(i,3)= 5.7;
    else
        data(i,3) = 0; % Zero in this case means out of range
    end

elseif data1(i,1)== 35
    if data1(i,2) == 20
        data(i,3)= 0.8;
    elseif data1(i,2) == 30
        data(i,3)= 1;
    elseif data1(i,2) == 40
        data(i,3)= 2.2;
    elseif data1(i,2) == 50
        data(i,3)= 2.68;
    elseif data1(i,2) == 60
        data(i,3)= 3.48;
    elseif data1(i,2) == 70
        data(i,3)= 4.24;
    elseif data1(i,2) == 80
        data(i,3)= 5.1;
    elseif data1(i,2) == 90
        data(i,3)= 5.4;
    else
        data(i,3) = 0; % Zero in this case means out of range
    end

elseif data1(i,1)== 40
     if data1(i,2) == 10
        data(i,3)= 0.36;
    elseif data1(i,2) == 20
        data(i,3)= 0.9;
    elseif data1(i,2) == 30
        data(i,3)= 1.52;
    elseif data1(i,2) == 40
        data(i,3)= 2.4;
    elseif data1(i,2) == 50
        data(i,3)= 3.42;
    elseif data1(i,2) == 60
        data(i,3)= 5.4;
    else
         data(i,3) = 0; % Zero in this case means out of range
     end
```

```matlab
    elseif data1(i,1)== 45
        if data1(i,2) == 10
            data(i,3)= 0.4;
        elseif data1(i,2) == 20
            data(i,3)= 0.9;
        elseif data1(i,2) == 30
            data(i,3)= 1.3;
        elseif data1(i,2) == 40
            data(i,3)= 3.3;
        elseif data1(i,2) == 50
            data(i,3)= 3.5;
        else
            data(i,3) = 0; % Zero in this case means out of range
        end
    else
        text3 = 'the data is out of range';
        disp(text3)
    end
        xlswrite('Augusst2013results.xlsx', data,'Sheet1','B2');
        T = sum(data,1);
        xlswrite('Augusst2013results.xlsx', T,'Sheet1','D32');
        xlswrite('Augusst2013results.xlsx', T,'Sheet1','B26');
        M = mean(data,1);
        %xlswrite('yieldperday.xlsx', M,'1','C3');
end
```

2. {EES code. This program calculates the rate of condensate extraction from a vapor
   compression cycle. It also calculate the system performance parameters}

```
R$='R22'                              {specified type of refrigerant}
T_ev_in=31[C]                         {air temperature at the evaporator inlet}
P_a=101.3[kPa]                        {air pressure at the evaporator inlet (atmospheric)}
R_ev_in=0.4                           {air relative humidity at the evaporator inlet}
t=24[h]                               {time}
V_dot_a=0.135[m^3/s]                  {volumetric flow rate of air_ evaporator}
omega_ev_in=humrat(AirH2O, T=T_ev_in, P=P_a,R=R_ev_in) {air humidity ratio at the
evaporator inlet}
T_ev_in_k=convertTemp(C,K,T_ev_in)         { evaporator inlet air temperature in Kelvin}
Cp_a=Cp(AirH2O, T=T_ev_in, P=P_a,R=R_ev_in)   {specific heat capacity of moist air at inlet
conditions}
rho_a_in=density(AirH2O, T=T_ev_in, P=P_a,R=R_ev_in)          {density of moist air}
m_dot_a=V_dot_a*rho_a_in                      {mass flow rate of air at the evaporator side}
h_ev_in=enthalpy(AirH2O, T=T_ev_in, P=P_a,R=R_ev_in)    {air enthalpy at  evaporator inlet}
V_dot_a_cd=0.73[m^3/s]                        {volumetric flow rate of air_ condenser}
T_cd_in=T_ev_in                               {condenser inlet air temperature}
R_cd_in=R_ev_in                               {condenser inlet air relative humidity}
Cp_a_cd=Cp(AirH2O,P=P_a,T=T_cd_in,R=R_cd_in) {specific heat capacity of moist air at inlet
conditions}
rho_a_cd_in=density(AirH2O,P=P_a,T=T_cd_in,R=R_cd_in)    {density of air at condenser side}
m_dot_a_cd=V_dot_a_cd*rho_a_cd_in           {condenser side air mass flow rate}
{T_4=5[C]}                                   {initial guess of refrigerant temperature}
```

```
omega_ev_min=HumRat(AirH2O,P=P_a,T=T_4,R=1)          {minimum humidity ratio of air}
h_ev_min=enthalpy(AirH2O,P=P_a,T=T_4,R=1)      {minimum enthalpy of outlet air}
{Q_dot_ev=4.747[kW]}                    {initial guess value of evaporator cooling capacity/load}
Q_dot_ev=m_dot_a*(h_ev_in-h_ev_out                 {evaporator air side heat transfer}
epsilon_ev=(h_ev_in-h_ev_out)/(h_ev_in-h_ev_min)        {enthalpy effectiveness relation}
epsilon_ev=(omega_ev_in-omega_ev_out)/(omega_ev_in-omega_ev_min)  {enthalpy
effectiveness relation}
T_ev_out=temperature(AirH2O,h=h_ev_out,w=omega_ev_out,P=P_a)   {evaporator outlet
temperature}
m_dot_c=m_dot_a*(omega_ev_in-omega_ev_out)          {rate of condensate removal from the
evaporator}
m_dot_c_kgph=m_dot_c*convert(kg/s,kg/h         {condensate yield in kg/h}
m_dot_c_kgph_pkw=m_dot_c_kgph/Q_dot_ev         {condensate yield in kg/kW-h}
T_c=T_ev_out    {assume condensate temperature equals evaporator outlet air temp}
{x_4=0.65}                          {initial guess value of vapor quality after expansion}
eta_ID=0.65                                {assumed ideal efficiency of compressor}
epsilon_cd=0.3[kW/K]      {assumed value of product of HX effectiveness and capacitance rate}
h_4=Enthalpy(R$,T=T_4,x=x_4)          {refrigerant specific enthalpy at evaporator inlet}
P_4=Pressure(R$,T=T_4,x=x_4)          {refrigerant low pressure of the conventional system}
T_1=T_4                         {assumed refrigerant evaporating at constant temperature}
h_1=Enthalpy(R$,T=T_1,x=1)                {enthalpy at compressor inlet}
s_1=Entropy(R$,P=P_4,x=1)             {refrigerant entropy at the compressor inlet}
h_2_ID=enthalpy(R$,P=P_2,s=s_1)    {discharge specific enthalpy assuming isentropic
compression}
Q_dot_ev=m_dot_r*(h_1-h_4)             {refrigerant side heat transfer rate in the evaporator}
W_c_ID=m_dot_r*(h_2_ID-h_1)              {compressor isentropic work}
{W_c=W_c_ID/eta_ID}                   {actual compressor work}
W_c=m_dot_r*(h_2-h_1)                    {energy balance across compressor}
Q_dot_cd=Q_dot_ev+W_c                              {overall
energy balance of the cycle}
Q_dot_cd=m_dot_r*(h_2-h_3)               {refrigerant side heat transfer rate in condenser}
Q_dot_cd=epsilon_cd*m_dot_a_cd*Cp_a_cd*(T_2-T_cd_in)    {heat transfer rate in condenser}
Q_dot_cd=m_dot_a_cd*Cp_a_cd*(T_out_cd-T_cd_in)   {air side heat transfer rate in condenser}
x_4=Quality(R$,T=T_4,h=h_4)                 {vapor quality after expansion}
P_2=Pressure(R$,h=h_3,T=T_3)              {refrigerant high pressure}
h_4=h_3                               {constant enthalpy across throttling valve}
T_L=(T_ev_in-T_ev_out)/ln(T_ev_in/T_ev_out)    {definition of low temperature for calculating
max. COP}
T_L_k=convertTemp(C,K,T_L)                {low temperature in Kelvin}
T_cd_in_k=convertTemp(C,K,T_cd_in)        {condenser inlet air temperature in Kelvin}
T_3=Temperature(R$,x=0,P=P_2)
T_2=Temperature(R$,h=h_2,P=P_2)               {compressor discharge temperature}
T_1=Temperature(R$,h=h_1,x=1)           {compressor suction temperature}
COP=Q_dot_ev/W_c                       {definition of coefficient of performance}
P_r=P_2/P_4                            {compressor pressure ratio}
COP_max=T_L_k/(T_cd_in_k-T_L_k)        {maximum/Carnot COP of the conventional system}
eta_II=COP/COP_max
```

3. Analytical code for option 'A': EES

```
{Precooler}
T_p_in=36[C]                              {air temperature at the precooler inlet}
P_a=101.3[kPa]                            {air pressure at the precooler inlet}
```

R_p_in=0.8   {air relative humidity at the precooler inlet}
{t=24[h]}   {time}
V_dot_a=0.146[m^3/s]
{volumetric flow rate of air_ evaporator}
omega_p_in=humrat(AirH2O, T=T_p_in, P=P_a,R=R_p_in) {air humidity ratio at the precooler inlet}

T_p_in_k=convertTemp(C,K,T_p_in)   {precooler inlet air temperature in kelvin}
Cp_a=Cp(AirH2O,P=P_a,T=T_p_in,R=R_p_in)   {specific heat capacity of moist air at inlet conditions}
rho_a_in=density(AirH2O,T=T_p_in,P=P_a,R=R_p_in)   {density of moist air}
m_dot_a=V_dot_a*rho_a_in   {mass flow rate of air}
h_p_in=enthalpy(AirH2O, T=T_p_in, P=P_a, R=R_p_in)   {enthalpy at precooler inlet}
T_p_w_in=24[C]   {inlet water temperature to precooler 1}
P_w_in=115.8[kPa]   {assumed water pressure in precooler 1}
Cp_w=Cp(Water,T=T_p_w_in,P=P_w_in)   {specific heat capacity of water}
epsilon_p=0.6   {precooler 1 effectiveness}
m_dot_w=0[kg/s]   {water flow rate in the evaporator precooler 1}
C_dot_p_a=m_dot_a*Cp_a   {air side capacitance in the evaporator precooler 1}
C_dot_p_w=m_dot_w*Cp_w   {water side capacitance in the evaporator precooler 1}
C_dot_min=MIN(C_dot_p_a,C_dot_p_w)   {minimum capacitance rate for precooler 1}
Q_dot_p=m_dot_w*Cp_w*(T_p_w_out-T_p_w_in) {cooling capacity of precooler 1}
Q_dot_p=m_dot_a*Cp_a*(T_p_in-T_p_out)   {energy balance}
Q_dot_p=epsilon_p*C_dot_min*(T_p_in-T_p_w_in) {cooling capacity of precooler 1}
omega_p_out=omega_p_in   {constant humidity ratio: sensible cooling}
T_p_out_k=convertTemp(C,K,T_p_out)   {precooler outlet air temperature in K}
T_dp=DewPoint(AirH2O,T=T_p_out,w=omega_p_out,P=P_a)   {dew point temperature of precooler outlet air}
R_p_out=RelHum(AirH2O,T=T_p_out,D=T_dp,P=P_a) {precooler outlet air relative humidity}
h_p_out=enthalpy(AirH2O, T=T_p_out, P=P_a, w=omega_p_in) {air enthalpy at precooler outlet}
DELTAT_p=(T_p_in-T_p_out)   {air temperature difference across precooler 1}

{T_cd_in=38[C]}   {condenser inlet air temperature}
R_cd_in=R_p_in   {condenser inlet air relative humidity}
V_dot_a_cd=0.73[m^3/s]   {volumetric flow rate of air_ condenser}
Cp_a_cd=Cp(AirH2O,P=P_a,T=T_cd_in,R=R_cd_in) {specific heat capacity of moist air at inlet conditions}
rho_a_cd_in=density(AirH2O,P=P_a,T=T_cd_in,R=R_cd_in) {density of air at condenser side}
m_dot_a_cd=V_dot_a_cd*rho_a_cd_in   {condenser side air mass flow rate}

{T_4=20[C]}   {initial guess of refrigerant temperature}
{Q_dot_ev=8[kW]}   {initial guess of evaporator cooling capacity/load}
omega_ev_min=HumRat(AirH2O,P=P_a,T=T_4,R=1)   {minimum humidity ratio of air}
h_ev_min=enthalpy(AirH2O,P=P_a,T=T_4,R=1)   {minimum enthalpy of outlet air}
Q_dot_ev=m_dot_a*(h_p_out-h_ev_out)   {evaporator air side heat transfer}
epsilon_ev=(h_p_in-h_ev_out)/(h_p_in-h_ev_min)   {enthalpy effectiveness relation}
epsilon_ev=(omega_p_out-omega_ev_out)/(omega_p_out-omega_ev_min)   {enthalpy effectiveness relation}
T_ev_out=temperature(AirH2O,h=h_ev_out,w=omega_ev_out,P=P_a) {evaporator outlet temperature}
Q_dot_ev_n=m_dot_a*(h_p_out-h_ev_out)   {new cooling load after in precooler 1}
m_dot_c=m_dot_a*(omega_p_out-omega_ev_out)   {rate of condensate removal from the evaporator}
m_dot_c_kgph=m_dot_c*convert(kg/s,kg/hr)   {condensate yield in kg/h}
m_dot_c_kgph_pkw=m_dot_c_kgph/Q_dot_ev   {condensate yield in kg/kW-h}
T_c=T_ev_out   {assume condensate temperature equals evaporator outlet air temp}

163

```
R$='R22'                              {specified type of refrigerant}
{x_4=0.43}                            {initial guess value of vapor quality after expansion}
eta_ID=0.65                                    {assumed ideal efficiency of compressor}
epsilon_cd=0.68[kW/K]      {assumed value of product of HX effectiveness and capacitance rate}
h_4=Enthalpy(R$,T=T_4,x=x_4)              {refrigerant specific enthalpy at evaporator inlet}
P_4=Pressure(R$,h=h_4,x=x_4)              {refrigerant low pressure}
T_1=T_4                       {assumed refrigerant evaporating at constant temperature}
h_1=Enthalpy(R$,T=T_1,x=1)                      {enthalpy at compressor inlet}
Q_dot_ev=m_dot_r*(h_1-h_4)         {refrigerant side heat transfer rate in the evaporator}
{s_1=Entropy(R$,P=P_4,x=1)}          {refrigerant entropy at the compressor inlet}
h_2_ID=enthalpy(R$,P=P_2,s=s_1) {discharge specific enthalpy assuming isentropic
compression}
P_2=Pressure(R$,h=h_2,T=T_2)                    {refrigerant high pressure}
T_2=Temperature(R$,h=h_2,P=P_2)
h_3=h_4
T_1=Temperature(R$,h=h_1,x=1)


W_c_ID=m_dot_r*(h_2_ID-h_1)                {compressor isentropic work}
W_c=W_c_ID/eta_ID                              {actual compressor work}
W_c=m_dot_r*(h_2-h_1)                     {energy balance across compressor}
Q_dot_cd=Q_dot_ev+W_c                    {overall energy balance of the cycle}
Q_dot_cd=m_dot_r*(h_2-h_3)               {refrigerant side heat transfer rate in condenser}
Q_dot_cd=epsilon_cd*m_dot_a_cd*(T_3-T_cd_in)      {heat transfer rate in condenser}
Q_dot_cd=m_dot_a_cd*Cp_a_cd*(T_out_cd-T_cd_in)  {air side heat transfer rate in condenser }
x_4=Quality(R$,T=T_4,h=h_4)                    {vapor quality after expansion}
COP=(Q_dot_ev+Q_dot_p)/W_c
T_L=(T_p_in-T_ev_out)/ln(T_p_in/T_ev_out) {defination of low temperature for calculating max.
COP}
T_L_k=convertTemp(C,K,T_L)                     {low temperature in Kelvin}
T_cd_in_k=convertTemp(C,K,T_cd_in)         {condensaer inlet air temperature in Kelvin}
P_r=P_2/P_4                              {compressor pressure ratio}
COP_max=T_L_k/(T_cd_in_k-T_L_k)       {maximum/Carnot COP of the conventional system}
eta_II=COP/COP_max                 {second low efficiency of the conventional system}
EER=3.412*Q_dot_ev/W_c

s_1=Entropy(R$,P=P_4,X=1)
s_2=Entropy(R$,P=P_2,h=h_2)
s_3=Entropy(R$,h=h_3,T=T_3)
s_4=Entropy(R$,h=h_4,x=x_4)

Ex_com=m_dot_r*(T_cd_in_k*(s_2-s_1))
Ex_cd=m_dot_r*(h_2-h_3-T_cd_in_k*(s_2-s_3))
Ex_vlv=m_dot_r*T_cd_in_k*(s_4-s_3)
Ex_ev=m_dot_r*(h_4-h_1-T_cd_in_k*(s_4-s_1))-(-Q_dot_ev*(1-T_cd_in_k/T_L_k))
W_min=-Q_dot_ev*(1-T_cd_in_k/T_L_k)
Ex_tot=Ex_com+Ex_cd+Ex_vlv+Ex_ev
eta_II_2=W_min/W_c

DELTAT_w_t=1.3[C]
{temperature change of water in the precooler}
m_dot_w_t=9.6[kg/min]                          {mass flow rate of precooler water}
m_dot_c_fresh=0.113[kg/min]               {mass flow rate of fresh condensate}
M_i=1000[kg]     {initial mass of water in the tank before }
T_i=24.8[C]            {initial water temp. in the tank before }
```

T_c_fresh=22[C]   {temperature of fresh condensate}
t_t=120[min]   {operating time for }
T_tank=(((m_dot_w_t*DELTAT_w_t)-
m_dot_c_fresh*T_c_fresh)*t_t)/(m_dot_c_fresh*t_t+M_i)+(T_i*M_i)/(m_dot_c_fresh*t_t+M_i)
{current water temperature in the tank at any time}
DELTAT_Tank=T_tank-T_i   {change in water temperature at a time interval}
T_tank_n=-
m_dot_c_fresh*T_c_fresh*t_t/(m_dot_c_fresh*t_t+M_i)+(T_i*M_i)/(m_dot_c_fresh*t_t+M_i)
M_t=m_dot_c_fresh*t_t+M_i

APPENDIX C: SAMPLE CALCULATIONS OF EXPERIMENTAL UNCERTAINTIES

The detail calculations of uncertainties the baseline results for severest conditions are given here. During this experiment, the data was saved at every minute for two hours. In this section, only the sample calculations for uncertainty values of the baseline experimental results conducted at severest weather conditions are given. From the experimental data and using Eq. (7.2), evaporator inlet air temperature $T_{a,ev,i} = 36.06\,°\text{C}$.

$$\delta_{T_{a,ev,i}} = \delta_{i,e} + \delta_{r,e}$$

$$\delta_{T_{a,ev,i}} = 0.2 + 0.00322 = \pm 0.2032\,°\text{C}.$$

Similarly, $T_{a,ev,e} = 22.67\,°\text{C}$, $\emptyset_i = 0.78$, $\emptyset_e = 0.94$, $T_L = 22.67\,°\text{C}$,

$h_{a,ev,i} = 113.2\,\text{kJ/kg}$, $h_{a,ev,e} = 56.56\,\text{kJ/kg}$, $I = 11.64\,A$, $\dot{W}_c = 2.56\,kW$,

$\dot{Q}_{ev} = 7.84\,kW$, $COP = 3.064$, $COP_{max} = 32.42$, $\eta_{II} = 0.0946$, $\dot{m}_a = 0.159\,kg/s$

$$\delta_{T_{a,ev,e}} = \pm 0.20572\,°\text{C}, \quad \delta_{T_H} = \pm 0.2296\,°\text{C}, \quad \delta_{\emptyset_i} = \pm 0.02628, \quad \delta_{\emptyset_e} = \pm 0.02562$$

$$\delta_I = \pm 0.237\,A, \quad \delta_{\dot{m}_a} = \pm 0.00318\,kg/s.$$

$$\frac{\partial h_{a,ev,i}}{\partial T_{a,ev,i}} = 1 + \frac{(1.1569)(0.78)(5.965)}{101.3 - 0.78(5.965)} = \frac{1.0557\,kJ}{kgK}$$

$$\frac{\partial h_{a,ev,i}}{\partial \emptyset_i} = \frac{(0.622)(5.965)(2501.3 + 1.86\,x\,36.06)(101.3 - 0.78(5.965) + 0.78)}{(101.3 - 0.78(5.965))^2}$$

$$\frac{\partial h_{a,ev,i}}{\partial \emptyset_i} = 99.39\,kJ/kg$$

$$\delta_{h_{a,ev,i}} = [(1.0557 \; x \; 0.2032)^2 + (99.39 \; x \; 0.02628)^2]^{1/2} = \pm 2.62 \frac{kJ}{kg}$$

$$\frac{\partial h_{a,ev,e}}{\partial T_{a,ev,e}} = 1 + \frac{(1.1569)(0.94)(2.755)}{101.3 - 0.78(2.755)} = \frac{1.0304 \; kJ}{kgK}$$

$$\frac{\partial h_{a,ev,e}}{\partial \emptyset_e} = \frac{(0.622)(2.755)(2501.3 + 1.86 \; x \; 36.06)(101.3 - 0.94(2.755) + 0.94)}{(101.3 - 0.78(2.755))^2}$$

$$\frac{\partial h_{a,ev,e}}{\partial \emptyset_e} = 44.56 \frac{kJ}{kg}$$

$$\delta_{h_{a,ev,e}} = [(1.0304 \; x \; 0.20572)^2 + (44.56 \; x \; 0.02562)^2]^{1/2} = \pm 1.16 \; kJ/kg$$

$$\delta_{\dot{m}_a} = \frac{2}{100} \; x \; 0.159 = \pm 0.00318 \; kg/s$$

$$\delta_{\dot{Q}_{ev}} = [(56.63 \; x \; 0.00318)^2 + (0.159 \; x \; 2.62)^2 + (-0.159 \; x \; 1.16)^2]^{1/2}$$

$$\delta_{\dot{Q}_{ev}} = \pm \boldsymbol{0.49 \; kW} = \pm \boldsymbol{6.25}\%$$

$$\delta_{\dot{W}_c} = 0.22 \; x \; 0.237 = \pm \boldsymbol{0.052 \; kW} = \pm \boldsymbol{2.03} \%$$

$$\delta_{COP} = [(0.39 \; x \; 0.49)^2 + (-1.196 \; x \; 0.052)^2]^{1/2}$$

$$\delta_{COP} = \pm \boldsymbol{0.2} = \pm \boldsymbol{6.56}\%$$

$$\delta_{T_L} = [(0.426 \; x \; 0.2032)^2 + (-0.595 \; x \; 0.2057)^2]^{1/2} = \pm 0.15 \, ^{\circ}\text{C} = 0.52 \; \%$$

$$\delta_{COP_{max}} = [(3.67 \; x \; 0.15)^2 + (3.469 \; x \; 0.2296)^2]^{1/2}$$

$$\delta_{COP_{max}} = \pm 0.96 = \pm 2.96\%$$

$$\delta_{\eta_{II}} = [(0.031 \; x \; 0.2)^2 + (-0.00295 \; x \; 0.96)^2]^{1/2}$$

$\delta_{\eta_{II}} = \pm 0.0068 = \pm 7.2\%$

Using the same calculation procedure, the uncertainty values of the experimental data for options 'A', 'B' and 'C' ware calculated and given in Tables 7.1 to 7.4.

REFERENCES

[1] M.I. Budaiwi, Air conditioning system operation strategies for intermittent occupancy buildings in a hot-humid climate, Proceedings of the 8th IBPSA conference. Eindhoven, Netherlands, August 2003; 11-14.

[2] M.A Esmail, E. Ashraf, Determinants of consumers' demand on energy-efficient air conditioners in Saudi Arabia, *Energy & environment* 2011; 22:711-722.

[3] P. Gandhidasan, H.I. Abualhamayel, Modelling and testing of a dew collection system, *Desalination* 2005; 180:47-51.

[4] R.V. Wahlgren, Atmospheric water vapor processor designs for potable water production: A Review, *Water Resources* 2001; 35:1-22.

[5] A. Khalil, Dehumidification of atmospheric air as a potential source of fresh water, *Desalination* 1993; 34:587-596.

[6] B.W. E. Alnaser, A. Barakat, Use of condensed water vapor from the atmosphere for irrigation in Bahrain, *Applied Energy* 2000; 65:3-18.

[7] B.A. Habeebullah, Potential use of evaporator coils for water extraction in hot and humid areas, *Desalination* 2009; 237:330-345.

[8] B.A. Habeebullah, Performance analysis of a combined heat pump-dehumidification system, *J. KAU: Engineering Science* 2010; 21:97-114.

[9] E. Elsarrag, Y.Al Horr. Experimental investigations on water recovery from the atmosphere in arid humid regions. CIBSE Technical symposium, DeMontfort University, Leicestern UK – 6th and 7th September 2011.

[10] J.A. Brayant, T. Ahmad. Condensate water collection for an institutional building in Doha, Qatar: an opportunity for water sustainability. Proceedings of the 16th symposium on improving building systems in hot and humid climates, Plano, TX, December 15 – 17, 2008.

[11] K. Guz. Sustainability: Condensate water recovery. *ASHRAE Journal* 2005; 47(6):54 – 56.

[12] S.A. Khan, S.N. Al-Zubaidy, Conservation of portable water using chilled water condensate from air conditioning machines in hot and humid climate, *Int. J. Engineering and Innovative Technology* 2013; 3(2):182-188.

[13] A.H. Mahvi, V. Alipour, L. Rezaei, Atmospheric moisture condensation to water recovery by home air conditioners, *American Journal of Applied Sciences* 2013;10(8): 917-923.

[14] K. Loveless, A. Farooq, N. Ghaffour, Collection of condensate: Global potential and water quality impacts, *Water Resource Management* 2013;27:1351-1361.

[15] W. A. Abderrahman, Energy and water in arid developing countries: Saudi Arabia, a case study, Water Resource Development, 2001; 17(2):247-255.

[16] N.R. Lakdawala, Water condensate recovery device, *US Patent* 4280334 (1981).

[17] F.B. Wachs, Refrigeration system with evaporative sub-cooling, *US Patent* 5113668 (1992).

[18] K. Teller, Non-drip high efficiency AC system utilizing condensate water for subcooling, US *Patent* 5979172 (1999).

[19] K.T.J. Dobmeier, Michael F. Taras, A. Lifson, Refrigerant Subcooling by Condensate. *US Patent* 7013658 B2 (2006).

[20] J. Chodak, S. Murphy, Improvement on the efficiency of condensing units Analysis of the AC precooling machine, MS thesis report, *Dept. of Mech. Eng. Tulane University, New Orleans, La*, 2005.

[21] E. Hajidavalloo, H. Eghtedari, Performance improvement of air-cooled refrigeration system by using evaporatively cooled air condenser, *Int. J. Refrigeration* 2010; 33:982-988.

[22] E. Hajidavalloo, H. Eghtedari, Application of evaporative cooling on the condenser of window-air-conditioner, *Applied Thermal Engineering* 2007; 27:1937-1943.

[23] S. Delfani, J. Esmaeelian, H. Pasdarshahri, M. Karami, Energy saving potential of an indirect evaporative cooler as a precooling unit for mechanical cooling systems in Iran, *Energy and Buildings* 2010; 42:2169-2176.

[24] M. Waly, W. Cakroun, N. K. Al-Mutawa, Effect of precooling of inlet air to condensers of air conditioning units., *Int. J. Energy Research* 2005; 29:718-794.

[25] R. Sawan, K. Ghali, M. Al-Hindi, Use of condensate drain to precool the inlet air to the condensers: A technique to improve the performance of split air-conditioning Units, *HVAC & R Research* 2012; 18(3):417-431.

[26] B. Cansevdi, U. Calli and H. Arif, Improving the energy performance of air-cooled chillers with water-spray mist: An application. *Unpublished paper, Dept. of Mech. Eng. Ege University Izmir, Turkey*. 2010.

[27] F.W. Yu, K.T. Chan, Improved energy performance of air-cooled chiller system with mist, *Applied Thermal Engineering* 2011; 31:537-544.

[28] J. Tissot, P. Boulet, F. Trinquet, L. Fournaison, H. Macchi-Tejeda, Air cooling by evaporating droplets in the upward flow of a condenser, *Int. J. Thermal Sc.* 2011; 50:2122-2131.

[29] Federal Technology Alert, Refrigerant sub-cooling, prepared by *New Technology Demonstration Program*, *US Department of energy,* Washington 1995.

[30] W.F. Stoeker, J.W. Jones. Refrigeration and air Conditioning 2nd Ed., *McGraw- Hill Publishing Company, New York,* 1982.

[31] B.O. Bolaji, Effect of subcooling on the performance of R12 alternatives in a domestic refrigeration system, Tammasat, *Int. J. Sc. Tech.*, 2010; 15(1):12-19

[32] M. Miller, Mechanical sub-cooling yields gains in efficiency, capacity, plus lower maintenance costs, *The Air Conditioning, Heating and Refrigeration News*, June 15, 1981.

[33] J.R. Khan, S.M. Zubair, Design and rating of an integrated mechanical sub-cooling vapour-compression refrigeration system, *Energy Conversion and Management*, 2000; 41:1201-1222.

[34] J.R. Khan, S.M. Zubair, Design and rating of dedicated mechanical sub-cooling vapour-compression refrigeration systems, *Journal of Power and Energy*, 2000; 214:455-471.

[35] B.A. Qureshi, M. Inam, M.A. Antar, S.M. Zubair, Experimental energetic analysis of a vapor compression refrigeration system with dedicated mechanical subcooling, *Applied Energy*, 2012; 1 02:1035-1041.

[36] O.M. Al-Rabghi, M. M. Akyurt, A survey on energy efficient strategies for effective air conditioning, *Energy conversion and management*, 2004; 45:1643-1654.

[37] M. Fatouh, Talaat A. Ibrahim, A. Mustafa, Experimental investigation on a solid desiccant system integrated with a R407C Compression air conditioner, *Energy conversion and management*, 2009; 50:2670-2679.

[38] L. Mei, Y.J. Dai, A Technical review on use of liquid-desiccant dehumidification for air conditioning application, *Renewable and sustainable Energy Review* 2008; 12:662-689.

[39] Y.J Dai, R.Z. Wang, H. F. Zhang, J.D Yu, Use of liquid desiccant cooling to improve the performance of vapor-compression air conditioning, *Applied thermal Engineering* 2001; 21:1185-1202.

[40] Y. Seiichi, J. Jeong, K. Saito, H. Miyauchi, M. Harada, Hybrid liquid desiccant air-conditioning system: experiment and simulations, *Applied Thermal Engineering*, 2011; 31:3741-3747.

[41] Y.J. Seiichi, Y. Kiyoshi S. Sunaok, Performance analysis of desiccant dehumidification systems driven by low-grade heat source, *Int. J. Refrigeration*, 2011; 928-945.

[42] B. Stefano, C. Anna, On the performance of a hybrid air-conditioning system in different climatic conditions, *Energy*, 2011; 36:5261-5273.

[43] I. Dincer, On thermal energy storage system and applications in buildings, *Energy and Buildings*, 2002; 34:377-388.

[44] M.J. Sebzali, P.A. Rubini, Analysis of ice cool thermal storage for a clinic building in Kuwait, *Energy Conversion and Management*, 2006; 47:3417-3434.

[45] M.J. Sebzali, P.A. Rubini, The impact of using chilled water storage systems on the performance of air cooled chillers in Kuwait, *Energy and Buildings* 2007; 39:975-984.

[46] Y.H. Yau, R. Behzad, A review on cool thermal storage technologies and operating strategies, *Renewable and Sustainable Energy Reviews* 2012; 16:787-797.

[47] W. Leidenfrost, K.H. Lee, B. Korenic, Conservation of energy estimated by second law analysis of a power-consuming process. *Energy* 1980; 5:47-61.

[48] A. Bejan, Theory of heat transfer – irreversible refrigeration plants. *Int. J. Heat Mass Transfer* 1989; 32:1631-1639.

[49] T.R. Strobridge, Cryogenic Refrigerators – An updated survey in: National Bureau of Standards Technical note. Vol. 655, Washington, DC, 1974.

[50] R.L. Akau, R.J. Schoenhals, The second law efficiency of a heat pump system. *Energy* 1980; 5:853-863.

[51] R.Yumrutas, M. Kunduz, M. Kanoglu, Exergy analysis of vapour compression refrigeration systems, *Exergy, An International Journal* 2002; 2:266-272.

[52] E.Bilgen, H. Takahashi, M. Kanoglu, Exergy analysis and experimental study of heat pump systems, *Exergy, an International Journal* 2002; 2:259-265.

[53] A. Arora, S.C. Kaushik, Theoretical analysis of a vapour compression heat pump refrigeration system with R502, R404A and R507A, *Int. Journal of Refrigeration* 2008; 31:998-1005.

[54] M. Mafi, S.M. Mousavi, M. Amidpour, Exergy analysis of multistage cascade low temperature refrigeration systems used in olefin plants, *Int. Journal of Refrigeration* 2008; 32:279-294.

[55] V.P. Venkataramanamurthy, P.S. Kumar, Experimental comparative energy, exergy flow and second law analysis of R22, R436b vapour compression refrigeration cycles, *Int. Journal of Engineering Science and Technology* 2010; 2:1399-1412.

[56] C. Aprea, C Renno, Experimental comparison of R22 with R417A performance in a vapor compression refrigeration plant subjected to a cold store, *Energy Conversion and Management*, 2004; 45:1807-1819.

[57] B.O. Bolaji, Exergetic performance of a domestic refrigerator using R12 and its alternative refrigerants, *Journal of Engineering Science and Technology* 2010; 5:435-446.

[58] A.E. Ozugur, A. Kabul, O. Kizilkan, Exergy analysis of refrigeration systems using an alternative refrigerant (hfo-1234yf) to R134a, *Int. Journal of Low Carbon Technologies* 2012; 0:1-7.

[59] J.U. Ahamed, R. Saidur, H.H. Masjuki, A review on exergy analysis of vapor compression refrigeration system, *Renewable and sustainable Energy Review* 2011; 12:1593-1600.

[60] Tzong-Shing Lee, Second law analysis to improve the energy efficiency of screw liquid chillers, *Entropy* 2010; 12:375-389.

[61] G.F. Nellis, S.A. Klien, Heat transfer, Cambridge University Press, 2009.

[62] S.A. Klein, F.L. Alvarado. *Engineering Equation Solver*, Academic Professional Version 8.609. F-Chart Software, Madison, WI, USA; 2009.

[63] T.H. Kuehn, J. W. Ramsey and J. L. Threlkeld, Thermal environmental engineering, 3rd Ed., Prentice Hall, 1998.

[64] ASHRAE, Fundamentals Handbook, (SI) 2005; 3.28: 4.1-4.10.

[65] F.C. McQuiston, J. D. Parker, J. D. Spitler. Heating, ventilating and air conditioning: Design and analysis, 6th Ed., John Wiley, New York, 2005.

[66] S.N. Sapali. Refrigeration and air conditioning, 2nd Ed., PHI Learning, 2009.

[67] M.M. Shah, "Chart correlation for saturated boiling heat transfer: equations and further study," *ASHRAE Trans* 1982; 88:185-196.

[68] W.M, Kays, A.L. London. Compact heat exchangers, 3rd Ed., McGraw Hill, New York, 1984.

[69] J.A. Duffie, W, Beckman, Solar engineering of thermal processes, 3rd Ed., Wiley, New York, 2006.

[70] http://www.techsciresearch.com/2012.

[71] Air-Conditioning and Refrigeration Institute (AIR). Forced-circulation air-cooling and air-heating coils. ANSI/ARI *Standard* 410-01. Arlington, VA. 2005.

[72] D. Westphalen, S. Koszalinski, Energy consumption characteristics of commercial building HVAC systems. Office of building technology state and community programs, U.S. Department of Energy. Contract No.: DE-AC01-96CE23798. October, 1999.

[73] J.P. Holman, Experimental methods for engineers, Eighth Ed. McGraw-Hill, 2011.

VITAE

Name   : Nasiru Ishaq. Ibrahim

Nationality   : Nigeria

Date of Birth   : 20/12/1981

Email   : nasir1301@yahoo.com

Academic Background   : **M.S. Mechanical Engineering, 2013**

                          King Fahd University of Petroleum and Minerals,

                          Dhahran, Saudi Arabia.

                          B.Sc. Mechanical Engineering, 2009

                          Bayero University Kano, Nigeria.

Publications   Abdulghani. A. Al-Farayedhi, Nasiru I. Ibrahim, P. Gandhidasan, **"A Novel Technique for Reducing Cooling Load of an Air Conditioning System Operating in Hot and Humid Climates"** *Proceedings of the ASME 2013 Summer Heat Transfer Conference, Minneapolis MN, July 14 – 19 USA*, DOI: 10.1115/HT2013-17712, pp.v002T04H025-;8 pages.